

On Classification of Models of Large Local-Type Non-Gaussianity

Teruaki Suyama¹, Tomo Takahashi², Masahide Yamaguchi³,
and Shuichiro Yokoyama⁴

¹*Research Center for the Early Universe, Graduate School of Science,
The University of Tokyo, Tokyo 113-0033, Japan*

²*Department of Physics, Saga University, Saga 840-8502, Japan*

³*Department of Physics, Tokyo Institute of Technology, Tokyo 152-8551, Japan*

⁴*Department of Physics and Astrophysics, Nagoya University, Aichi 464-8602, Japan*

Abstract

We classify models generating large local-type non-Gaussianity into some categories by using some “consistency relations” among the non-linearity parameters $f_{\text{NL}}^{\text{local}}$, $\tau_{\text{NL}}^{\text{local}}$ and $g_{\text{NL}}^{\text{local}}$, which characterize the size of bispectrum for the former and trispectrum for the later two. Then we discuss how one can discriminate models of large local-type non-Gaussianity with such relations. We first classify the models by using the ratio of $\tau_{\text{NL}}^{\text{local}}/(6f_{\text{NL}}^{\text{local}}/5)^2$, which is unity for “single-source” models and deviates from unity for “multi-source” ones. We can make a further classification of models in each category by utilizing the relation between $f_{\text{NL}}^{\text{local}}$ and $g_{\text{NL}}^{\text{local}}$. Our classification suggests that observations of trispectrum would be very helpful to distinguish models of large non-Gaussianity and may reveal the generation mechanism of primordial fluctuations.

Contents

1	Introduction	1
2	Formalism	2
3	Models of local-type non-Gaussianity	4
3.1	A classification of local type	4
3.2	Single-source model	5
3.2.1	Pure curvaton model	9
3.2.2	Pure modulated reheating model	11
3.2.3	Modulated-curvaton model	13
3.2.4	Inhomogeneous end of hybrid inflation	16
3.2.5	Inhomogeneous end of thermal inflation	19
3.2.6	Modulated trapping mechanism	20
3.3	Multi-source model	22
3.3.1	Mixed model with inflaton fluctuations	24
3.3.2	Multi-curvaton model	26
3.3.3	Multi-field inflation model	31
3.4	Constrained multi-source model	46
3.4.1	Expressions including loop contributions	47
3.4.2	Ungaussiton model	48
3.5	Other models	49
4	Discussion and Summary	50
A	Full expression for ζ in multi-curvaton model	53
B	Full expressions including one-loop corrections	55
C	Full order calculation	56

1 Introduction

Non-Gaussianity of primordial fluctuations is now one of the important observables to probe the physics of the early Universe. Although the inflaton, which acquires quantum fluctuations during inflation and generates (almost) scale-invariant and adiabatic primordial fluctuations, has been considered to be responsible for the origin of density fluctuations in the Universe, this scenario might not be the one realized in the nature. Primordial fluctuations generated from the inflaton during slow-roll inflation are expected to be almost Gaussian, however, current observations such as WMAP indicate that the primordial fluctuations might deviate from Gaussian ones and the deviation could be relatively large compared to the one expected from the “slow-rolling” inflation models. (For recent analyses, see [1–4].) The degrees of non-Gaussianity are often represented by a so-called non-linearity parameter f_{NL} , which characterizes the size of bispectrum of the curvature perturbation. Depending on the momentum distribution of the bispectrum or the shape of three point function, three types of f_{NL} have been discussed in the literature [1, 5]: local, equilateral and orthogonal types. The limits on these f_{NL} s have been obtained as [1]: $-10 < f_{\text{NL}}^{\text{local}} < 74$ for the local type, $-214 < f_{\text{NL}}^{\text{equil}} < 266$ for the equilateral type and $-410 < f_{\text{NL}}^{\text{orthog}} < 6$ for the orthogonal type (95% C.L.). Although all of these are still consistent with Gaussian fluctuations, they may give some hint of non-Gaussian ones since the central value of f_{NL} for some types is away from the zero. If the primordial fluctuations are confirmed to be deviated from Gaussian ones in the future, which may well be probed with more precise observations such as Planck [6], fluctuations from the “slow-rolling” inflaton would be excluded at least as a dominant mechanism of the generation of density fluctuations. However, many other mechanisms have also been discussed in the literature and quite a few of them can generate large non-Gaussianity.

Now we have plenty of models generating large non-Gaussian primordial fluctuations. Thus the question we should ask next is “how can we differentiate these models?” In this paper, we discuss this issue by using bispectrum and trispectrum of the curvature perturbation. Although, as mentioned above, we can divide models into some categories depending on the shape of the three point functions (local, equilateral and orthogonal types)^{#1}, the shape is not enough to differentiate models since there remain many models for each type of the shape. Furthermore, f_{NL} predicted in those models can fall onto almost the same value by tuning some model parameters. Thus, obviously, the determination of f_{NL} is not enough to pin down the models of large non-Gaussianity even if f_{NL} is found to be large in the future. The purpose of this paper is to pursue the strategy of how one can differentiate models of large non-Gaussianity. To this end, we consider higher order statistics such as the trispectrum in addition to the bispectrum^{#2}. The size of the

^{#1} There are various inflationary models that can produce large $f_{\text{NL}}^{\text{equil}}$, where scalar fields have some non-canonical kinetic terms [7–13]. The orthogonal-type $f_{\text{NL}}^{\text{orthog}}$ approximately arises from a linear combination of higher-derivative scalar-field interaction terms [5, 12].

^{#2} Another possible direction may be the one using the scale dependence of f_{NL} [14–19].

trispectrum can be parametrized by other non-linearity parameters τ_{NL} and g_{NL} ^{#3} and the importance of the trispectrum has been emphasized in some literature [20–25]. However, here we give a systematic study of the bispectrum and the trispectrum of models with large non-Gaussianity and make some classifications by using the “consistency relations” between the non-linearity parameters f_{NL} , τ_{NL} and g_{NL} .

Among three types mentioned above (local, equilateral and orthogonal types), we focus on local-type models in this paper. As will be shown, by using the “consistency relations,” we may be able to discriminate models of large non-Gaussianity.

The organization of this paper is as follows. In the next section, we summarize the formalism for the discussion of local-type non-Gaussianity of primordial fluctuations. Then in Section 3, we first make a classification of models by using some relation between the non-linearity parameters f_{NL} , τ_{NL} and g_{NL} in a systematic manner. Some example models will also be discussed. The final section is devoted to summary and conclusion of this paper.

2 Formalism

First we summarize the formalism to discuss local-type non-Gaussianity of primordial fluctuations, which is expected to be generated from super-horizon dynamics of curvature fluctuations. For this purpose, we adopt the δN formalism [26–29]. In this formalism, the super-horizon scale curvature perturbation on the uniform energy density hypersurface ζ at some time $t = t_f$ is given by the perturbation in the number of e -folding measured from the initial time t_* to the time t_f . Here we take the initial time t_* to be the time shortly after the horizon crossing and the initial hypersurface to be a flat one. Then the curvature perturbation is given, up to the third order, as

$$\zeta(t_f) \simeq N_a \delta\varphi_*^a + \frac{1}{2} N_{ab} \delta\varphi_*^a \delta\varphi_*^b + \frac{1}{6} N_{abc} \delta\varphi_*^a \delta\varphi_*^b \delta\varphi_*^c, \quad (1)$$

where a subscript a, b and c labels a scalar field, which is assumed to be Gaussian fluctuations $\delta\varphi^a$ at $t = t_*$ in the following discussion, and $N_a = dN/d\varphi_*^a$ and so on. The summation is implied for repeated indices.

The power spectrum P_ζ , bispectrum B_ζ and trispectrum T_ζ of the curvature perturbation are given by

$$\langle \zeta_{\vec{k}_1} \zeta_{\vec{k}_2} \rangle = (2\pi)^3 P_\zeta(k_1) \delta(\vec{k}_1 + \vec{k}_2), \quad (2)$$

$$\langle \zeta_{\vec{k}_1} \zeta_{\vec{k}_2} \zeta_{\vec{k}_3} \rangle = (2\pi)^3 B_\zeta(k_1, k_2, k_3) \delta(\vec{k}_1 + \vec{k}_2 + \vec{k}_3), \quad (3)$$

^{#3} Current observational limits for $\tau_{\text{NL}}^{\text{local}}$ and $g_{\text{NL}}^{\text{local}}$ are given by $-0.6 \times 10^4 < \tau_{\text{NL}}^{\text{local}} < 3.3 \times 10^4$ (95% C.L.) and $-7.4 \times 10^5 < g_{\text{NL}}^{\text{local}} < 8.2 \times 10^5$ (95% C.L.) from cosmic microwave background observations [23]. The authors of [24] also obtained $-3.5 \times 10^5 < g_{\text{NL}}^{\text{local}} < 8.2 \times 10^5$ (95% C.L.) from large scale structure observations by assuming that $f_{\text{NL}}^{\text{local}} = 0$ and $\tau_{\text{NL}}^{\text{local}} = 0$.

$$\langle \zeta_{\vec{k}_1} \zeta_{\vec{k}_2} \zeta_{\vec{k}_3} \zeta_{\vec{k}_4} \rangle = (2\pi)^3 T_\zeta(k_1, k_2, k_3, k_4) \delta(\vec{k}_1 + \vec{k}_2 + \vec{k}_3 + \vec{k}_4), \quad (4)$$

where B_ζ and T_ζ can be written as

$$B_\zeta(k_1, k_2, k_3) = \frac{6}{5} f_{\text{NL}}^{\text{local}} (P_\zeta(k_1)P_\zeta(k_2) + P_\zeta(k_2)P_\zeta(k_3) + P_\zeta(k_3)P_\zeta(k_1)), \quad (5)$$

$$T_\zeta(k_1, k_2, k_3, k_4) = \tau_{\text{NL}}^{\text{local}} (P_\zeta(k_{13})P_\zeta(k_3)P_\zeta(k_4) + 11 \text{ perms.}) \\ + \frac{54}{25} g_{\text{NL}}^{\text{local}} (P_\zeta(k_2)P_\zeta(k_3)P_\zeta(k_4) + 3 \text{ perms.}), \quad (6)$$

with $k_{13} = |\vec{k}_1 + \vec{k}_3|$. Here $f_{\text{NL}}^{\text{local}}$, $\tau_{\text{NL}}^{\text{local}}$ and $g_{\text{NL}}^{\text{local}}$ are non-linearity parameters of the local type. From Eq. (1), the power spectrum of the curvature perturbation is given by

$$P_\zeta(k) = N_a N^a P_\delta(k), \quad (7)$$

where $P_\delta(k)$ is the power spectrum for fluctuations of a scalar field:

$$\langle \delta\varphi_{*\vec{k}_1}^a \delta\varphi_{*\vec{k}_2}^b \rangle \equiv (2\pi)^3 \delta^{ab} \delta(\vec{k}_1 + \vec{k}_2) P_\delta(k_1) = (2\pi)^3 \delta^{ab} \delta(\vec{k}_1 + \vec{k}_2) \frac{2\pi^2}{k_1^3} \mathcal{P}_\delta(k_1), \quad (8)$$

with $\mathcal{P}_\delta(k) = (H_*/2\pi)^2$ and H_* being the Hubble parameter at $t = t_*$.

Since $\delta\varphi_a$ are Gaussian fields, the leading order contributions to the bispectrum are given by four-point functions of $\delta\varphi_a$. The next leading order contributions are given by six-point functions. As is explained in detail in [30, 31], we can systematically classify those contributions by assigning a diagram to each contribution. In terms of the diagram approach, the four-point function of $\delta\varphi_a$ is represented by the tree diagram and the six-point function by the diagram containing a single loop. This can be easily generalized to higher order correlation functions of ζ (and also to the power spectrum). The leading order contributions to the n -point function of ζ are given by $2(n-1)$ -point function of $\delta\varphi_a$, which are represented by the tree diagrams. The next leading order contributions are given by $2n$ -point function, which are represented by the one-loop diagrams.

In many cases, the contributions from the loop diagrams are tiny and can be safely neglected. Therefore, we first drop the loop corrections and consider only tree contributions. We will discuss a case in which effects from loop corrections cannot be neglected in a later section and an appendix.

By calculating the bispectrum and the trispectrum at the tree level, we obtain the non-linearity parameters f_{NL} , τ_{NL} and g_{NL} as [20, 32, 33]

$$\frac{6}{5} f_{\text{NL}}^{\text{local}} = \frac{N_a N_b N^{ab}}{(N_c N^c)^2}, \quad (9)$$

$$\tau_{\text{NL}}^{\text{local}} = \frac{N_a N_b N^{ac} N_c^b}{(N_d N^d)^3}, \quad (10)$$

$$\frac{54}{25}g_{\text{NL}}^{\text{local}} = \frac{N_{abc}N^aN^bN^c}{(N_dN^d)^3}. \quad (11)$$

In the following, since we concentrate on non-Gaussianity of the local-type models, we omit a superscript “local” unless some confusions arise.

3 Models of local-type non-Gaussianity

3.1 A classification of local type

Even if we limit ourselves to models generating large local-type non-Gaussianity, there still remain many possibilities. To discuss how we discriminate those models, here we classify the local-type models into some categories. For this purpose, we first give a particular attention to the relation between f_{NL} and τ_{NL} . Notice that, when a single scalar field σ is only responsible for density fluctuations in the Universe, δN formalism indicates:

$$\frac{6}{5}f_{\text{NL}} = \frac{N_{\sigma\sigma}}{N_\sigma^2}, \quad \tau_{\text{NL}} = \frac{N_{\sigma\sigma}^2}{N_\sigma^4}, \quad \frac{54}{25}g_{\text{NL}} = \frac{N_{\sigma\sigma\sigma}}{N_\sigma^3}. \quad (12)$$

From these equations, we can easily find the following relation between f_{NL} and τ_{NL} :

$$\tau_{\text{NL}} = \left(\frac{6}{5}f_{\text{NL}}\right)^2. \quad (13)$$

Since some simple models such as the pure curvaton and the pure modulated reheating scenarios fall onto this type, we use the above relation to make a classification. We call models in which Eq. (13) is satisfied as “single-source model.” Notice that τ_{NL} is determined once f_{NL} is given in models of this class.

The next category is for models which do not have a universal relation between f_{NL} and τ_{NL} , although there exists an inequality as given below. This is a general situation where there are multiple sources of density fluctuations. Thus we call this category “multi-source model.” An example of this type includes mixed fluctuation models, where fluctuations from both of the inflaton and another scalar field such as the curvaton can be responsible for density fluctuations. Since the inflaton gives almost Gaussian fluctuations, non-Gaussianity mostly originates from fluctuations of the other source in such a case.

The third category would be for models where there is some universal relation between f_{NL} and τ_{NL} . In fact, this definition includes models of the first class discussed above as a special case. However, the “single source model” is somewhat a very special type, and thus we treat them as a separate category. One of examples of this third category is so-called “ungaussiton” model [34–36], in which the relation $\tau_{\text{NL}} \propto f_{\text{NL}}^{4/3}$ holds. In this model, the second order perturbation of the “ungaussiton” field dominates the linear order one. Since the dominance of the second order perturbations indicates that the fluctuations are completely non-Gaussian, we need another source which gives a Gaussian perturbation at

linear order. Thus this model would require multi-sources of fluctuations in this sense. Hence we call models in this third category “constrained multi-source model.”

Here it is worth noting that the following inequality holds in the $f_{\text{NL}}\text{-}\tau_{\text{NL}}$ plane:

$$\tau_{\text{NL}} \geq \left(\frac{6}{5}f_{\text{NL}}\right)^2, \quad (14)$$

which can be obtained by using Cauchy-Schwarz inequality and was first found by two of the present authors (T.S. and M.Y.) [37]. The derivation of this inequality (14) in [37] was based on the expressions for f_{NL} and τ_{NL} given in Eqs. (9) and (10), which are valid at the tree level. In this paper, we further show that, even when some loop corrections are dominant in f_{NL} and τ_{NL} , the inequality (14) holds as far as loop contributions are subdominant in the power spectrum, which is required from current observations. Since all models generating large local-type non-Gaussianity known to date satisfy the above assumptions, the inequality (14) is very important to test the local-type models. Thus we call the inequality (14) “local-type inequality” in the following. We discuss this issue in detail again in Section 3.4. Also notice that single-source models correspond to the boundary of this local-type inequality.

In the following sections, we discuss various models for each category. We start with “single-source model,” then discuss “multi-source model” and “constrained multi-source model” afterwards. In Fig. 1, some models of these categories are shown in the “ $f_{\text{NL}}\text{-}\tau_{\text{NL}}$ ” diagram, from which we can have some idea of to what extent models of each category can give different predictions on f_{NL} and τ_{NL} . We also give a summary of the categories and their examples in Table 1.

Now we have categorized models of local-type into three classes by using the key quantity $\tau_{\text{NL}}/(6f_{\text{NL}}/5)^2$. However, since each category still includes some (or many) possible models, we may need another quantity to discriminate them. For this purpose, we can further utilize the relation between f_{NL} and g_{NL} . Although the $f_{\text{NL}}\text{-}g_{\text{NL}}$ relation can change depending on the model parameters, we can roughly divide models into three types further by looking at their relative size. As we will argue in the following sections, the relation $|g_{\text{NL}}| \sim |f_{\text{NL}}|$ holds in some models, then we call such models “linear g_{NL} type.” In other models, g_{NL} could be suppressed compared to f_{NL} , i.e. $g_{\text{NL}} \sim (\text{suppression factor}) \times f_{\text{NL}}$, which we denote this type of models as “suppressed g_{NL} type.” The other type is “enhanced g_{NL} type” in which the relation between f_{NL} and g_{NL} can be given as $g_{\text{NL}} \sim f_{\text{NL}}^n$ with $n > 1$ (but in most models discussed in this paper, $n = 2$). By using the $f_{\text{NL}}\text{-}\tau_{\text{NL}}$ and $f_{\text{NL}}\text{-}g_{\text{NL}}$ relations, we may be able to discriminate models well. In Table 1, the $f_{\text{NL}}\text{-}g_{\text{NL}}$ relations for example models are shown and depicted in Fig. 2.

3.2 Single-source model

If future observations confirm the relation $\tau_{\text{NL}} = (6f_{\text{NL}}/5)^2$, models of large non-Gaussianity we should pursue would be the ones in this category. Models categorized in this class in-

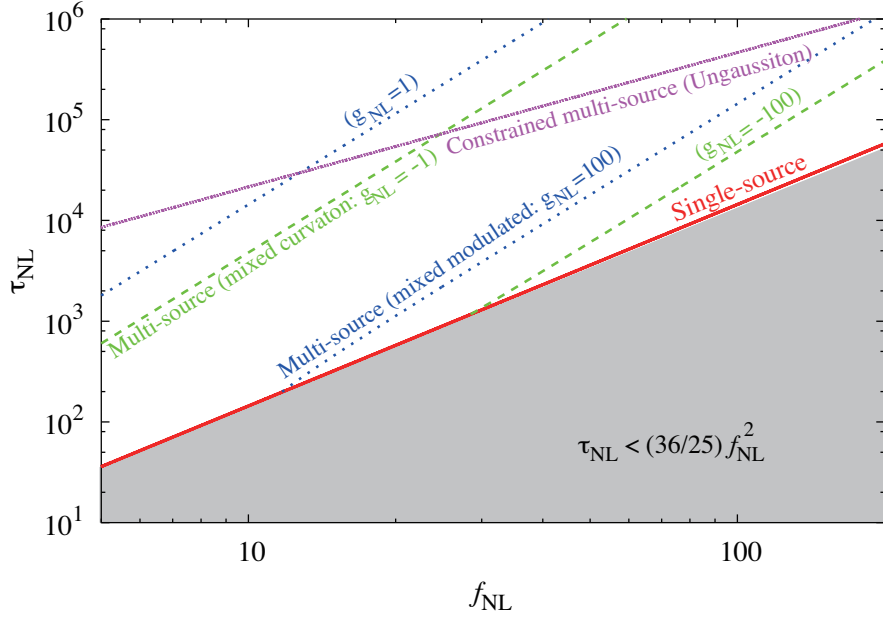


Figure 1: $f_{\text{NL}}-\tau_{\text{NL}}$ diagram. The relation between f_{NL} and τ_{NL} is shown for three categories: single-source, multi-source and constrained multi-source models. For multi-source and constrained multi-source models, the cases for some representative explicit models (mixed curvaton and inflaton, mixed modulated reheating and inflaton, and ungaussiton models) are plotted. All the three categories satisfy the inequality $\tau_{\text{NL}} \gtrsim (6f_{\text{NL}}/5)^2$ as far as loop contributions are subdominant in the power spectrum. The region with $\tau_{\text{NL}} < (6f_{\text{NL}}/5)^2$ is shaded with gray.

Category	$f_{\text{NL}}\text{-}\tau_{\text{NL}}$ relation	Examples and $f_{\text{NL}}\text{-}g_{\text{NL}}$ relation
Single-source	$\tau_{\text{NL}} = (6f_{\text{NL}}/5)^2$	(pure) curvaton (w/o self-interaction) [$g_{\text{NL}} = -(10/3)f_{\text{NL}} - (575/108)$] ^(a)
		(pure) curvaton (w/ self-interaction) [$g_{\text{NL}} = A_{\text{NQ}}f_{\text{NL}}^2 + B_{\text{NQ}}f_{\text{NL}} + C_{\text{NQ}}$] ^(b)
		(pure) modulated reheating [$g_{\text{NL}} = 10f_{\text{NL}} - (50/3)$] ^(c)
		modulated-curvaton scenario [$g_{\text{NL}} = 3r_{\text{dec}}^{1/2}f_{\text{NL}}^{3/2}$] ^(d)
		Inhomogeneous end of hybrid inflation [$g_{\text{NL}} = (10/3)\eta_{\text{cr}}f_{\text{NL}}$]
		Inhomogeneous end of thermal inflation [$g_{\text{NL}} = -(10/3)f_{\text{NL}} - (50/27)$] ^(e)
		Modulated trapping [$g_{\text{NL}} = (2/9)f_{\text{NL}}^2$] ^(f)
		Multi-source
mixed modulated and inflaton [$g_{\text{NL}} = 10(R/(1+R))f_{\text{NL}} - (50/3)(R/(1+R))^3$] ^(h)		
mixed modulated trapping and inflaton [$g_{\text{NL}} = (2/9)((1+R)/R)f_{\text{NL}}^2 = (25/162)\tau_{\text{NL}}$] ⁽ⁱ⁾		
multi-curvaton [$g_{\text{NL}} = C_{\text{mc}}f_{\text{NL}}, g_{\text{NL}} = (4/15)f_{\text{NL}}^2$] ^(j)		
Multi-brid inflation (quadratic potential) [$g_{\text{NL}} = -(10/3)\eta f_{\text{NL}}, g_{\text{NL}} = 2f_{\text{NL}}^2$] ^(k)		
Multi-brid inflation (linear potential) [$g_{\text{NL}} = 2f_{\text{NL}}^2$] ^(l)		
Constrained multi-source	$\tau_{\text{NL}} = Cf_{\text{NL}}^n$	

^(a)For the case with $r_{\text{dec}} \ll 1$.

^(b) $A_{\text{NQ}}, B_{\text{NQ}}$ and C_{NQ} are given in Eqs. (23)-(25) and this expression is for $r_{\text{dec}} \ll 1$.

^(c) $\Gamma_{\sigma\sigma\sigma} = 0$ is assumed.

^(d)This relation holds in the Region 2. For other cases, see text.

^(e) $g''' = 0$ is assumed.

^(f) $\lambda = \sigma/M$ and $m = g\sigma$ are assumed.

^(g)A quadratic potential and $r_{\text{dec}} \ll 1$ are assumed for the curvaton sector. $R \equiv P_{\zeta}^{(\sigma)}/P_{\zeta}^{(\phi)}$ is the ratio of the power spectra. This relation can also be written as $g_{\text{NL}} \simeq -(24/5)(f_{\text{NL}}^3/\tau_{\text{NL}}) - (9936/625)(f_{\text{NL}}^6/\tau_{\text{NL}}^3)$.

^(h) $\Gamma_{\sigma\sigma\sigma} = 0$ is assumed for the modulated reheating sector. This relation can also be written as $g_{\text{NL}} \simeq (72/5)(f_{\text{NL}}^3/\tau_{\text{NL}}) - (31104/625)(f_{\text{NL}}^6/\tau_{\text{NL}}^3)$.

⁽ⁱ⁾ $\lambda = \sigma/M$ and $m = g\sigma$ are assumed for the modulator sector.

^(j)The former and the latter relations are for the cases where both curvatons are subdominant and dominant at their decay, respectively. C_{mc} is $\mathcal{O}(1)$ coefficient and always negative.

^(k)The former and the latter relations are for the equal mass and the large mass ratio cases, respectively.

^(l)For the equal mass case with $g_1 = g_2$.

Table 1: Summary of the categories and their examples.

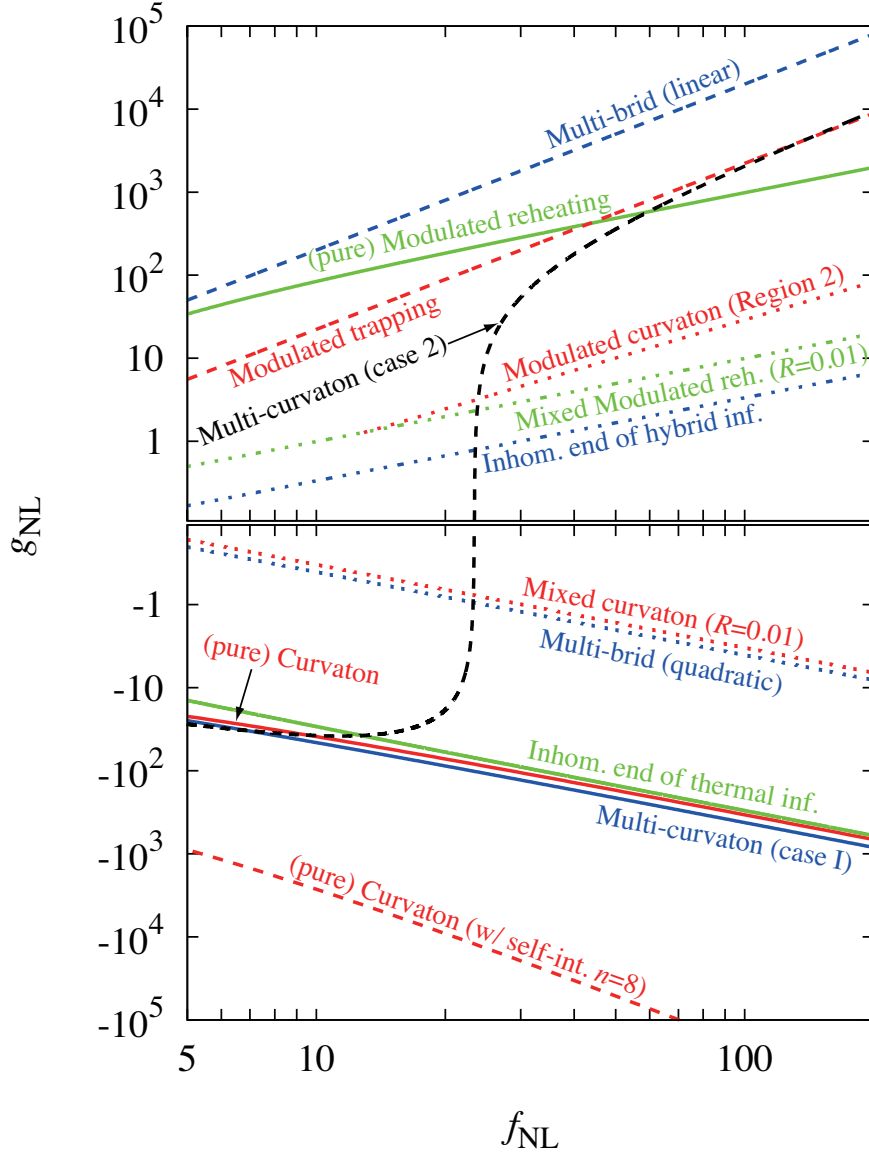


Figure 2: $f_{\text{NL}}-g_{\text{NL}}$ diagram. The relation between g_{NL} and f_{NL} is plotted for models given in Table 1.

clude the pure curvaton and the pure modulated reheating scenarios, and so on. In the following, we look at some of models in this class more closely.

3.2.1 Pure curvaton model

To make a prediction on the non-linearity parameters in the pure curvaton model [38–40]^{#4}, first we need to specify the curvaton potential. Although in most study of the curvaton [41–51], a quadratic potential is adopted, it is also possible to have a self-interaction term. Thus we assume the following potential [21, 22, 52–55]^{#5}:

$$V(\sigma) = \frac{1}{2}m_\sigma^2\sigma^2 + \lambda m_\sigma^4 \left(\frac{\sigma}{m_\sigma}\right)^n, \quad (15)$$

where m_σ is the mass of the curvaton, λ is the coupling and n is the power for a self-interaction term. In the following discussion, we assume that the self-interaction term is subdominant compared to the quadratic one. In general, it is possible that a self-interaction term dominates first, and then the quadratic term becomes dominant at later time. However, in such a case, rigorous numerical calculations will be needed. Thus we restrict ourselves to the “nearly” quadratic potential case when we include a self-interaction term^{#6}.

In fact, to make a concrete prediction on non-Gaussianity in this model, we need to specify the decay rate Γ_σ , the mass m_σ and the initial value for the curvaton σ_* . However, as far as the non-linearity parameters are concerned, the information on these quantities is encoded into the parameter r_{dec} , which corresponds to the ratio of the energy density of the curvaton to the total one at the decay^{#7}. The definition of r_{dec} and its approximate expression using Γ_σ , m_σ and σ_* are given by

$$r_{\text{dec}} \equiv \frac{3\rho_\sigma}{4\rho_{\text{rad}} + 3\rho_\sigma} \Big|_{\text{dec}} \sim \frac{\sigma_*^2}{M_{\text{pl}}^2 \sqrt{\Gamma_\sigma/m_\sigma}}, \quad (16)$$

where $M_{\text{pl}} \simeq 2.4 \times 10^{18}$ GeV is the reduced Planck mass. Thus in the following, we do not specify explicit values for Γ_σ , m_σ and σ_* .

In the curvaton model, adopting the sudden-decay approximation and assuming radiation-dominated background from the period of the start of its oscillation to its decay^{#8}, the

^{#4} We later also consider a mixed model where density fluctuations originate both from the curvaton and the inflaton. To be definite, we call the model where only the curvaton generates density fluctuations the pure curvaton model.

^{#5} For the analyses of other non-quadratic type potentials, see [56–59].

^{#6} For a general case, see [54, 55].

^{#7} When the initial amplitude for the curvaton is large enough, the curvaton can drive the second inflation after the standard inflation. In this case, this statement does not hold true. However, the value of f_{NL} is $\mathcal{O}(1)$ in such a situation, hence we do not discuss such a case here.

^{#8} In Ref. [22], it has been shown that the background equation of state also affects the curvature perturbation generated from the curvaton, in particular, its non-Gaussianity.

curvature perturbation can be given by^{#9},

$$\begin{aligned}\zeta_{\text{cur}} = & \frac{2}{3}r_{\text{dec}}\frac{\sigma'_{\text{osc}}}{\sigma_{\text{osc}}}\delta\sigma_* + \frac{1}{9}\left[3r_{\text{dec}}\left(1 + \frac{\sigma_{\text{osc}}\sigma''_{\text{osc}}}{\sigma'^2_{\text{osc}}}\right) - 4r_{\text{dec}}^2 - 2r_{\text{dec}}^3\right]\left(\frac{\sigma'_{\text{osc}}}{\sigma_{\text{osc}}}\right)^2(\delta\sigma_*)^2 \\ & + \frac{4}{81}\left[\frac{9r_{\text{dec}}}{4}\left(\frac{\sigma_{\text{osc}}^2\sigma'''_{\text{osc}}}{\sigma'^3_{\text{osc}}} + 3\frac{\sigma_{\text{osc}}\sigma''_{\text{osc}}}{\sigma'^2_{\text{osc}}}\right) - 9r_{\text{dec}}^2\left(1 + \frac{\sigma_{\text{osc}}\sigma''_{\text{osc}}}{\sigma'^2_{\text{osc}}}\right)\right. \\ & \left. + \frac{r_{\text{dec}}^3}{2}\left(1 - 9\frac{\sigma_{\text{osc}}\sigma''_{\text{osc}}}{\sigma'^2_{\text{osc}}}\right) + 10r_{\text{dec}}^4 + 3r_{\text{dec}}^5\right]\left(\frac{\sigma'_{\text{osc}}}{\sigma_{\text{osc}}}\right)^3(\delta\sigma_*)^3,\end{aligned}\quad (17)$$

where σ_{osc} denotes the value of the curvaton field at the time of the start of oscillation and the prime indicates a derivative with respect to σ_* , namely $\sigma'_{\text{osc}} = d\sigma_{\text{osc}}/d\sigma_*$ and so on. σ_{osc} and its derivatives represent the non-linear evolution of the curvaton after the horizon exit.

From the expression of the curvature perturbation given above, the non-linearity parameters f_{NL} and g_{NL} can be evaluated as

$$\frac{6}{5}f_{\text{NL}} = \frac{3}{2r_{\text{dec}}}\left(1 + \frac{\sigma_{\text{osc}}\sigma''_{\text{osc}}}{\sigma'^2_{\text{osc}}}\right) - 2 - r_{\text{dec}},\quad (18)$$

$$\begin{aligned}\frac{54}{25}g_{\text{NL}} = & \frac{9}{4r_{\text{dec}}^2}\left(\frac{\sigma_{\text{osc}}^2\sigma'''_{\text{osc}}}{\sigma'^3_{\text{osc}}} + 3\frac{\sigma_{\text{osc}}\sigma''_{\text{osc}}}{\sigma'^2_{\text{osc}}}\right) - \frac{9}{r_{\text{dec}}}\left(1 + \frac{\sigma_{\text{osc}}\sigma''_{\text{osc}}}{\sigma'^2_{\text{osc}}}\right) \\ & + \frac{1}{2}\left(1 - 9\frac{\sigma_{\text{osc}}\sigma''_{\text{osc}}}{\sigma'^2_{\text{osc}}}\right) + 10r_{\text{dec}} + 3r_{\text{dec}}^2.\end{aligned}\quad (19)$$

When the potential has a pure quadratic form, we have

$$\frac{\sigma'_{\text{osc}}}{\sigma_{\text{osc}}} = \frac{1}{\sigma_*}, \quad \sigma''_{\text{osc}} = 0, \quad \sigma'''_{\text{osc}} = 0.\quad (20)$$

Thus, in this case with $r_{\text{dec}} \ll 1$, we can find the following relation between f_{NL} and g_{NL} [21]:

$$g_{\text{NL}} = -\frac{10}{3}f_{\text{NL}} - \frac{575}{108} + O(r_{\text{dec}}).\quad (21)$$

On the other hand, when we cannot neglect the contribution from a self-interaction term, the non-linear evolution of the curvaton field after the horizon exit changes the relation between f_{NL} and g_{NL} , for $r_{\text{dec}} \ll 1$, as

$$g_{\text{NL}} \simeq A_{\text{NQ}}f_{\text{NL}}^2 + B_{\text{NQ}}f_{\text{NL}} + C_{\text{NQ}},\quad (22)$$

^{#9} In the curvaton model, isocurvature fluctuations can also be generated. However, we do not consider such a case here. For the study of isocurvature fluctuations in the model, see [41, 43, 49, 50].

where the coefficients are given by

$$A_{\text{NQ}} = \frac{2}{3} \left(\frac{\sigma_{\text{osc}}^2 \sigma_{\text{osc}}'''}{\sigma_{\text{osc}}'^3} + 3 \frac{\sigma_{\text{osc}} \sigma_{\text{osc}}''}{\sigma_{\text{osc}}'^2} \right) \left(1 + \frac{\sigma_{\text{osc}} \sigma_{\text{osc}}''}{\sigma_{\text{osc}}'^2} \right)^{-2}, \quad (23)$$

$$B_{\text{NQ}} = -\frac{10}{3} \left(1 - 5 \frac{\sigma_{\text{osc}} \sigma_{\text{osc}}''}{\sigma_{\text{osc}}'^2} - 2 \frac{\sigma_{\text{osc}}^2 \sigma_{\text{osc}}'''}{\sigma_{\text{osc}}'^3} \right) \left(1 + \frac{\sigma_{\text{osc}} \sigma_{\text{osc}}''}{\sigma_{\text{osc}}'^2} \right)^{-2}, \quad (24)$$

$$C_{\text{NQ}} = -\frac{50}{27} \left(3 - \frac{\sigma_{\text{osc}}^2 \sigma_{\text{osc}}'''}{\sigma_{\text{osc}}'^3} \right) \left(1 + \frac{\sigma_{\text{osc}} \sigma_{\text{osc}}''}{\sigma_{\text{osc}}'^2} \right)^{-2} - \frac{25}{108} \left(1 - 9 \frac{\sigma_{\text{osc}} \sigma_{\text{osc}}''}{\sigma_{\text{osc}}'^2} \right). \quad (25)$$

These coefficients depend on the power of a self-interaction term and its relative size to the mass term, which can be calculated numerically [21, 22]. There is a clear distinction in the relation between f_{NL} and g_{NL} depending on the contribution from a self-interaction term. From the viewpoint of the $f_{\text{NL}}-g_{\text{NL}}$ relation, the model with and without a self-interaction term can be regarded as “enhanced g_{NL} ” and “linear g_{NL} ” types, respectively. Thus once f_{NL} and g_{NL} are determined by observations with some accuracy, it may be even possible to probe the form of the potential [21, 22] as well. In Fig. 2, we show the case with $V(\sigma) = (1/2)m_\sigma^2\sigma^2$ (pure quadratic potential) and $V(\sigma) = (1/2)m_\sigma^2\sigma^2 + \lambda\sigma^8/m_\sigma^4$ (with a self-interaction term). As seen from the figure, we can easily see the difference in the $f_{\text{NL}}-g_{\text{NL}}$ relation between the cases with and without a self-interaction.

3.2.2 Pure modulated reheating model

In the modulated reheating scenario [60, 61], the decay rate of the inflaton Γ fluctuates in space^{#10} because of its dependence on a modulus field σ , which acquires quantum fluctuations during inflation, and large non-Gaussianity can be generated [37, 64, 65]. In this scenario, the level of non-Gaussianity is highly dependent on the assumption of the decay rate. Thus we need to specify the dependence of Γ on σ to give a concrete prediction. Furthermore, in fact, we also need to specify the form of the inflaton potential and the interaction for the decay. But we first give a general expression for the curvature perturbations ζ in this scenario, taking into account the above mentioned uncertainties. ζ in this scenario can be given by [37, 65]

$$\begin{aligned} \zeta_{\text{mod}} = & A(x) \frac{\Gamma_\sigma}{\Gamma} \delta\sigma_* + \frac{1}{2} \left(A(x) \frac{\Gamma_{\sigma\sigma}}{\Gamma} + B(x) \frac{\Gamma_\sigma^2}{\Gamma^2} \right) \delta\sigma_*^2 \\ & + \frac{1}{6} \left(A(x) \frac{\Gamma_{\sigma\sigma\sigma}}{\Gamma} + 3B(x) \frac{\Gamma_\sigma \Gamma_{\sigma\sigma}}{\Gamma^2} + C(x) \frac{\Gamma_\sigma^3}{\Gamma^3} \right) \delta\sigma_*^3. \end{aligned} \quad (26)$$

Here $\Gamma_\sigma = d\Gamma/d\sigma$, $\Gamma_{\sigma\sigma} = d^2\Gamma/d\sigma^2$ and so on. $A(x), B(x)$ and $C(x)$ are functions of $x \equiv \Gamma/H_c$ with H_c being the Hubble parameter after several oscillations of the inflaton field. Since the number of e -folds after inflation only depends on the quantity $x = \Gamma/H_c$,

^{#10} Thus, the reheating temperature after inflation also fluctuates in space in this model, which may generate significant isocurvature fluctuations and give severe constraints in some settings [62, 63].

which can be confirmed by a dimensional analysis of the background evolution equations, the coefficients such as A, B and C depend only on x . From the above expression, we obtain the non-linearity parameters for this model as

$$\frac{6}{5}f_{\text{NL}} = \frac{B(x)}{A(x)^2} + \frac{1}{A(x)} \frac{\Gamma\Gamma_{\sigma\sigma}}{\Gamma_{\sigma}^2}, \quad (27)$$

$$\frac{54}{25}g_{\text{NL}} = \frac{C(x)}{A(x)} + \frac{3B(x)}{A(x)} \frac{\Gamma\Gamma_{\sigma\sigma}}{\Gamma_{\sigma}^2} + \frac{\Gamma^2\Gamma_{\sigma\sigma\sigma}}{\Gamma_{\sigma}^3}. \quad (28)$$

To make some explicit predictions for these parameters, we need to know the values of $A(x), B(x)$ and $C(x)$ for a given x , which requires us to specify the interaction responsible for the decay and the potential under which the inflaton oscillates. Furthermore, some numerical analysis may be needed. However, some approximations are available which can give quite accurate results, in particular, for the case of $x \ll 1$ [37, 65].

To evaluate to what extent the non-linearity parameters can be large, here we assume that the potential of the inflaton is $V \propto \phi^2$ and the inflaton decays through $\mathcal{L}_{\text{int}} = -y\phi\bar{\psi}\psi$. Then the coefficients are evaluated as $A = -1/6, B = 1/6$ and $C = -1/3$ (for other types of potentials and interactions, see [65]). In this case, the non-linearity parameters are given by

$$\frac{6}{5}f_{\text{NL}} = 6 - 6 \frac{\Gamma\Gamma_{\sigma\sigma}}{\Gamma_{\sigma}^2}, \quad (29)$$

$$\frac{54}{25}g_{\text{NL}} = 36 \left(2 - 3 \frac{\Gamma\Gamma_{\sigma\sigma}}{\Gamma_{\sigma}^2} + \frac{\Gamma^2\Gamma_{\sigma\sigma\sigma}}{\Gamma_{\sigma}^3} \right). \quad (30)$$

To get some numbers for f_{NL} and g_{NL} , we further need to assume an explicit form for Γ . Here we take the following form:

$$\Gamma = \Gamma_0 \left(1 + \alpha \frac{\sigma}{M} + \beta \frac{\sigma^2}{M^2} \right), \quad (31)$$

where α and β are some coefficients, M is some scale and we assume $|\sigma| \ll M$ to justify the expansion in terms of σ/M . With this form of Γ , the non-linearity parameters are given by^{#11}

$$\frac{6}{5}f_{\text{NL}} \simeq 6 \left(1 - \frac{2\beta}{\alpha^2} \right), \quad \frac{54}{25}g_{\text{NL}} \simeq 36 \left(2 - \frac{6\beta}{\alpha^2} \right). \quad (32)$$

^{#11} Although here we assume that the curvature perturbation is totally generated from this mechanism, in general, fluctuations from the inflaton would also contribute, in particular to the power spectrum. In order that the contribution from the inflaton is negligible at linear order, $M/M_{\text{pl}} \lesssim 0.2\alpha\sqrt{\epsilon}$ should be satisfied with ϵ being the slow-roll parameter for the inflaton, which is obtained by requiring that $\zeta_{\text{mod}} > \zeta_{\text{inf}}$ with ζ_{inf} being the curvature perturbation generated from the inflaton. Another requirement comes from the constraint on the tensor-to-scalar ratio $r \lesssim 0.1$, from which we obtain $M/M_{\text{pl}} < 0.01\alpha$. These relations can be satisfied by taking the scale M appropriately.

Thus, for example, if we take $\alpha = 1/2$ and $\beta = -1$, then one can have $f_{\text{NL}} \sim 45$ and $g_{\text{NL}} \sim 430$.

In fact, we can find a relation between f_{NL} and g_{NL} independent of the form of Γ as far as the third derivative $\Gamma_{\sigma\sigma\sigma}$ is negligible. After some algebra, one can derive the relation between f_{NL} and g_{NL} as [37]

$$g_{\text{NL}} = 10f_{\text{NL}} - \frac{50}{3}. \quad (33)$$

Notice that the signs of f_{NL} and g_{NL} are the same for large values of f_{NL} , which is different from the one in the curvaton model. Thus once the signs of f_{NL} and g_{NL} are determined from observations, we can discriminate between the curvaton and the modulated reheating models (see also Fig. 2). In both models, the simple cases predict that g_{NL} is of the same order of f_{NL} as given in Eqs. (21) and (33), which is what we call “linear g_{NL} ” type. Thus, as far as the modulated reheating scenario is concerned, larger g_{NL} may suggest a non-negligible third derivative of the decay rate $\Gamma_{\sigma\sigma\sigma}$.

3.2.3 Modulated-curvaton model

In the modulated reheating scenario, density fluctuations originate from those of a modulus field. Such a field may also play a role of the curvaton at later time after it “modulates” the reheating. In this case, the fluctuations become a mixture of those generated from the modulated reheating and the curvaton mechanism although the source of fluctuations is a single field σ . In fact, this kind of possibility has not been well explored in the literature. Therefore, we here discuss this scenario in some detail.

The curvature perturbation ζ in this scenario can be written as the sum of the contributions from the modulated reheating and the curvaton mechanism:

$$\begin{aligned} \zeta &= \zeta_{\text{cur}} + \zeta_{\text{mod}} \\ &= \left(\frac{2r_{\text{dec}}}{3\sigma_*} - \frac{\Gamma_{\sigma}}{6\Gamma} \right) \delta\sigma_* + \left[\frac{1}{9\sigma_*^2} (3r_{\text{dec}} - 4r_{\text{dec}}^2 - 2r_{\text{dec}}^3) - \frac{1}{12} \left(\frac{\Gamma_{\sigma\sigma}}{\Gamma} - \frac{\Gamma_{\sigma}^2}{\Gamma^2} \right) \right] \delta\sigma_*^2 \\ &\quad + \left[\frac{4}{81\sigma_*^3} \left(-9r_{\text{dec}}^2 + \frac{r_{\text{dec}}^3}{2} + 10r_{\text{dec}}^4 + 3r_{\text{dec}}^5 \right) - \frac{1}{36} \left(\frac{2\Gamma_{\sigma}^3}{\Gamma^3} - \frac{3\Gamma_{\sigma}\Gamma_{\sigma\sigma}}{\Gamma^2} + \frac{\Gamma_{\sigma\sigma\sigma}}{\Gamma} \right) \right] \delta\sigma_*^3, \end{aligned} \quad (34)$$

where ζ_{cur} and ζ_{mod} are the curvature perturbations generated from the curvaton mechanism and the modulated reheating, and are given in Eqs. (17) and (26). Here we assume that the curvaton potential is quadratic and the potential for the inflaton is $V \propto \phi^2$. The

non-linearity parameters are then given by

$$\frac{6}{5}f_{\text{NL}} = 2\left(-\frac{4r_{\text{dec}}}{\sigma_*} + \frac{\Gamma_\sigma}{\Gamma}\right)^{-2} \left[3\left(\frac{\Gamma_\sigma^2}{\Gamma^2} - \frac{\Gamma_{\sigma\sigma}}{\Gamma}\right) + \frac{4r_{\text{dec}}}{\sigma_*^2}(3 - 4r_{\text{dec}} - 2r_{\text{dec}}^2) \right], \quad (35)$$

$$\begin{aligned} \frac{54}{25}g_{\text{NL}} = & -36\left(-\frac{4r_{\text{dec}}}{\sigma_*} + \frac{\Gamma_\sigma}{\Gamma}\right)^{-3} \\ & \times \left[-\frac{2\Gamma_\sigma^3}{\Gamma^3} + \frac{3\Gamma_\sigma\Gamma_{\sigma\sigma}}{\Gamma^2} - \frac{\Gamma_{\sigma\sigma\sigma}}{\Gamma} + \frac{8r_{\text{dec}}^2}{9\sigma_*^3}(-18 + r_{\text{dec}} + 20r_{\text{dec}}^2 + 6r_{\text{dec}}^3) \right]. \end{aligned} \quad (36)$$

To discuss the prediction of this model more explicitly, we need to specify the form of the decay rate. Here we again adopt the form given by Eq. (31). Since this model includes both cases of the curvaton and the modulated reheating, some limits should be identical to those models. However, notice that which part gives a dominant contribution to the total curvature perturbation ζ can be different order by order. Assuming $\sigma_*/M \ll 1$ and $r_{\text{dec}} \ll 1$, the condition in which $\zeta_{\text{cur}} > \zeta_{\text{mod}}$ at the first order can be given by

$$r_{\text{dec}} > |C_1| \frac{\sigma_*}{M}, \quad (37)$$

where $C_1 = \alpha/4$ is a constant. In the second order, the corresponding condition is

$$r_{\text{dec}} > |C_2| \left(\frac{\sigma_*}{M}\right)^2, \quad (38)$$

where $C_2 = (2\beta - \alpha^2)/4$. For the third order, it is given by

$$r_{\text{dec}} > \sqrt{|C_3|} \left(\frac{\sigma_*}{M}\right)^{3/2}, \quad (39)$$

where $C_3 = (\alpha^3 - 3\alpha\beta)/8$. As far as the parameters α, β are $\mathcal{O}(1)$, the constants C_1, C_2 and C_3 are also $\mathcal{O}(1)$. From the inequalities above, one can easily notice that there can exist, for example, the case where the curvaton part dominates over the modulated reheating part in the second order, however, in the third order, the modulated reheating part gives a more contribution. When $\alpha, \beta = \mathcal{O}(1)$, the parameters r_{dec} in the curvaton and σ_*/M in the modulated reheating totally determine the size of ζ in each order. From the conditions Eqs. (37), (38) and (39), we can divide the parameter space in the $\sigma_*/M - r_{\text{dec}}$ plane into four regions, which is shown in Fig. 3. Since we consider the case of $\sigma_*/M \ll 1$, for a fixed value of σ_*/M , the corresponding values of r_{dec} for each region are:

$$r_{\text{dec},4} < |C_2| \left(\frac{\sigma_*}{M}\right)^2 < r_{\text{dec},3} < \sqrt{|C_3|} \left(\frac{\sigma_*}{M}\right)^{3/2} < r_{\text{dec},2} < |C_1| \left(\frac{\sigma_*}{M}\right) < r_{\text{dec},1}, \quad (40)$$

where the subscript i which appears in $r_{\text{dec},i}$ indicates the region shown in Fig. 3. Region 1 corresponds to the case where the curvaton fluctuations always dominate over those from

the modulated reheating. In Region 2, only at linear order $\zeta_{\text{mod}}^{(1)} > \zeta_{\text{cur}}^{(1)}$ holds, but in the second and third orders, $\zeta_{\text{cur}}^{(2)} > \zeta_{\text{mod}}^{(2)}$ and $\zeta_{\text{cur}}^{(3)} > \zeta_{\text{mod}}^{(3)}$ are satisfied. In Region 3, only in the second order, $\zeta_{\text{cur}}^{(2)} > \zeta_{\text{mod}}^{(2)}$ holds, but in linear and the third orders, fluctuations from the modulated reheating give dominant contributions. Region 4 corresponds to the pure modulated reheating case.

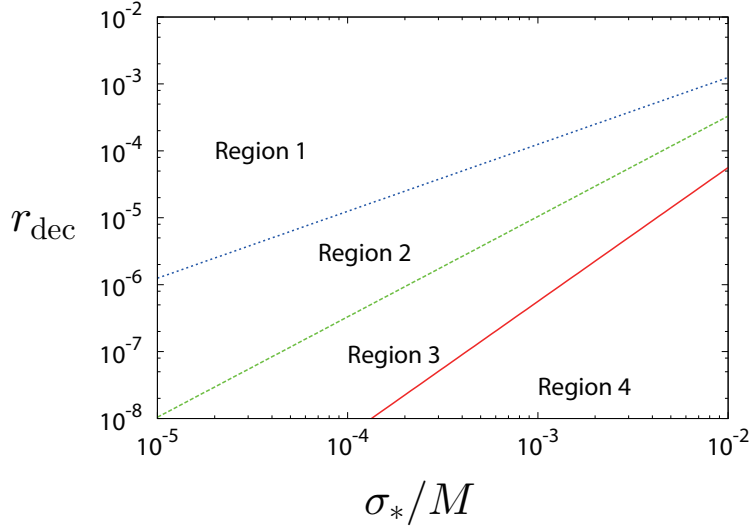


Figure 3: Parameter regions where the curvaton fluctuations dominate over those from the modulated reheating in all orders (Region 1), and the fluctuations from modulated reheating dominate the curvaton ones, in the first and the third orders (Region 2), only in the second order (Region 3), and in all orders (Region 4). Note that here “all orders” just means “up to the third order” since we consider fluctuations only up to this order. We used $\alpha = \frac{1}{2}$ and $\beta = -1$ for illustrative purpose.

Now we look at each case in order. In Region 1, r_{dec} should satisfy $r_{\text{dec}} > |C_1|\sigma_*/M$, which is required to have $\zeta_{\text{cur}} > \zeta_{\text{mod}}$ at all (up to the third) orders. Here we assume that $\sigma_* > \delta\sigma_* = H_*/2\pi$, which guarantees the linear order perturbation always dominates over the second order one. Since ζ_{cur} should be equal to the observed amplitude of fluctuation, we require $\zeta_{\text{cur}} \sim 10^{-5}$, which yields another condition $r_{\text{dec}} \sim 10^{-5}\sigma_*/H_*$. By eliminating r_{dec} from the above two conditions, we find that M must satisfy a bound $M > 10^5|C_1|H_*$.

In Region 2, although the curvature fluctuations from the modulated reheating give more contribution than those from the curvaton at linear order, the curvaton dominates over the modulated reheating both in the second and third orders. In this case, the relation between f_{NL} and g_{NL} can be given by

$$g_{\text{NL}} \sim 3r_{\text{dec}}^{1/2}f_{\text{NL}}^{3/2}. \quad (41)$$

Although g_{NL} is proportional to $f_{\text{NL}}^{3/2}$, the size of g_{NL} cannot be very large, comparing to

that of f_{NL} , due to the suppression by r_{dec} . (Notice that $r_{\text{dec}} \lesssim \sigma_*/M$ in this region.) Furthermore, parameter sets in Region 2 generally give too large f_{NL} . The expression for f_{NL} in Region 2 is approximately given by

$$\frac{6}{5}f_{\text{NL}} \simeq \frac{24r_{\text{dec}}}{\alpha^2} \left(\frac{\sigma_*}{M}\right)^{-2}. \quad (42)$$

r_{dec} should satisfy the inequality of Eq. (40), from which we can find

$$\frac{6}{\sqrt{\sigma_*/M}} \lesssim \frac{6}{5}f_{\text{NL}} \lesssim \frac{6}{\sigma_*/M}. \quad (43)$$

Since here we assume that $\sigma_*/M \ll 1$, f_{NL} is expected to be large. For example, if we take $\sigma_*/M < 10^{-3}$, $f_{\text{NL}} \sim 200$, which is already outside the current limit. But, in fact, by fine-tuning some parameters such as α and β , we can have the situation where $f_{\text{NL}} < 100$. For example, if one takes $\beta \simeq \alpha^2/3$, this choice of parameters effectively enlarges Region 2 since $C_3 \sim 0$ (see Eq. (40)). We show such a case in Fig. 2.

In Region 3, the relation between f_{NL} and g_{NL} can be written as

$$g_{\text{NL}} \sim \left(\frac{\sigma_*}{M}\right)^2 \frac{f_{\text{NL}}}{r_{\text{dec}}}. \quad (44)$$

In this region, the inequality $(\sigma_*/M)^2/r_{\text{dec}} < 1$ should be satisfied (see Eq. (40)), thus g_{NL} tends to be smaller than f_{NL} as in the case of Region 2, which can be regarded as ‘‘suppressed g_{NL} ’’ type.

Region 4 corresponds to the limit of the pure modulated reheating case. Thus this region follows the argument in the previous subsection 3.2.2.

As a final remark on this scenario, it should be noted that the linear order term can be canceled to vanish for some parameter values of r_{dec} and σ_*/M even if $\sigma_* > \delta\sigma_*$ is satisfied. In this situation, by introducing the fluctuations from the inflaton, this scenario becomes like the ungaussiton model which is discussed later.

3.2.4 Inhomogeneous end of hybrid inflation

In this subsection, we discuss a hybrid inflation model, where a light scalar field other than inflaton exists and fluctuations of such a field give cosmic density perturbations [66–70]. In usual hybrid inflation models, the inflationary phase ends due to the tachyonic instability of a waterfall field and the end of inflation homogeneously occurs. If, however, such a waterfall field is coupled with a light scalar field, then the fluctuations of the light scalar field can drive the inhomogeneous end of inflation, from which the curvature perturbation can be generated.

Here let us consider one of the simplest models introduced in Ref. [68], where the potential for the model is given by

$$V = \frac{\lambda}{4} \left(\frac{v^2}{\lambda} - \chi^2\right)^2 + \frac{1}{2}g^2\phi^2\chi^2 + \frac{1}{2}m_\phi^2\phi^2 + \frac{1}{2}f^2\sigma^2\chi^2 + \frac{1}{2}m_\sigma^2\sigma^2, \quad (45)$$

where g , f and λ are some coupling constants and v is a vacuum expectation value (VEV). m_ϕ and m_σ are the masses for the inflaton ϕ and a light scalar field σ , respectively. χ is the waterfall field. Here we assume that only σ acquires fluctuations^{#12}. The effective mass squared of the waterfall field is

$$m_\chi^2 = -v^2 + g^2\phi^2 + f^2\sigma^2, \quad (46)$$

and then a critical value of the inflaton field corresponding to $m_\chi^2 = 0$ is given by

$$\phi_{\text{cr}} = \frac{\sqrt{v^2 - f^2\sigma^2}}{g}. \quad (47)$$

Here, we have assumed that $v^2 > f^2\sigma^2$. Notice that the critical value of the inflaton can fluctuate due to the fluctuations of the light field σ . Assuming that the inflation ends at $\phi = \phi_{\text{cr}}$ because of the tachyonic instability of the waterfall field (hence we adopt a sudden-end approximation), the total e -folding number during inflation can be estimated as

$$N = -\frac{1}{M_{\text{Pl}}^2} \int_{\phi_*}^{\phi_{\text{cr}}} \frac{V}{V_\phi} d\phi, \quad (48)$$

where we have used the slow-roll approximation. Since the fluctuations of the light field σ affect the perturbation of the e -folding number, which corresponds to the total curvature perturbation ζ , through the fluctuation of the critical value of the inflaton ϕ_{cr} , we have

$$\begin{aligned} \zeta &= \frac{\partial N}{\partial \phi_{\text{cr}}} \frac{d\phi_{\text{cr}}}{d\sigma} \delta\sigma_* + \frac{1}{2} \left[\frac{\partial^2 N}{\partial \phi_{\text{cr}}^2} \left(\frac{d\phi_{\text{cr}}}{d\sigma} \right)^2 + \frac{\partial N}{\partial \phi_{\text{cr}}} \frac{d^2 \phi_{\text{cr}}}{d\sigma^2} \right] \delta\sigma_*^2 \\ &+ \frac{1}{6} \left[\frac{\partial^3 N}{\partial \phi_{\text{cr}}^3} \left(\frac{d\phi_{\text{cr}}}{d\sigma} \right)^3 + 3 \frac{\partial^2 N}{\partial \phi_{\text{cr}}^2} \left(\frac{d\phi_{\text{cr}}}{d\sigma} \right) \left(\frac{d^2 \phi_{\text{cr}}}{d\sigma^2} \right) + \frac{\partial N}{\partial \phi_{\text{cr}}} \frac{d^3 \phi_{\text{cr}}}{d\sigma^3} \right] \delta\sigma_*^3. \end{aligned} \quad (49)$$

Hence, the non-linearity parameters are given by

$$\frac{6}{5} f_{\text{NL}} = \left. \frac{N_{\phi\phi}}{N_\phi^2} \right|_{\phi=\phi_{\text{cr}}} + \frac{1}{N_\phi} \left. \frac{\phi_{\text{cr}}''}{\phi_{\text{cr}}'^2} \right|_{\phi=\phi_{\text{cr}}}, \quad (50)$$

$$\frac{54}{25} g_{\text{NL}} = \left. \frac{N_{\phi\phi\phi}}{N_\phi^3} \right|_{\phi=\phi_{\text{cr}}} + 3 \left. \frac{N_{\phi\phi}}{N_\phi^3} \right|_{\phi=\phi_{\text{cr}}} \frac{\phi_{\text{cr}}''}{\phi_{\text{cr}}'^2} + \left. \frac{1}{N_\phi^2} \right|_{\phi=\phi_{\text{cr}}} \frac{\phi_{\text{cr}}'''}{\phi_{\text{cr}}'^3}, \quad (51)$$

where the prime denotes the derivative with respect to σ . Since in the ordinary hybrid inflation model the slow-roll conditions are satisfied until $\phi = \phi_{\text{cr}}$, we find that the first terms in Eqs. (50) and (51) are suppressed by the slow-roll parameters. In order to realize the large non-Gaussianity in this model, large contributions from the second terms in

^{#12} For the case where fluctuations of ϕ also contribute to ζ , which becomes a multi-source case, see the discussion in Sec. 3.3.3.

Eqs. (50) and (51) or the third term in Eq. (51) are needed. Neglecting the terms suppressed by slow-roll parameters, the expressions for non-linearity parameters are reduced to

$$\frac{6}{5}f_{\text{NL}} \simeq -\sqrt{2\epsilon_{\text{cr}}}\frac{\phi_{\text{cr}}''}{\phi_{\text{cr}}'^2}, \quad (52)$$

$$\frac{54}{25}g_{\text{NL}} \simeq -(2\epsilon_{\text{cr}} - \eta_{\text{cr}})\frac{18}{5}f_{\text{NL}} + 2\epsilon_{\text{cr}}\frac{\phi_{\text{cr}}'''}{\phi_{\text{cr}}'^3}, \quad (53)$$

where ϵ and η are the slow-roll parameters defined by

$$\epsilon \equiv \frac{1}{2}M_{\text{Pl}}^2\left(\frac{V_\phi}{V}\right)^2, \quad \eta \equiv M_{\text{Pl}}^2\frac{V_{\phi\phi}}{V}, \quad (54)$$

and we denote the quantities evaluated at $\phi = \phi_{\text{cr}}$ by a subscript “cr.”

From Eq. (47), we have

$$\frac{d\phi_{\text{cr}}}{d\sigma} = -\frac{f^2\sigma}{g^2\phi_{\text{cr}}}, \quad (55)$$

$$\frac{d^2\phi_{\text{cr}}}{d\sigma^2} = -\frac{f^2}{g^2\phi_{\text{cr}}}\left(\frac{v^2}{g^2\phi_{\text{cr}}^2}\right), \quad (56)$$

$$\frac{d^3\phi_{\text{cr}}}{d\sigma^3} = -3\frac{f^4\sigma}{g^4\phi_{\text{cr}}^3}\left(\frac{v^2}{g^2\phi_{\text{cr}}^2}\right). \quad (57)$$

Then, the non-linearity parameters can be written as

$$\frac{6}{5}f_{\text{NL}} = \eta_{\text{cr}}\frac{v^2}{f^2\sigma^2}, \quad (58)$$

$$\frac{54}{25}g_{\text{NL}} = 6\eta_{\text{cr}}^2\frac{v^2}{f^2\sigma^2}, \quad (59)$$

where we have used $\eta = M_{\text{Pl}}\sqrt{2\epsilon}/\phi$ since $\sqrt{2\epsilon} = M_{\text{Pl}}m_\phi^2\phi/V$ and $\eta = M_{\text{Pl}}^2m_\phi^2/V$ during inflation in this model. Furthermore we have also adopted the approximation $\epsilon_{\text{cr}} \ll \eta_{\text{cr}} \ll 1$, which is satisfied as in a usual hybrid inflation. Hence, when $v^2 \gg f^2\sigma^2/\eta_{\text{cr}}$, large f_{NL} can be generated in this scenario. Notice that, in general, fluctuations from the inflaton would also exist, which gives another condition for neglecting the inflaton fluctuations: $f^2\sigma > g^2\phi_{\text{cr}}(\epsilon_{\text{cr}}/\epsilon_*)^{1/2}$. This relation can hold by taking the value of σ appropriately. Then, we can find the following relation between f_{NL} and g_{NL} :

$$g_{\text{NL}} = \eta_{\text{cr}}\frac{10}{3}f_{\text{NL}}. \quad (60)$$

Compared to the modulated reheating scenario, the ratio of the non-linearity parameters $g_{\text{NL}}/f_{\text{NL}}$ is suppressed by the slow-roll parameter η in this scenario and thus this model can be regarded as “suppressed g_{NL} ” type. Another simple model introduced by Alabidi and Lyth [70] also predicts that $g_{\text{NL}}/f_{\text{NL}}$ is suppressed by the slow-roll parameter.

3.2.5 Inhomogeneous end of thermal inflation

Primordial fluctuations can also be generated by modulating the end of thermal inflation [71] (see also [72] for the discussion on the generation of primordial fluctuation from inhomogeneous cosmological phase transition). Here we briefly review the mechanism following [71].

The thermal inflation [73] can be realized by using a flaton field ϕ , a flat direction in supersymmetric theories, whose effective potential can be given by

$$V_{\text{eff}} = V_{\text{cons}} + \frac{1}{2} (gT^2 - m^2) \phi^2 + \frac{\lambda}{6} \frac{1}{M_{\text{Pl}}^2} \phi^6, \quad (61)$$

where $(1/2)gT^2$ is a thermal correction to the potential due to the interaction of the flaton field with some particles in the thermal bath with g being an effective coupling between them and T being the cosmic temperature. When $\sqrt{g} T > m$, the flaton field is trapped at the minimum $\phi = 0$, then at some time when the energy density of the flaton given by V_{cons} becomes larger than the background energy density, the Universe is dominated by the false vacuum in the potential, which drives a mini-inflation. However, when the temperature decreases down to $T_c = m/\sqrt{g}$, the flaton rolls down to the VEV, then the mini-inflation ends. The total number of e -folding from the time t_i when the mini-inflation begins to the time t_f when the flaton rolls down to the VEV is given by

$$N(t_c, t_{\text{in}}) = \int_{t_{\text{in}}}^{t_c} H dt = \ln \left(\frac{a_c}{a_{\text{in}}} \right) = -\ln \left(\frac{T_c}{T_{\text{in}}} \right), \quad (62)$$

where T_{in} is the temperature when the mini-inflation begins. If the coupling g depends on a light scalar field σ as $g = g(\sigma)$, the coupling g can fluctuate since a light scalar field σ can acquire quantum fluctuations during inflation, which gives rise to fluctuation in the number of e -folding, that is, the curvature fluctuation. By utilizing the δN formalism, the curvature perturbation can be given by

$$\begin{aligned} \zeta = \delta N &= -\frac{\delta T_c}{T_c} + \frac{1}{2} \left(\frac{\delta T_c}{T_c} \right)^2 - \frac{1}{3} \left(\frac{\delta T_c}{T_c} \right)^3 \\ &= \frac{1}{2} \left\{ \frac{g'}{g} \delta \sigma_* + \frac{1}{2} \left[\frac{g''}{g} - \left(\frac{g'}{g} \right)^2 \right] \delta \sigma_*^2 + \frac{1}{6} \left[\frac{g'''}{g} - 3 \frac{g'' g'}{g^2} + 2 \left(\frac{g'}{g} \right)^3 \right] \delta \sigma_*^3 \right\}, \end{aligned} \quad (63)$$

from which we can derive the non-linearity parameters in this model as

$$\frac{6}{5} f_{\text{NL}} = 2 \left[\frac{g''/g}{(g'/g)^2} - 1 \right], \quad (64)$$

$$\frac{54}{25} g_{\text{NL}} = 4 \left[\frac{g'''/g}{(g'/g)^3} - 3 \frac{g''/g}{(g'/g)^2} + 2 \right], \quad (65)$$

where the prime represents the derivative with respect to σ_* . When g''' is negligible, the following relation holds between f_{NL} and g_{NL} :

$$g_{\text{NL}} = -\frac{10}{3}f_{\text{NL}} - \frac{50}{27}. \quad (66)$$

Thus this model can be considered as “linear g_{NL} ” type in terms of the $f_{\text{NL}}-g_{\text{NL}}$ relation. Although the mechanism is quite similar to the modulated reheating scenario and the inhomogeneous end of hybrid inflation discussed in the previous subsection, the relation between f_{NL} and g_{NL} is different. In particular, the relative sign between f_{NL} and g_{NL} differs from the one in the modulated reheating although the size of f_{NL} and g_{NL} is almost the same order. On the other hand, the size of g_{NL} is larger than that for the case of the inhomogeneous end of hybrid inflation, where $g_{\text{NL}}/f_{\text{NL}}$ is suppressed by the slow-roll parameter.

3.2.6 Modulated trapping mechanism

During inflation, the resonant particle production can occur because of the coupling of the inflaton to other particles [74–76]. If the relevant coupling λ depends on a light scalar field σ , dubbed as modulaton in [77], the curvature perturbation can be generated through fluctuations of σ which originate from quantum fluctuations during inflation. Such a mechanism is called modulated trapping, which was proposed in [77].

Here we briefly discuss this mechanism, following closely [77], and give some relation between f_{NL} and g_{NL} in the model. Let us consider the following interaction for the inflaton ϕ :

$$\mathcal{L}_{\text{int}} = -\frac{1}{2}\mathcal{N}(m - \lambda\phi)\bar{\chi}\chi, \quad (67)$$

where χ is a fermion coupled to the inflaton and \mathcal{N} is the number of species of particles with the same mass. When the inflaton crosses the value $\phi = \phi_{\text{pp}} = m/\lambda$, χ field becomes effectively massless, then they are resonantly produced. At this moment, the occupation number for χ abruptly increases from zero to

$$n_{\text{pp}} = \frac{\lambda^{3/2}}{2\pi^3}|\dot{\phi}_{\text{pp}}|^{3/2}, \quad (68)$$

where “pp” indicates that the quantities are evaluated at the time of particle production. Once the particles are produced, its number density just decreases with the cosmic expansion, thus after its production, the number density can be written as

$$n(t) = n_{\text{pp}} \left(\frac{a}{a_{\text{pp}}} \right)^{-3} \Theta(t - t_{\text{pp}}). \quad (69)$$

By using the above expression and adopting the Hartree approximation in the equation of motion for ϕ , we can evaluate the effect of the backreaction of the particle production

to ϕ . The equation of motion for ϕ can be written as

$$\ddot{\phi} + 3H\dot{\phi} + \frac{dV(\phi)}{d\phi} = \mathcal{N}\lambda n_{\text{pp}} \left(\frac{a}{a_{\text{pp}}} \right)^{-3} \Theta(t - t_{\text{pp}}). \quad (70)$$

Assuming that the particle production and its dilution occur in a short time scale compared to the cosmic expansion during inflation, H_* and $dV(\phi_*)/d\phi$ can be regarded as constants during the particle production. Defining

$$\Delta\phi(t) \equiv \phi(t, \lambda \neq 0) - \phi(t, \lambda = 0), \quad (71)$$

then, from the equation of motion above, we obtain

$$\Delta\dot{\phi}(t > t_{\text{pp}}) = \mathcal{N}\lambda n_{\text{pp}} \exp[-3H_{\text{pp}}(t - t_{\text{pp}})](t - t_{\text{pp}}). \quad (72)$$

Now we evaluate the curvature perturbation by using the δN formalism. The number of e -folding which is attributed to the particle production can be given as

$$\Delta N^{(\lambda \neq 0)} = -H_{\text{pp}} \frac{\Delta\phi}{\dot{\phi}_{\text{pp}}}. \quad (73)$$

By integrating $\Delta\dot{\phi}$ given in Eq. (72) from the time of particle production, we obtain $\Delta\phi$ as

$$\Delta\phi = \int_{t_*}^{\infty} \Delta\dot{\phi} dt = \frac{\mathcal{N}\lambda n_{\text{pp}}}{9H_{\text{pp}}^2}. \quad (74)$$

Thus $\Delta N^{(\lambda \neq 0)}$ can be evaluated as

$$\Delta N^{(\lambda \neq 0)} = -H_* \frac{\Delta\phi}{\dot{\phi}_{\text{pp}}} = \frac{\lambda^{5/2} \mathcal{N} |\dot{\phi}_{\text{pp}}|^{1/2}}{18\pi^3 H_{\text{pp}}}, \quad (75)$$

from which the curvature perturbation due to the fluctuations of σ is given by the formula in the δN formalism:

$$\zeta = (\Delta N^{(\lambda \neq 0)})_{,\sigma} \delta\sigma_* + \frac{1}{2} (\Delta N^{(\lambda \neq 0)})_{,\sigma\sigma} (\delta\sigma_*)^2 + \frac{1}{6} (\Delta N^{(\lambda \neq 0)})_{,\sigma\sigma\sigma} (\delta\sigma_*)^3. \quad (76)$$

To give some explicit expressions for the non-linearity parameters such as f_{NL} and g_{NL} , we need to assume the functional form or σ dependence of λ and m , which is somewhat model-dependent. As discussed in [77], in the case where λ is independent of σ , but the mass depends on σ as $m = g\sigma$, the non-linearity parameters cannot be much larger than unity. Thus we do not consider such a case here. When the coupling λ and the mass m depend on σ as $\lambda = \sigma/M$ and $m = g\sigma$ with M being some energy scale, f_{NL} and g_{NL} are evaluated as

$$\frac{6}{5} f_{\text{NL}} = \frac{9}{5e\beta}, \quad (77)$$

$$\frac{54}{25} g_{\text{NL}} = \frac{27}{25e^2\beta^2}, \quad (78)$$

where β is the “efficiency factor”, which is defined and given as

$$\beta \equiv \frac{\text{Max}(\Delta\dot{\phi})}{|\dot{\phi}_{\text{pp}}|} = \frac{\mathcal{N}\lambda^{5/2}|\dot{\phi}_{\text{pp}}|^{1/2}}{6\pi^3 e H_{\text{pp}}}. \quad (79)$$

Since the particle production occurs at the cost of reducing the kinetic energy of the inflaton, β cannot exceed 1. If we take $\beta \simeq 0.01$, f_{NL} can be as large as $f_{\text{NL}} \simeq 55$ [77]. Furthermore, from the above expression, we can find the relation between f_{NL} and g_{NL} as

$$g_{\text{NL}} = \frac{2}{9}f_{\text{NL}}^2, \quad (80)$$

which is “enhanced g_{NL} ” type. In fact, the relation $g_{\text{NL}} \sim f_{\text{NL}}^2$ holds even if we assume somewhat general type of functional form for $\lambda = (\sigma/M)^p$. Thus this mechanism predicts a large values for g_{NL} relative to f_{NL} compared to some other “modulated coupling” scenarios such as modulated reheating and inhomogeneous end of thermal inflation, which give $|g_{\text{NL}}| \sim |f_{\text{NL}}|$.

3.3 Multi-source model

Although the origin of density fluctuations is usually assumed to be a single source, in general, it is possible that multiple sources can be simultaneously responsible for density fluctuations [51, 65, 78–81]. For example, in the curvaton scenario, the curvaton field alone is usually supposed to generate the curvature perturbation, however, even in this scenario, the inflaton should exist to drive the superluminal expansion at the early epoch and it can acquire quantum fluctuations. Thus in general, both the inflaton and the curvaton fields can be responsible for cosmic density fluctuations today. In a case where fluctuations from multiple sources can simultaneously give a sizable contribution to observed ones, the relations among the non-linearity parameters are different from those discussed in Section 3.2.

Here we discuss the case where two scalar fields ϕ and σ generate density fluctuations. In this case, the curvature perturbation can be generally written as

$$\begin{aligned} \zeta = & N_{\phi}\delta\phi_* + N_{\sigma}\delta\sigma_* \\ & + \frac{1}{2}\left(N_{\phi\phi}(\delta\phi_*)^2 + 2N_{\phi\sigma}\delta\phi_*\delta\sigma_* + N_{\sigma\sigma}(\delta\sigma_*)^2\right) \\ & + \frac{1}{6}\left(N_{\phi\phi\phi}(\delta\phi_*)^3 + 3N_{\phi\phi\sigma}(\delta\phi_*)^2\delta\sigma_* + 3N_{\phi\sigma\sigma}\delta\phi_*(\delta\sigma_*)^2 + N_{\sigma\sigma\sigma}(\delta\sigma_*)^3\right). \end{aligned} \quad (81)$$

Then the non-linearity parameters can be given by

$$f_{\text{NL}} = \left(\frac{1}{1+R} \right)^2 \left[f_{\text{NL}}^{(\phi)} + 2R f_{\text{NL}}^{(\phi\sigma)} + R^2 f_{\text{NL}}^{(\sigma)} \right], \quad (82)$$

$$\tau_{\text{NL}} = \left(\frac{1}{1+R} \right)^3 \left[\left(\frac{6}{5} f_{\text{NL}}^{(\phi)} + R \frac{6}{5} f_{\text{NL}}^{(\phi\sigma)} \right)^2 + R^3 \left(\frac{6}{5} f_{\text{NL}}^{(\sigma)} + \frac{1}{R} \frac{6}{5} f_{\text{NL}}^{(\phi\sigma)} \right)^2 \right], \quad (83)$$

$$g_{\text{NL}} = \left(\frac{1}{1+R} \right)^3 \left[g_{\text{NL}}^{(\phi)} + 3R g_{\text{NL}}^{(\phi\phi\sigma)} + 3R^2 g_{\text{NL}}^{(\phi\sigma\sigma)} + R^3 g_{\text{NL}}^{(\sigma)} \right], \quad (84)$$

where we have defined non-linearity parameters for each contribution as

$$\begin{aligned} \frac{6}{5} f_{\text{NL}}^{(\phi)} &= \frac{N_{\phi\phi}}{N_\phi^2}, & \frac{6}{5} f_{\text{NL}}^{(\phi\sigma)} &= \frac{N_{\phi\sigma}}{N_\phi N_\sigma}, & \frac{6}{5} f_{\text{NL}}^{(\sigma)} &= \frac{N_{\sigma\sigma}}{N_\sigma^2}, \\ \frac{54}{25} g_{\text{NL}}^{(\phi)} &= \frac{N_{\phi\phi\phi}}{N_\phi^3}, & \frac{54}{25} g_{\text{NL}}^{(\phi\phi\sigma)} &= \frac{N_{\phi\phi\sigma}}{N_\phi^2 N_\sigma}, & \frac{54}{25} g_{\text{NL}}^{(\phi\sigma\sigma)} &= \frac{N_{\phi\sigma\sigma}}{N_\phi N_\sigma^2}, & \frac{54}{25} g_{\text{NL}}^{(\sigma)} &= \frac{N_{\sigma\sigma\sigma}}{N_\sigma^3}. \end{aligned} \quad (85)$$

R represents the ratio of the power spectrum for the curvature perturbation from fluctuations of ϕ and σ :

$$R \equiv \frac{P_\zeta^{(\sigma)}(k_{\text{ref}})}{P_\zeta^{(\phi)}(k_{\text{ref}})}, \quad (86)$$

where

$$P_\zeta^{(\phi)}(k_{\text{ref}}) = N_\phi^2 P_\delta(k_{\text{ref}}), \quad P_\zeta^{(\sigma)}(k_{\text{ref}}) = N_\sigma^2 P_\delta(k_{\text{ref}}), \quad (87)$$

with P_δ being defined in Eq. (8) and the power spectra are evaluated at some reference scale k_{ref} . Then, we obtain the following relation,

$$\tau_{\text{NL}} = \left(\frac{1+\bar{R}}{\bar{R}} \right) \left(\frac{6}{5} f_{\text{NL}} \right)^2 \geq \left(\frac{6}{5} f_{\text{NL}} \right)^2, \quad (88)$$

where the ratio \bar{R} is defined as

$$\bar{R} \equiv \frac{1}{R} \left(\frac{R_{f_{\text{NL}}} + R^2}{R_{f_{\text{NL}}} - R} \right)^2 \geq 0, \quad (89)$$

with

$$R_{f_{\text{NL}}} \equiv \frac{f_{\text{NL}}^{(\phi)} + R f_{\text{NL}}^{(\phi\sigma)}}{f_{\text{NL}}^{(\sigma)} + (1/R) f_{\text{NL}}^{(\phi\sigma)}}. \quad (90)$$

These formulae can be applied for a general two-field case.

3.3.1 Mixed model with inflaton fluctuations

In a special case where ϕ is the inflaton field and σ is some other light field, ϕ does not contribute to non-Gaussianity because non-linearity parameters are suppressed by the slow-roll of ϕ . Then, the curvature perturbation can be written as

$$\begin{aligned}\zeta &= \zeta^{(\phi)} + \zeta^{(\sigma)} \\ &= N_\phi \delta\phi_* + N_\sigma \delta\sigma_* + \frac{1}{2} N_{\sigma\sigma} (\delta\sigma_*)^2 + \frac{1}{6} N_{\sigma\sigma\sigma} (\delta\sigma_*)^3,\end{aligned}\tag{91}$$

where $\zeta^{(\phi)}$ and $\zeta^{(\sigma)}$ represent the contributions to the curvature perturbation from $\delta\phi$ and $\delta\sigma$, respectively^{#13}. In most cases, the inflaton and the other light scalar field can be considered to be uncorrelated and non-linearity in the inflaton sector is generally suppressed by the slow-roll, here we set $f_{\text{NL}}^{(\phi)} = f_{\text{NL}}^{(\phi\sigma)} = 0$, which indicates that $R_{f_{\text{NL}}} = 0$ and $\overline{R} = R$. Furthermore, in this case, we can also set $g_{\text{NL}}^{(\phi)} = g_{\text{NL}}^{(\phi\phi\sigma)} = g_{\text{NL}}^{(\phi\sigma\sigma)} = 0$. Then we have the relation among f_{NL} , τ_{NL} and g_{NL} as

$$\tau_{\text{NL}} = \left(\frac{1+R}{R}\right) \left(\frac{6}{5} f_{\text{NL}}\right)^2,\tag{92}$$

and

$$\frac{g_{\text{NL}} \tau_{\text{NL}}}{f_{\text{NL}}^3} = \left(\frac{6}{5}\right)^2 \frac{g_{\text{NL}}^{(\sigma)}}{f_{\text{NL}}^{(\sigma)}}.\tag{93}$$

This equation can be applied for a scenario where one of two sources of fluctuations alone contributes to non-Gaussianity. Also notice that when R is small, it corresponds to the situation where $\tau_{\text{NL}} \gg (6f_{\text{NL}}/5)^2$. Thus large $\tau_{\text{NL}}/f_{\text{NL}}^2$ may indicate that (almost) Gaussian field gives a large contribution to the power spectrum, but non-Gaussianity comes from the other source^{#14}.

In most models, the relation between $f_{\text{NL}}^{(\sigma)}$ and $g_{\text{NL}}^{(\sigma)}$ for a single field sector can be given by the following form:

$$g_{\text{NL}}^{(\sigma)} = C_{1\sigma} \left(f_{\text{NL}}^{(\sigma)}\right)^p + C_{2\sigma},\tag{94}$$

where $C_{1\sigma}$ and $C_{2\sigma}$ are numerical constants and p is the power of $f_{\text{NL}}^{(\sigma)}$. For example, in the curvaton model with a quadratic potential, these parameters are given as $C_{1\sigma} = -(10/3)$, $C_{2\sigma} = -(575/108)$ and $p = 1$ as can be read off from Eq. (21). By assuming the

^{#13} In some literature, the notation ζ_ϕ indicates that the curvature perturbation on the slice where the energy density of ϕ is uniform. Here $\zeta^{(\phi)}$ just represents the contribution to ζ from $\delta\phi$.

^{#14} Here it should also be noted that, for certain parameter values of this kind of mixed models, the second order fluctuations give the leading contribution in $\zeta^{(\sigma)}$. In this case, the model becomes like ‘‘ungaussiton’’ model, categorized as ‘‘constrained multi-field type,’’ which will be discussed in the later section.

form of Eq. (94) for the σ sector, we can write the relation between f_{NL} and g_{NL} for the mixed model with the inflaton as,

$$g_{\text{NL}} = C_{1\sigma} \left(\frac{R}{1+R} \right)^{3-2p} f_{\text{NL}}^p + C_{2\sigma} \left(\frac{R}{1+R} \right)^3. \quad (95)$$

We can also write this equation by using τ_{NL} and eliminating R as,

$$g_{\text{NL}} = \left(\frac{6}{5} \right)^{6-4p} C_{1\sigma} \frac{f_{\text{NL}}^{6-3p}}{\tau_{\text{NL}}^{3-2p}} + \left(\frac{6}{5} \right)^6 C_{2\sigma} \frac{f_{\text{NL}}^6}{\tau_{\text{NL}}^3}. \quad (96)$$

As an explicit example, first we give the formula for the case of the mixed curvaton and inflaton fluctuations. As mentioned above, even in the curvaton scenario, the fluctuations from the inflaton can also give some contribution to the curvature perturbations as well as those from the curvaton. Here we denote σ as the curvaton field. As discussed in Section 3.2.1, assuming that the potential of the curvaton is quadratic, $f_{\text{NL}}^{(\sigma)}$ and $g_{\text{NL}}^{(\sigma)}$ are related as Eq. (21) for $r_{\text{dec}} \ll 1$. Putting the relation into Eq. (93) or (96), we find the relation among the non-linearity parameters for the case with $r_{\text{dec}} \ll 1$ as [78],

$$g_{\text{NL}} = -\frac{24}{5} \frac{f_{\text{NL}}^3}{\tau_{\text{NL}}} - \frac{9936}{625} \frac{f_{\text{NL}}^6}{\tau_{\text{NL}}^3}. \quad (97)$$

This relation can be rewritten as

$$g_{\text{NL}} = -\frac{10}{3} \left(\frac{R}{1+R} \right) f_{\text{NL}} - \frac{575}{108} \left(\frac{R}{1+R} \right)^3, \quad (98)$$

which recovers the pure curvaton case Eq. (21) in the limit of $R \rightarrow \infty$. When $R \sim 1$, g_{NL} is of the same order of f_{NL} , but when $R \ll 1$, g_{NL} is suppressed by the factor R .

A similar relation can be obtained for a mixed model of the modulated reheating and the inflaton fluctuations. As discussed in Section 3.2.2, when the term with $\Gamma_{\sigma\sigma\sigma}$ is negligible, $f_{\text{NL}}^{(\sigma)}$ is related to $g_{\text{NL}}^{(\sigma)}$ as in Eq. (33). By adopting the relation, we obtain the corresponding equation in this model as [65]

$$g_{\text{NL}} = \frac{72}{5} \frac{f_{\text{NL}}^3}{\tau_{\text{NL}}} - \frac{31104}{625} \frac{f_{\text{NL}}^6}{\tau_{\text{NL}}^3} = 10 \left(\frac{R}{1+R} \right) f_{\text{NL}} - \frac{50}{3} \left(\frac{R}{1+R} \right)^3, \quad (99)$$

which reduces to the pure modulated reheating case (33) in the limit of $R \rightarrow \infty$. Notice that g_{NL} is again suppressed by R when $R \ll 1$.

Another example is the modulated trapping model with a sizable contribution from the inflaton fluctuations. Here σ is assumed to be modulator. For some functional forms of λ and m , the relation between $f_{\text{NL}}^{(\sigma)}$ and $g_{\text{NL}}^{(\sigma)}$ can be given as Eq. (80). In this model, the following relation holds:

$$g_{\text{NL}} = \frac{2}{9} \left(\frac{1+R}{R} \right) f_{\text{NL}}^2 = \frac{25}{162} \tau_{\text{NL}}. \quad (100)$$

In general, the inflaton fluctuations can also contribute to the primordial fluctuations even if we consider another source. The discussion above is applicable for other models regarding σ as the one in other single-source models. If the corresponding single-source model predicts the $f_{\text{NL}}-g_{\text{NL}}$ relation of the linear type, the counterpart of its mixed model with the inflaton gives “suppressed g_{NL} ” type due to the ratio R when $R \ll 1$, although $|f_{\text{NL}}| \sim |g_{\text{NL}}|$ when $R \sim 1$.

As a final remark, we comment on the spectral index n_s and tensor-to-scalar ratio r in this type of mixed models. n_s and r in this scenario are generally given by

$$n_s - 1 = -2\epsilon - \frac{4\epsilon - 2\eta}{1 + R}, \quad (101)$$

$$r = \frac{16\epsilon}{1 + R}, \quad (102)$$

where ϵ and η are slow-roll parameters for the inflaton defined as in Eq. (54). The limit of $R \rightarrow 0$ corresponds to the case where only inflaton fluctuations are responsible for today’s density fluctuations.

On the other hand, the limit of $R \rightarrow \infty$ corresponds to a single-source model. As seen from the above equation, the tensor-to-scalar ratio r becomes very small in this limit. Thus r is considered to be generally very small in models with large non-Gaussianity. However, when $R \sim 1$, large r is possible while non-Gaussianity can also be large. Thus a mixed model discussed in this section is interesting in this respect as well.

3.3.2 Multi-curvaton model

In a usual curvaton model, there exists only one curvaton field. However, it may also be possible that multiple fields can play a role of the curvaton. Some authors have already considered this kind of the scenario [82, 83], which is called “multi-curvaton” model. Here we discuss this model focusing on its non-linearity parameters.

In the following, we basically follow the arguments in [83]. Here we adopt the sudden decay approximation and assume that two curvaton fields, denoted as a and b , are responsible for the present-day density fluctuations. We also assume that the curvaton field a decays first (i.e., the decay rates for a and b are assumed to be $\Gamma_a > \Gamma_b$). At an infinitesimal time before and after the first curvaton decay, the total curvature perturbation ζ_1 at the first curvaton decay, the curvature perturbations on the constant curvaton a and b hypersurfaces ζ_a and ζ_b are related as

$$(1 - \Omega_{a1} - \Omega_{b1})e^{-4\zeta_1} + \Omega_{a1}e^{3(\zeta_a - \zeta_1)} + \Omega_{b1}e^{3(\zeta_b - \zeta_1)} = 1, \quad (103)$$

$$(1 - \Omega_{b1})e^{4(\zeta_{\gamma 1} - \zeta_1)} + \Omega_{b1}e^{3(\zeta_b - \zeta_1)} = 1, \quad (104)$$

where $\Omega_{a1} = \rho_{a1}/\rho_1$ and $\Omega_{b1} = \rho_{b1}/\rho_1$ with ρ_1, ρ_{a1} and ρ_{b1} being energy densities of the total component, the curvaton a and b at the first curvaton decay, respectively. At the time just before the second curvaton decay, the following equation holds:

$$(1 - \Omega_{b2})e^{4(\zeta_{\gamma 1} - \zeta_2)} + \Omega_{b2}e^{3(\zeta_b - \zeta_2)} = 1, \quad (105)$$

where $\Omega_{b2} = \rho_{b2}/\rho_2$ with ρ_2 and ρ_{b2} being energy densities of the total component and the curvaton b at the second curvaton decay, respectively. Here ζ_{γ_1} is the curvature perturbation on the constant radiation hypersurface at the first curvaton decay. ζ_2 is the curvature perturbation after the second curvaton decay. Here the subscripts 1 and 2 indicate that the quantities are the ones at the time of the first and the second curvatons (the curvatons a and b) decays, respectively.

Since we are interested in the final curvature perturbation after the second curvaton decays, we evaluate ζ_2 up to third order, then find non-linearity parameters in the model. The curvature perturbations ζ_a and ζ_b are related to the field perturbations of the curvatons a and b , denoted as δa and δb , by

$$\zeta_a = \frac{1}{3} \log(1 + \delta a) = \frac{2}{3} \frac{\delta a}{a} - \frac{1}{3} \left(\frac{\delta a}{a} \right)^2 + \frac{2}{9} \left(\frac{\delta a}{a} \right)^3, \quad (106)$$

$$\zeta_b = \frac{1}{3} \log(1 + \delta b) = \frac{2}{3} \frac{\delta b}{b} - \frac{1}{3} \left(\frac{\delta b}{b} \right)^2 + \frac{2}{9} \left(\frac{\delta b}{b} \right)^3, \quad (107)$$

where $\delta_i = \delta\rho_i/\rho_i$ and we truncated at the third order. Here we have assumed that the potentials for the curvatons are quadratic. Hence the field values a, b and their perturbations $\delta a, \delta b$ are regarded as the ones evaluated at the time of horizon crossing.

By using an iterative method, we can express ζ_2 as the series in ζ_a and ζ_b . Denoting the first order parts for the curvatons a and b in Eqs. (106) and (107) as $\zeta_{a(1)}$ and $\zeta_{b(1)}$, respectively, we can generally write ζ_2 as

$$\begin{aligned} \zeta_2 = & C_a \zeta_{a(1)} + C_b \zeta_{b(1)} + C_{aa} \zeta_{a(1)}^2 + C_{bb} \zeta_{b(1)}^2 + C_{ab} \zeta_{a(1)} \zeta_{b(1)} \\ & + C_{aaa} \zeta_{a(1)}^3 + C_{bbb} \zeta_{b(1)}^3 + C_{aab} \zeta_{a(1)}^2 \zeta_{b(1)} + C_{abb} \zeta_{a(1)} \zeta_{b(1)}^2. \end{aligned} \quad (108)$$

Here the coefficients such as C_a and so on are functions of f_{a1}, f_{b1} and f_{b2} which are defined as

$$f_{a1} = \frac{3\Omega_{a1}}{4 - \Omega_{a1} - \Omega_{b1}}, \quad (109)$$

$$f_{b1} = \frac{3\Omega_{b1}}{4 - \Omega_{a1} - \Omega_{b1}}, \quad (110)$$

$$f_{b2} = \frac{3\Omega_{b2}}{4 - \Omega_{b2}}. \quad (111)$$

These quantities roughly represent the ratio of the energy density of the curvatons a and b to the total one at the first and second curvaton decays.

Since the expression for the coefficients are very complicated in general, here we consider only some limiting cases where non-Gaussianity can be large. We give the full expression of the curvature perturbation in Appendix A.

• **Case I: Both curvatons are subdominant at their decays**

When the curvatons are both subdominant at their decays, which corresponds to the case of $f_{a1}, f_{b2} \ll 1$ (and $f_{b1} < f_{b2}$ being implicitly assumed), the curvature perturbation after the second curvaton decay can be given by

$$\begin{aligned} \zeta_2 = & f_{a1}\zeta_{a(1)} + f_{b2}\zeta_{b(1)} + \frac{3f_{a1}}{4}\zeta_{a(1)}^2 + \frac{3f_{b2}}{4}\zeta_{b(1)}^2 \\ & - \frac{3f_{a1}^2}{2}\zeta_{a(1)}^3 - \frac{3f_{b2}^2}{2}\zeta_{b(1)}^3 - \frac{9}{4}f_{a1}f_{b2}\zeta_{a(1)}^2\zeta_{b(1)} - \frac{9}{4}f_{a1}f_{b2}\zeta_{a(1)}\zeta_{b(1)}^2, \end{aligned} \quad (112)$$

where we have kept f_{a1} and f_{b2} only at the leading order.

Then we can find the non-linearity parameters for this case as

$$\frac{6}{5}f_{\text{NL}} \simeq \frac{3}{2} \frac{f_{a1}^3 + f_{b2}^3 K^2}{(f_{a1}^2 + f_{b2}^2 K)^2}, \quad (113)$$

$$\tau_{\text{NL}} \simeq \frac{9}{4} \frac{f_{a1}^4 + f_{b2}^4 K^3}{(f_{a1}^2 + f_{b2}^2 K)^3}, \quad (114)$$

$$\frac{54}{25}g_{\text{NL}} \simeq -9 \frac{f_{a1}^5 + 3f_{a1}^3 f_{b2}^2 K + 3f_{a1}^2 f_{b2}^3 K^2 + f_{b2}^5 K^3}{(f_{a1}^2 + f_{b2}^2 K)^3}, \quad (115)$$

where K is the ratio of the power spectra of the curvatons a and b , denoted as P_{ζ_a} and P_{ζ_b} , respectively:

$$K = \frac{P_{\zeta_b}}{P_{\zeta_a}}. \quad (116)$$

With this definition, the ratio R defined by Eq. (86) in Section 3.3 can be written as

$$R \simeq \frac{f_{b2}^2}{f_{a1}^2} K. \quad (117)$$

In the language of Section 3.3, we have

$$\tau_{\text{NL}} = \left(\frac{1 + \bar{R}}{\bar{R}} \right) \left(\frac{6}{5} f_{\text{NL}} \right)^2, \quad \bar{R} = \frac{1}{R} \left[\frac{f_{a1}^3 + f_{b2}^3 K^2}{f_{a1}^2 (f_{a1} - f_{b2} K)} \right]^2. \quad (118)$$

Regarding the relation between g_{NL} and f_{NL} , we find

$$\frac{10}{3} f_{\text{NL}} < -g_{\text{NL}} < 10 f_{\text{NL}}. \quad (119)$$

Thus, g_{NL} is of the same order of f_{NL} with the opposite sign in this case and we could write as

$$g_{\text{NL}} = C_{\text{mc}}(f_{a1}, f_{b2}, K) f_{\text{NL}}, \quad (120)$$

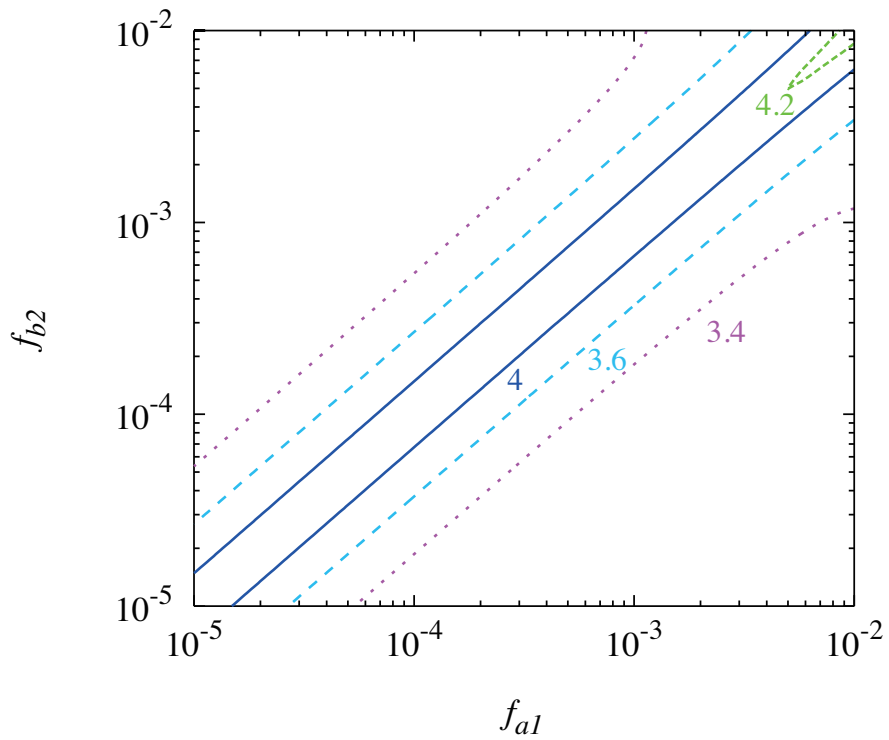


Figure 4: Contours of $-C_{\text{mc}}$ in the f_{a1} - f_{b2} plane. Here we take $K = 1$. Notice that, in the lower right and upper left region, $C_{\text{mc}} \rightarrow -(10/3)$, which corresponds to the single curvaton case.

where C_{mc} is a negative coefficient of $\mathcal{O}(1)$, which slightly depends on the parameters f_{a1} , f_{b2} and K . In Fig. 4, contours of $-C_{\text{mc}}$ are plotted in the $f_{a1}-f_{b2}$ plane, from which we can see that C_{mc} is generally $\mathcal{O}(1)$.

We also find the following inequalities for three non-linearity parameters:

$$-\frac{125}{27} \leq \frac{f_{\text{NL}} g_{\text{NL}}}{\tau_{\text{NL}}} \leq 0, \quad (121)$$

$$\frac{\tau_{\text{NL}} g_{\text{NL}}}{f_{\text{NL}}^3} \leq -\frac{24}{5}, \quad (122)$$

which may be useful for discriminating this case from other ones.

• Case II: Both curvatons are dominant at their decay

It was first noted in [83] that large non-Gaussianity can be generated even if the curvatons are dominant when it decays. This is possible only when there are two curvatons. For this case, we assume that $f_{a1} = 1$ and $f_{b1} \ll 1$. Although we also assume that $f_{b2} \simeq 1$, we keep f_{b2} up to the leading order, i.e., we expand the expressions for ζ_2 and non-linearity parameters around $f_{b2} = 1$. The limit $K \rightarrow \infty$ corresponds to the case where the first curvaton effectively homogeneous and only the second curvaton fluctuates. This situation is exactly the same as the standard (one-field) curvaton case. However, the case of $K \rightarrow 0$ is quite different from the standard curvaton model, which we are going to consider here. Taking the limit $K \rightarrow 0$, which corresponds to the case where the second curvaton is effectively homogeneous, the curvature perturbation is given by

$$\begin{aligned} \zeta_2 = & (1 - f_{b2})\zeta_{a(1)} + f_{b2}\zeta_{b(1)} + \frac{5}{4(1 - f_{b2})}[(1 - f_{b2})\zeta_{a(1)} + f_{b2}\zeta_{b(1)}]^2 \\ & + \frac{5}{12(1 - f_{b2})^2}[(1 - f_{b2})\zeta_{a(1)} + f_{b2}\zeta_{b(1)}]^3, \end{aligned} \quad (123)$$

from which we can find that this case effectively reduces to the single-source case by regarding $(1 - f_{b2})\zeta_{a(1)} + f_{b2}\zeta_{b(1)}$ being a Gaussian field. The non-linearity parameters for this case can be evaluated as

$$\frac{6}{5}f_{\text{NL}} = \frac{5}{2(1 - f_{b2})}, \quad (124)$$

$$\frac{54}{25}g_{\text{NL}} = \frac{5}{2(1 - f_{b2})^2}. \quad (125)$$

Then we have the following consistency relations:

$$\tau_{\text{NL}} = \frac{36}{25}f_{\text{NL}}^2, \quad (126)$$

$$g_{\text{NL}} = \frac{4}{15}f_{\text{NL}}^2. \quad (127)$$

In this case, g_{NL} is proportional to f_{NL}^2 and hence may become relatively large, which could be categorized as “enhanced g_{NL} ” type.

3.3.3 Multi-field inflation model

As is well known, the non-linearity parameters in the standard single field inflation models are suppressed by the slow-roll parameters evaluated at the time of horizon crossing. Due to the special property of the single field model that the curvature perturbation is conserved on super-horizon scales, the breakdown of the slow-roll conditions at the end of inflation does not induce additional corrections to the non-linearity parameters. One may then expect that the situation changes either if we go on to multi-field inflation models where more than one field contribute to the inflation dynamics, or if more than one field enter the game at the end of inflation where the slow-roll conditions are violated^{#15}. This is what we want to address in this subsection.

We first briefly review the general argument which shows that, from a naive order counting, f_{NL} , τ_{NL} and g_{NL} generated during the slow-roll inflation are suppressed by the slow-roll parameters. Then we consider a counter example given in [84–86], where the non-linearity parameters can be large during the slow-roll inflation. Then, we also consider another multi-field inflation model called multi-brid inflation model, where large non-Gaussianity is generated at the end of inflation.

We set M_{Pl} to be unity only in this subsection to simplify the equations.

• General slow-roll multi-field inflation model

Here we just present the formula for f_{NL} in a (multi-field) slow-roll inflation model with canonical kinetic terms. The formula for f_{NL} at some time t_f during inflation when the slow-roll approximation is valid can be written in terms of the potential of scalar fields V as [87, 88]

$$\frac{6}{5}f_{\text{NL}} = (N_*^d N_{d*})^{-2} \left[N_{ab}^f \Theta^a(N_f) \Theta^b(N_f) + \int_{N_*}^{N_f} dN N_a(N) Q_{bc}^a(N) \Theta^b(N) \Theta^c(N) \right], \quad (128)$$

where $N_*^a = N^a(N_*)$ and N_{ab}^f is given by

$$N_{ab}^f = \left(\frac{V^2}{V'^2} \right)_{N=N_f} \left[\eta_{ab} + 2 \frac{V^c V^d V_a V_b}{(V'^2)^2} \eta_{cd} + \frac{V_a V_b}{V^2} - 4 \frac{\eta_{c(a} V_b) V^c}{V'^2} \right]_{N=N_f}. \quad (129)$$

Here we introduced a notation for tensor indices as $t_{(ab)} = (1/2)(t_{ab} + t_{ba})$ and $V_a = \partial V / \partial \phi^a$, $\eta_{ab} = V_{ab} / V$ and $V'^2 = V_a V^a$. All the quantities on the right hand side in Eq. (128) are evaluated on the background trajectory in field space and the e-folding number is used as

^{#15}The special cases belonging to this class have already been discussed in 3.2.4 and 3.2.5.

the time coordinate (N_f and N_* are respectively the e-folding numbers corresponding to t_f and t_*). Here, we have taken the final hypersurface at $N = N_f$ to be the $V = \text{constant}$ one, which is approximately corresponding to the uniform energy density one under the slow-roll approximation. The index is raised by the inverse of the field space metric, which is assumed to be δ^{ab} here. To define N_a and Θ^a , it is convenient to introduce the propagator

$$\Lambda^a{}_b(N, N') = \left[T \exp \left(\int_{N'}^N P(N'') dN'' \right) \right]_b^a, \quad (130)$$

where T means that the matrices P_b^a are ordered in time when the exponential is expanded in power of P_b^a and

$$P^a{}_b(N) \equiv -\frac{V^a{}_b}{V} + \frac{V^a V_b}{V^2}. \quad (131)$$

Using this propagator, N_a and Θ^a are defined as

$$N_a(N) = N_b^f \Lambda^b{}_a(N_f, N), \quad \Theta^a(N) \equiv \Lambda^a{}_b(N, N_*) N_*^b, \quad (132)$$

with

$$N_b^f = \left. \frac{V V_b}{V_a V^a} \right|_{N=N_f}. \quad (133)$$

$N_a(N)$ and $\Theta^a(N)$ respectively satisfy the following equation of motion:

$$\frac{d}{dN} N_a(N) = -P_a{}^b N_b(N), \quad (134)$$

$$\frac{d}{dN} \Theta^a(N) = P_b{}^a \Theta^b(N). \quad (135)$$

The boundary conditions are given by $N_a(N_f) = N_a^f$ and $\Theta^a(N_*) = N^a(N_*)$, respectively. The three point interaction $Q^a{}_{bc}$ is given by

$$Q^a{}_{bc}(N) \equiv -\frac{V^a{}_{bc}}{V} + \frac{V^a{}_b V_c}{V^2} + \frac{V^a{}_c V_b}{V^2} + \frac{V^a V_{bc}}{V^2} - 2 \frac{V^a V_b V_c}{V^3}. \quad (136)$$

In a naive sense, the slow-roll conditions require that the potential of the inflaton is a smooth function of ϕ^a and hence higher order differentiations with respect to ϕ^a are more suppressed^{#16}. Using the similar slow-roll parameters as defined in Eq. (54) and assuming those for every field as of the same order $\mathcal{O}(\epsilon)$, P_b^a and $Q^a{}_{bc}$ can be estimated to be of $O(\epsilon)$ and $O(\epsilon^{3/2})$, respectively. Since the duration of the inflation is roughly estimated as

$$N = O\left(\frac{V}{dV/dN}\right) = O\left(\frac{HV}{V'\phi}\right) = O(\epsilon^{-1}), \quad (137)$$

^{#16} The assumption of this kind of scaling would be natural to obtain an almost scale-invariant spectrum although it is not strictly required [89].

the exponential factor in Λ_b^a defined in Eq. (130) is $\mathcal{O}(1)$. Furthermore, the value of N_a^f is estimated as

$$N_a^f = \frac{VV_a}{V^b V_b} = \mathcal{O}(\epsilon^{-1/2}). \quad (138)$$

Hence, one can see that N_a and Θ^a are $\mathcal{O}(\epsilon^{-1/2})$. Substituting these estimates into Eq. (128), we find that $f_{NL} = \mathcal{O}(\epsilon)$. This rough estimate indicates that f_{NL} is typically smaller than $\mathcal{O}(1)$ within the range of validity of our present approximation.

However, when there are some large hierarchy between the slow-roll parameters, which is possible for a multi-field case, f_{NL} can be much larger than $\mathcal{O}(\epsilon)$. For example, let us consider the case where there is huge difference in size between ϵ_1 and ϵ_2 (which are slow-roll parameters for ϕ_1 and ϕ_2 , respectively). Assuming $\epsilon_1 \gg \epsilon_2$, f_{NL} can be estimated as $f_{NL} \sim \mathcal{O}(\epsilon) \times (\epsilon_1/\epsilon_2)$, which can be large even though $\epsilon_1, \epsilon_2 < \mathcal{O}(1)$. Hence, a multi-field inflation model can generate large non-Gaussianity although a typical estimate of f_{NL} is $\mathcal{O}(\epsilon)$.

Furthermore, the formulation given above is applicable only when the slow-roll condition is satisfied. However, when the slow-roll condition is violated, in particular, at the end of hybrid inflation, one could have large f_{NL} . Some explicit example models of large f_{NL} will be discussed in the following.

The above discussion on f_{NL} , of course, can be applied to the higher order non-linearity parameters, i.e., τ_{NL} and g_{NL} . Following Ref. [31], τ_{NL} and g_{NL} are respectively given by

$$\tau_{NL} = \frac{1}{(N_*^b N_{*b})^3} \Omega_a(N_*) \Omega^a(N_*), \quad (139)$$

$$\begin{aligned} \frac{54}{25} g_{NL} = \frac{1}{(N_*^b N_{*b})^3} & \left[N_{abc}^f \Theta(N_f) \Theta^b(N_f) \Theta^c(N_f) + \int_{N_*}^{N_f} dN N_a(N) S_{bcd}^a(N) \Theta^b(N) \Theta^c(N) \Theta^d(N) \right. \\ & \left. + 3 \int_{N_*}^{N_f} dN \Omega_a(N) Q_{bc}^a(N) \Theta^b(N) \Theta^c(N) \right], \quad (140) \end{aligned}$$

where $\Omega^a(N)$ is a new vector variable obtained by solving

$$\frac{d}{dN} \Omega_a(N) = -\Omega_b(N) P_a^b(N) - N_b(N) Q_{ac}^b(N) \Theta^c(N), \quad (141)$$

with the boundary condition $\Omega_a(N_f) = N_{ab}^f \Theta^b(N_f)$. N_{abc}^f is given by

$$\begin{aligned} N_{abc}^f = \left(\frac{V^2}{V'^2} \right) & \left[\frac{V_{abc}}{V} + 6 \frac{V_a V_b V_c}{V^3} - 2 \frac{V_a V_b V_c V^d V^e V^f V_{def}}{(V'^2)^3} - 4 \eta_{de} \frac{V^d V^e V_a V_b V_c}{V (V'^2)^2} \right. \\ & - 4 \eta_{de} \frac{V^{ef} V^d V_f V_a V_b V_c}{(V'^2)^3} + 6 \frac{V_{de(a} V^d V^e V_b V_c)}{V (V'^2)^2} + 12 \eta^{de} \frac{V_d V_{e(a} V_b V_c)}{(V'^2)^2} \\ & \left. - 6 \frac{V^d}{V} \eta_{d(a} \frac{V_b V_c)}{V'^2} - 3 \frac{V^d V_{(a} V_{bc)d}}{V'^2} - 6 \eta_{d(a} \frac{V_b V_c^d)}{V'^2} + 6 \eta_{de} \frac{V^d V^e V_{(a} N_{bc)}^f}{V V'^2} - 6 \frac{V^d}{V} \eta_{d(a} N_{bc)}^f \right], \quad (142) \end{aligned}$$

and the four point interaction $S_{bcd}^a(N)$ is given by differentiating Q_{bc}^a with respect to ϕ^a . Then, based on the standard slow-roll approximation, where $V_{ab}/V = O(\epsilon)$, $V_{abc}/V = O(\epsilon^{3/2})$ and $V_{abcd}/V = O(\epsilon^2)$, the orders of the non-linearity parameters τ_{NL} and g_{NL} are respectively estimated as

$$\tau_{\text{NL}} = O(\epsilon^2), \quad g_{\text{NL}} = O(\epsilon^2). \quad (143)$$

From this rough estimation, we find that τ_{NL} and g_{NL} are more suppressed by the slow-roll parameters than f_{NL} .

As in the case of f_{NL} , the magnitudes of τ_{NL} and g_{NL} are not necessarily suppressed like $O(\epsilon^2)$ and can be much larger than the rough estimation in some situations. Furthermore, if slow-roll conditions are violated, we may have a chance to generate large non-Gaussianity, which is not accommodated in this formalism. Indeed, some explicit multi-field inflation models have been constructed that can produce large non-Gaussianity. In the following, we consider the generation of non-Gaussianity in those models.

• Two-field slow-roll inflation

In Ref. [84–86], the authors have shown that the large non-Gaussianity can be generated even during the slow-roll inflation. As an example, we consider the potential of the form:

$$V(\phi_1, \phi_2) = V_{\text{inf}} \exp\left(\frac{1}{2}\eta_1\phi_1^2 + \frac{1}{2}\eta_2\phi_2^2\right). \quad (144)$$

In the following, we assume that $|\eta_1\phi_1^2| \ll 1$, $|\eta_2\phi_2^2| \ll 1$ and V_{inf} is constant. In fact, the above type of potential can lead to large *negative* f_{NL} in order to have a red-tilted spectral index, which is required to be consistent with current observations. Since *positive* f_{NL} is favored at this moment, this model might not be so attractive in this respect, however, we briefly discuss this model as an example, in which large non-Gaussianity may be generated even during a slow-roll inflation when two fields exist.

By using slow-roll solutions, we can write the inflaton field values during inflation as

$$\phi_1 = \phi_{1*} e^{-\eta_1 N}, \quad \phi_2 = \phi_{2*} e^{-\eta_2 N}. \quad (145)$$

Here, we consider only the slowly-rolling phase and do not specify how the end of inflation is triggered. Hence we evaluate the curvature perturbation on the uniform energy density hypersurface, which can be determined by $V = \text{constant}$ hypersurface as in the “general slow-roll multi-field inflation” model discussed above.

The spectral index and the tensor-to-scalar ratio are calculated as

$$n_s - 1 = -2\epsilon_* + 2 \frac{(\eta_1 - 2\epsilon e^{2\eta_1 N})\epsilon_1 e^{-2\eta_1 N} + (\eta_2 - 2\epsilon e^{2\eta_2 N})\epsilon_2 e^{-2\eta_2 N}}{2\epsilon_1 e^{-2\eta_1 N} + 2\epsilon_2 e^{-2\eta_2 N}}, \quad (146)$$

$$r = \frac{16\epsilon^2}{2\epsilon_1 e^{-2\eta_1 N} + 2\epsilon_2 e^{-2\eta_2 N}}. \quad (147)$$

The non-linearity parameter f_{NL} can be evaluated as

$$\frac{6}{5}f_{\text{NL}} = \frac{-\epsilon(\eta_1\epsilon_1 + \eta_2\epsilon_2 e^{4(\eta_1-\eta_2)N}) + (2/\epsilon)\epsilon_1\epsilon_2(\eta_1\epsilon_2 + \eta_2\epsilon_1)(1 - e^{2(\eta_1-\eta_2)N})^2}{(\epsilon_1 + \epsilon_2 e^{2(\eta_1-\eta_2)N})^2}, \quad (148)$$

where the slow-roll parameters ϵ_1 and ϵ_2 are defined for ϕ_1 and ϕ_2 , respectively, in the same manner as in Eq. (54) and $\epsilon = \epsilon_1 + \epsilon_2$. It has been shown that large non-Gaussianity can be generated when the following condition is met^{#17}:

$$\frac{\dot{\phi}_2^2}{\dot{\phi}_1^2 + \dot{\phi}_2^2} \simeq \frac{\epsilon_2}{\epsilon_1 + \epsilon_2} \ll 1. \quad (149)$$

In this case, we can have simpler formulae for n_s , r and f_{NL} as follows,

$$n_s - 1 \simeq \frac{2(\eta_1 + R\eta_2)}{1 + R}, \quad (150)$$

$$r \simeq \frac{16\epsilon_*}{1 + R}, \quad (151)$$

$$\frac{6}{5}f_{\text{NL}} \simeq \frac{R}{(1 + R)^2} \eta_2 e^{2(\eta_1-\eta_2)N}, \quad (152)$$

where R is defined as $R = N_{\phi_2}^2/N_{\phi_1}^2 = (\epsilon_2/\epsilon_1) e^{2(\eta_1-\eta_2)N}$ (see Eq. (86)). From the above expressions, we find that $\eta_2 > 0$ should be satisfied to have large positive f_{NL} . However, large f_{NL} requires $\eta_1 > \eta_2$ to have a big factor from $e^{2(\eta_1-\eta_2)N}$, which gives blue-tilted spectral index. Thus, to have a consistent value of n_s with current observations^{#18}, f_{NL} should be negative even though its size can be very large. Thus, in this sense, this model might not be a promising one from the viewpoint of current observations. However, one could consider another potential, which may give different predictions for n_s , r and f_{NL} .

As a final remark, we mention the relation between f_{NL} and g_{NL} , which holds for the case considered here [85]:

$$g_{\text{NL}} = \frac{10}{3} \frac{R(\eta_1 - 2\eta_2) - \eta_2}{1 + R} f_{\text{NL}}. \quad (153)$$

Thus, this model can be regarded as ‘‘suppressed g_{NL} ’’ type. For τ_{NL} , we do not find anything more than the relation given by Eq. (92).

^{#17} In fact, there is another case where large non-Gaussianity can be generated. However, such another case follows the same argument here by changing some parameters appropriately because of the symmetry of the potential [85].

^{#18} Current limit for the spectral index is $n_s = 0.963 \pm 0.012$ (68%CL) [1].

• **Multi-field hybrid (Multi-brid) inflation**

Here, we discuss a multi-field hybrid inflation (dubbed as multi-brid inflation [90]) model. The analysis of the non-Gaussianity in this model is similar to that in the previous multi-field slow-roll inflation model, where multiple (inflaton) fields can affect the dynamics of inflation. The difference between this multi-brid model and the previous multi-field slow-roll model is mainly the assumption on how the inflation ends: in the multi-brid model, the end of inflation is characterized by an ellipse in the field space^{#19}. In the following, we discuss two types of potential in the multi-brid inflation model.

A. Quadratic potential model

Let us first consider the model whose potential is approximately quadratic [93]:

$$V = V_0 \exp\left(\frac{1}{2}\eta_1\phi_1^2 + \frac{1}{2}\eta_2\phi_2^2\right), \quad (154)$$

where

$$V_0 = \frac{1}{2}G(\phi_1, \phi_2)\chi^2 + \frac{\lambda}{4}\left(\chi^2 - \frac{v^2}{\lambda}\right)^2, \quad (155)$$

$$G(\phi_1, \phi_2) = g_1^2(\phi_1 \cos \alpha + \phi_2 \sin \alpha)^2 + g_2^2(-\phi_1 \sin \alpha + \phi_2 \cos \alpha)^2. \quad (156)$$

Here η_1 and η_2 can be regarded as the masses squared for the inflatons ϕ_1 and ϕ_2 normalized by V_0 , respectively. χ is a water-fall field and its VEV is characterized by v . The angle α corresponds to the rotation of the ellipse of $G(\phi_1, \phi_2) = \text{const.}$ in the field space relative to the ϕ_1 axis. The slow-roll equation of motion for ϕ_i is given by

$$\frac{d\phi_i}{dN} = \eta_i\phi_i, \quad (157)$$

where N is the number of e -folds and $dN = -Hdt$, from which we obtain

$$N = \frac{1}{\eta_1} \ln \phi_1 - \frac{1}{\eta_1} \ln \phi_{1,f}. \quad (158)$$

The inflation ends when the following condition is satisfied,

$$v^2 = g_1^2(\phi_{1,f} \cos \alpha + \phi_{2,f} \sin \alpha)^2 + g_2^2(-\phi_{1,f} \sin \alpha + \phi_{2,f} \cos \alpha)^2, \quad (159)$$

^{#19} There are several related studies [91, 92]. This model, in fact, includes the inhomogeneous end of hybrid inflation model, discussed in section 3.2.4, as a single source limit.

where $\phi_{i,f}$ denotes the field value at the end of inflation. In order to parameterize $\phi_{i,f}$, we introduce an angular parameter γ defined as

$$\frac{v}{g_1} \cos \gamma \equiv \phi_{1,f} \cos \alpha + \phi_{2,f} \sin \alpha, \quad (160)$$

$$\frac{v}{g_2} \sin \gamma \equiv -\phi_{1,f} \sin \alpha + \phi_{2,f} \cos \alpha. \quad (161)$$

These equations imply

$$\phi_{1,f} = \frac{v}{g_1} \cos \alpha \cos \gamma - \frac{v}{g_2} \sin \alpha \sin \gamma, \quad (162)$$

$$\phi_{2,f} = \frac{v}{g_1} \sin \alpha \cos \gamma + \frac{v}{g_2} \cos \alpha \sin \gamma. \quad (163)$$

The angle γ represents the position of the inflationary trajectory at the end of inflation^{#20}. From the equation of motion, we can show that $\phi_1^{\eta_1}/\phi_2^{\eta_2}$ is a constant of motion, from which we can derive the following equation:

$$\begin{aligned} \frac{1}{\eta_1} \ln \phi_1 - \frac{1}{\eta_2} \ln \phi_2 &= \frac{1}{\eta_1} \ln \phi_{1,f} - \frac{1}{\eta_2} \ln \phi_{2,f} \\ &= \frac{1}{\eta_1} \ln \left[\frac{v}{g_1 g_2} (g_2 \cos \alpha \cos \gamma - g_1 \sin \alpha \sin \gamma) \right] \\ &\quad - \frac{1}{\eta_2} \ln \left[\frac{v}{g_1 g_2} (g_2 \sin \alpha \cos \gamma + g_1 \cos \alpha \sin \gamma) \right]. \end{aligned} \quad (164)$$

By expanding N given in Eq. (158), we can obtain δN , up to the third order, as

$$\begin{aligned} \delta N &= \frac{1}{\eta_1} \left[\frac{\delta \phi_1}{\phi_1} - \frac{1}{2} \left(\frac{\delta \phi_1}{\phi_1} \right)^2 + \frac{1}{3} \left(\frac{\delta \phi_1}{\phi_1} \right)^3 - \frac{\partial \ln \phi_{1,f}}{\partial \gamma} (\delta_{(1)}\gamma + \delta_{(2)}\gamma + \delta_{(3)}\gamma) \right. \\ &\quad \left. - \frac{1}{2} \frac{\partial^2 \ln \phi_{1,f}}{\partial \gamma^2} (\delta_{(1)}\gamma + \delta_{(2)}\gamma)^2 - \frac{1}{6} \frac{\partial^3 \ln \phi_{1,f}}{\partial \gamma^3} (\delta_{(1)}\gamma)^3 \right], \end{aligned} \quad (165)$$

where $\delta_{(1)}\gamma$, $\delta_{(2)}\gamma$ and $\delta_{(3)}\gamma$ are respectively the first, the second and the third order perturbations of γ . Since they can be described in terms of $\delta\phi_i$ by the relation given by Eq. (164), the resultant expression of δN or the curvature perturbation ζ with

^{#20} The definitions of α and γ are shown schematically in Fig. 1 of [93].

respect to $\delta\phi_i$ is given by

$$\begin{aligned}
\zeta = \delta N = & \frac{1}{F(\gamma)} \left[-A_2 \frac{\delta\phi_1}{\phi_1} + A_1 \frac{\delta\phi_2}{\phi_2} \right] \\
& + \frac{1}{2F(\gamma)} \left[A_2 \left(\frac{\delta\phi_1}{\phi_1} \right)^2 - A_1 \left(\frac{\delta\phi_2}{\phi_2} \right)^2 + \frac{G(\gamma)}{F(\gamma)^2} \left(\eta_2 \frac{\delta\phi_1}{\phi_1} - \eta_1 \frac{\delta\phi_2}{\phi_2} \right)^2 \right] \\
& + \frac{1}{6F(\gamma)} \left\{ -2A_2 \left(\frac{\delta\phi_1}{\phi_1} \right)^3 + 2A_1 \left(\frac{\delta\phi_2}{\phi_2} \right)^3 \right. \\
& \quad \left. - 3 \frac{G(\gamma)}{F(\gamma)^2} \left(\eta_2 \frac{\delta\phi_1}{\phi_1} - \eta_1 \frac{\delta\phi_2}{\phi_2} \right) \left[\eta_2 \left(\frac{\delta\phi_1}{\phi_1} \right)^2 - \eta_1 \left(\frac{\delta\phi_2}{\phi_2} \right)^2 \right] \right. \\
& \quad \left. + \frac{1}{F(\gamma)^4} (G'(\gamma)F(\gamma) - 3G(\gamma)F'(\gamma)) \left(\eta_2 \frac{\delta\phi_1}{\phi_1} - \eta_1 \frac{\delta\phi_2}{\phi_2} \right)^3 \right\}, \quad (166)
\end{aligned}$$

where a prime denotes the derivative with respect to γ , and A_1, A_2, F and G are defined as

$$A_1 = \frac{\partial \ln \phi_{1,f}}{\partial \gamma}, \quad A_2 = \frac{\partial \ln \phi_{2,f}}{\partial \gamma}, \quad (167)$$

$$F(\gamma) = \eta_2 A_1 - \eta_1 A_2, \quad G(\gamma) = A_1' A_2 - A_1 A_2'. \quad (168)$$

The spectral index and the tensor-to-scalar ratio are respectively given by

$$n_s - 1 = 2 \frac{\eta_1 A_2^2 / \phi_1^2 + \eta_2 A_1^2 / \phi_2^2}{A_2^2 / \phi_1^2 + A_1^2 / \phi_2^2} - (\eta_1^2 \phi_1^2 + \eta_2^2 \phi_2^2), \quad (169)$$

$$r = \frac{8F^2}{A_2^2 / \phi_1^2 + A_1^2 / \phi_2^2}. \quad (170)$$

Here it is worth noting that the tensor-to-scalar ratio r can be relatively large even when f_{NL} is large in this model [93]. As mentioned in Section 3.3.1, the tensor-to-scalar ratio r tends to be very small in most models generating large non-Gaussianity. However, the multi-brid inflation model is one of those which can realize large tensor-to-scalar ratio and large non-Gaussianity simultaneously.

For the non-linearity parameters, we obtain

$$\frac{6}{5} f_{\text{NL}} = \frac{F}{(A_2^2 / \phi_1^2 + A_1^2 / \phi_2^2)^2} \left(\frac{A_2^3}{\phi_1^4} - \frac{A_1^3}{\phi_2^4} \right) + \frac{G/F}{(A_2^2 / \phi_1^2 + A_1^2 / \phi_2^2)^2} \left(\eta_1 \frac{A_1}{\phi_2^2} + \eta_2 \frac{A_2}{\phi_1^2} \right)^2, \quad (171)$$

$$\begin{aligned}
\tau_{\text{NL}} = & \frac{F^2}{(A_2^2 / \phi_1^2 + A_1^2 / \phi_2^2)^3} \left(\frac{A_2^4}{\phi_1^6} + \frac{A_1^4}{\phi_2^6} \right) \\
& + \frac{G^2 / F^2}{(A_2^2 / \phi_1^2 + A_1^2 / \phi_2^2)^3} \left(\frac{\eta_2^2}{\phi_1^2} + \frac{\eta_1^2}{\phi_2^2} \right) \left(\eta_1 \frac{A_1}{\phi_2^2} + \eta_2 \frac{A_2}{\phi_1^2} \right)^2 \\
& + 2 \frac{G}{(A_2^2 / \phi_1^2 + A_1^2 / \phi_2^2)^3} \left(\eta_1 \frac{A_1}{\phi_2^2} + \eta_2 \frac{A_2}{\phi_1^2} \right) \left(\eta_2 \frac{A_2^2}{\phi_1^4} - \eta_1 \frac{A_1^2}{\phi_2^4} \right), \quad (172)
\end{aligned}$$

$$\begin{aligned}
\frac{54}{25}g_{\text{NL}} = & 2\frac{F^2}{(A_2^2/\phi_1^2 + A_1^2/\phi_2^2)^3} \left(\frac{A_2^4}{\phi_1^6} + \frac{A_1^4}{\phi_2^6} \right) \\
& + 3\frac{G}{(A_2^2/\phi_1^2 + A_1^2/\phi_2^2)^3} \left(\eta_1 \frac{A_1}{\phi_2^2} + \eta_2 \frac{A_2}{\phi_1^2} \right) \left(\eta_2 \frac{A_2^2}{\phi_1^4} - \eta_1 \frac{A_1^2}{\phi_2^4} \right) \\
& - \frac{G/F}{(A_2^2/\phi_1^2 + A_1^2/\phi_2^2)^3} \left(\frac{G'}{G} - 3\frac{F'}{F} \right) \left(\eta_1 \frac{A_1}{\phi_2^2} + \eta_2 \frac{A_2}{\phi_1^2} \right)^3. \quad (173)
\end{aligned}$$

Since these expressions are rather complicated in general, we consider three limiting cases, which may generate large non-Gaussianity: Single-source case, equal mass case ($\eta_1 = \eta_2 = \eta$), and large mass ratio case ($\eta_1 \gg \eta_2$).

I. Single source case

The setup of the multi-brid inflation model includes the inhomogeneous end of hybrid inflation discussed in section 3.2.4 as a limiting case where fluctuations of a single field, ϕ_1 or ϕ_2 , only contribute to the curvature fluctuation and the angle $\alpha = 0$. Here we regard ϕ_1 as the inflaton and ϕ_2 as another light scalar field, denoted as σ in Section 3.2.4, in which the mass of the inflaton is much bigger than that of a light scalar field (i.e. $\eta_1 \gg \eta_2$). In this limit, we also assume that the inflaton does not contribute to the power spectrum, which is represented by the following condition:

$$\frac{A_2^2}{\phi_1^2} \ll \frac{A_1^2}{\phi_2^2} \iff g_1^2 \phi_{1,f}^2 \phi_2 \ll g_2^2 \phi_{2,f}^2 \phi_1 \quad \left(\iff g_1^2 \phi_{1,f} \ll g_2^2 \phi_{2,f} \right). \quad (174)$$

The last inequality applies only when $\eta_1 N \lesssim 1$, which leads to the relation $\phi_{1,f}/\phi_1 \simeq \phi_{2,f}/\phi_2$. In order to realize large non-Gaussianity, we further assume that $A_1^2 \ll A_2^2$, which is equivalent to consider the situation where $g_2^2 \phi_{2,f}^2 \ll g_1^2 \phi_{1,f}^2 \simeq v^2$. Putting these conditions to the above general expressions with $\alpha = 0$, we obtain the following formulae,

$$\frac{6}{5}f_{\text{NL}} \simeq \eta_1 \frac{g_1^2 \phi_{1,f}^2}{g_2^2 \phi_{2,f}^2} \simeq \eta_1 \frac{v^2}{g_2^2 \phi_{2,f}^2}, \quad (175)$$

$$\frac{54}{25}g_{\text{NL}} \simeq 6\eta_1(\eta_1 - 2\eta_2) \frac{g_1^2 \phi_{1,f}^2}{g_2^2 \phi_{2,f}^2} \simeq \frac{36}{5}\eta_1 f_{\text{NL}}, \quad (176)$$

$$\tau_{\text{NL}} \simeq \left(\frac{6}{5}f_{\text{NL}} \right)^2, \quad (177)$$

where the following equations have been used:

$$F(\gamma) \simeq -\eta_1 \frac{g_1 \phi_{1,f}}{g_2 \phi_{2,f}}, \quad G(\gamma) \simeq -2 \frac{g_1 \phi_{1,f}}{g_2 \phi_{2,f}}. \quad (178)$$

These results reproduce those obtained for the inhomogeneous end of hybrid inflation model discussed in Section 3.2.4 and again notice that $g_{\text{NL}}/f_{\text{NL}}$ is suppressed by the slow-roll parameter η_1 .

II. Equal mass case ($\eta_1 = \eta_2 = \eta$)

In the equal mass limit ($\eta_1 = \eta_2 = \eta$), α -dependence disappears [93] because of the symmetry. Hence, we can set $\alpha = 0$ without loss of generality. In such a case, we have

$$A_1 = -\frac{g_2\phi_{2,f}}{g_1\phi_{1,f}} = -\tan\gamma, \quad A_2 = \frac{g_1\phi_{1,f}}{g_2\phi_{2,f}} = -\frac{1}{A_1}, \quad (179)$$

$$F = -\frac{\eta}{\sin\gamma\cos\gamma}, \quad G = -\frac{2}{\sin\gamma\cos\gamma} = \frac{2}{\eta}F. \quad (180)$$

Then, the tensor-to-scalar ratio and the spectral index are reduced to

$$r = \frac{8\eta^2 v^2 e^{2\eta N_k}}{(g_1^2 \cos^2 \gamma + g_2^2 \sin^2 \gamma)}, \quad (181)$$

$$n_s - 1 = 2\eta - \frac{r}{8g_1^2 g_2^2} (g_1^2 \cos^2 \gamma + g_2^2 \sin^2 \gamma) (g_1^2 \sin^2 \gamma + g_2^2 \cos^2 \gamma), \quad (182)$$

where we have used $\phi_i = \phi_{i,f} e^{\eta N_k}$. The non-linearity parameters in this limit are given by

$$\frac{6}{5}f_{\text{NL}} = -\frac{\eta}{(g_1^2 \cos^2 \gamma + g_2^2 \sin^2 \gamma)^2} \left[g_1^4 \cos^2 \gamma + g_2^4 \sin^2 \gamma - 2(g_1^2 - g_2^2)^2 \sin^2 \gamma \cos^2 \gamma \right], \quad (183)$$

$$\tau_{\text{NL}} = \frac{\eta^2}{(g_2^2 \sin^2 \gamma + g_1^2 \cos^2 \gamma)^3} \left[g_1^6 \cos^2 \gamma + g_2^6 \sin^2 \gamma - 4(g_1^2 - g_2^2)^2 (g_1^2 \cos^2 \gamma + g_2^2 \sin^2 \gamma) \sin^2 \gamma \cos^2 \gamma \right], \quad (184)$$

$$\frac{54}{25}g_{\text{NL}} = \frac{2\eta^2}{(g_2^2 \sin^2 \gamma + g_1^2 \cos^2 \gamma)^3} \left\{ g_1^6 \cos^2 \gamma + g_2^6 \sin^2 \gamma - (g_1^2 - g_2^2)^2 \sin^2 \gamma \cos^2 \gamma [3(g_1^2 + g_2^2) + 2(g_1^2 - g_2^2)(\cos^2 \gamma - \sin^2 \gamma)] \right\}. \quad (185)$$

After some algebra, we can find the simple relation between f_{NL} and g_{NL} :

$$g_{\text{NL}} = -\frac{10}{3}\eta f_{\text{NL}} - \frac{50}{27}\eta^2. \quad (186)$$

As is the same with the single-source case, the ratio of the non-linearity parameters $g_{\text{NL}}/f_{\text{NL}}$ is suppressed by the slow-roll parameter η in this case as well. We also obtain the following relation,

$$\tau_{\text{NL}} = \left(\frac{1 + \bar{R}}{\bar{R}}\right) \left(\frac{6}{5}f_{\text{NL}}\right)^2, \quad (187)$$

where the ratio \bar{R} is given by

$$\bar{R} = \left[\frac{g_1^4 \cos^2 \gamma + g_2^4 \sin^2 \gamma - 2(g_1^2 - g_2^2) \sin^2 \gamma \cos^2 \gamma}{g_1 g_2 (g_1^2 - g_2^2) \sin \gamma \cos \gamma} \right]^2, \quad (188)$$

from which we can calculate the size of τ_{NL} relative to f_{NL}^2 .

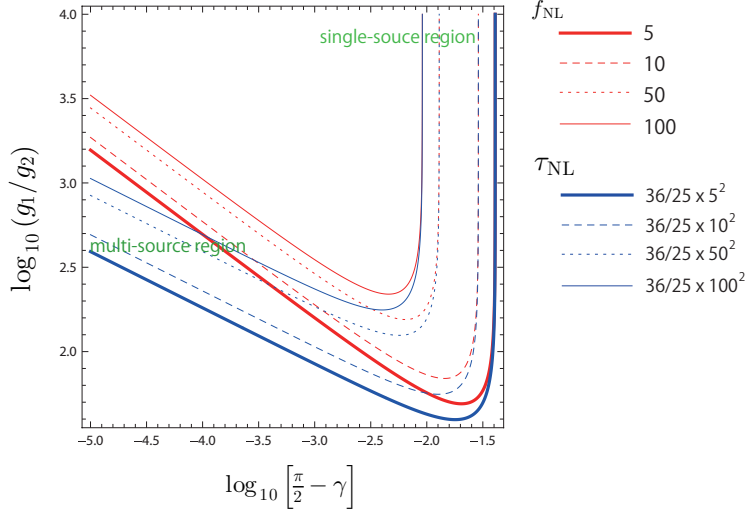


Figure 5: Contours of f_{NL} (red lines) and τ_{NL} (blue lines) on the γ - g_1/g_2 plane for the equal mass case. The blue lines are for $f_{\text{NL}} = 5$ (thick solid), 10 (dashed), 50 (dotted) and 100 (thin solid). The red lines are for $\tau_{\text{NL}} = 36/25 \times 5^2$ (thick solid), $36/25 \times 10^2$ (dashed), $36/25 \times 50^2$ (dotted) and $36/25 \times 100^2$ (thin solid). We set $\eta_1 = \eta_2 = \eta = 0.01$ here. From this figure, we can find that the upper right region on this plane corresponds to the single-source case because the equality $\tau_{\text{NL}} = 36/25 \times f_{\text{NL}}^2$ is satisfied, which holds in the single source case.

In Fig. 5, we depict contours of f_{NL} (red lines) and τ_{NL} (blue lines) on the γ - g_1/g_2 plane. As seen from this figure, we can find that the upper right region

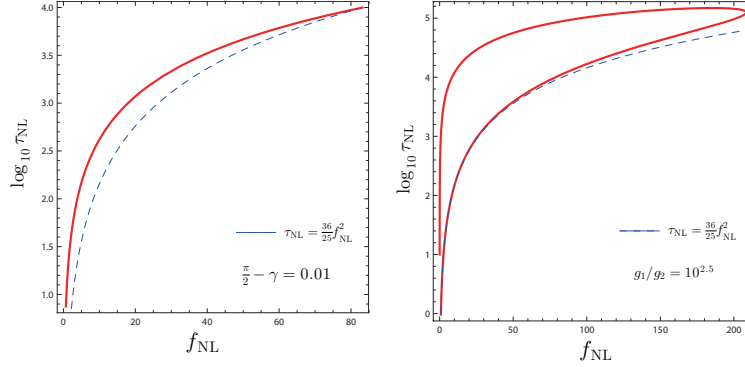


Figure 6: $f_{\text{NL}}-\tau_{\text{NL}}$ diagrams for the equal mass case. In the left panel, the red solid line is for the case with $\frac{\pi}{2} - \gamma = 0.01$ and g_1/g_2 being varied. In the right panel, the red solid line is for the case with $g_1/g_2 = 10^{2.5}$ and γ being varied. In both the panels, the blue dashed lines indicate the equality $\tau_{\text{NL}} = 36/25 \times f_{\text{NL}}^2$. We set $\eta_1 = \eta_2 = \eta = 0.01$ and $\alpha = 0$ here.

on this plane corresponds to the single source case because the equality $\tau_{\text{NL}} = 36/25 \times f_{\text{NL}}^2$, which holds in the single-source case, is approximated satisfied.

In Fig. 6, we also show the $f_{\text{NL}}-\tau_{\text{NL}}$ diagrams in this limiting case. In the left panel, the red solid line is for the case with $\frac{\pi}{2} - \gamma = 0.01$. In the right panel, the red solid line is for the case with $g_1/g_2 = 10^{2.5}$. In both the panels, the blue dashed lines show the equality $\tau_{\text{NL}} = 36/25 \times f_{\text{NL}}^2$.

III. Large mass ratio case ($\eta_1 \gg \eta_2$) with $A_2 \ll 1$

In order to study the case of large mass ratio, we have set $A_2 = 0$ in the expressions for the non-linearity parameters Eqs. (171)–(173). However, we would like to stress that, as already pointed out in Ref. [93], our expressions apply for an arbitrary mass ratio as long as $A_2 = 0$. From the expression for δN given in Eq. (165), we can easily find that the condition $A_2 = 0$ corresponds to neglecting the linear contribution from $\delta\gamma$. In such a case, the non-linearity parameters are given by

$$\frac{6}{5}f_{\text{NL}} = \eta_2 \left[-1 + \left(\frac{\eta_1}{\eta_2} \right)^2 \frac{1}{A_1^2} \right], \quad (189)$$

$$\tau_{\text{NL}} = \left(\frac{6}{5}f_{\text{NL}} \right)^2 + \frac{\eta_2^2 \phi_2^2}{\eta_1^2 \phi_1^2} \eta_2^2 \left(\frac{\eta_1}{\eta_2} \right)^4 \frac{1}{A_1^4}, \quad (190)$$

$$\frac{54}{25}g_{\text{NL}} = -3(\eta_1 + \eta_2) \frac{6}{5}f_{\text{NL}} - \eta_2^2 - 3\eta_2\eta_1 + 3 \left(1 - \frac{\eta_2}{\eta_1} \right) \eta_2^2 \left(\frac{\eta_1}{\eta_2} \right)^4 \frac{1}{A_1^4}. \quad (191)$$

From these equations, we find that, even if A_1 is order of unity, large mass ratio $\eta_1 \gg \eta_2$ can generate the large non-Gaussianity. For large f_{NL} , we can

approximately obtain the following relations,

$$\frac{6}{5}f_{\text{NL}} \simeq \eta_2 \left(\frac{\eta_1}{\eta_2} \right)^2 \frac{1}{A_1^2}, \quad (192)$$

$$\tau_{\text{NL}} \simeq \left(1 + \frac{\eta_2^2 \phi_2^2}{\eta_1^2 \phi_1^2} \right) \left(\frac{6}{5}f_{\text{NL}} \right)^2, \quad (193)$$

$$\frac{54}{25}g_{\text{NL}} \simeq 3 \left(1 - \frac{\eta_2}{\eta_1} \right) \left(\frac{6}{5}f_{\text{NL}} \right)^2 - (\eta_1 + \eta_2) \frac{18}{5}f_{\text{NL}}. \quad (194)$$

Here, it should be noticed that g_{NL} is of the order of f_{NL}^2 and can become relatively large. This is because both fields significantly contribute to the non-linearity parameters as well as the power spectrum despite their large mass ratio.

It should also be noted that, in the single source case discussed earlier, we have assumed not only the large mass ratio but also the large ratio of the field values, ϕ_1 and ϕ_2 , in order to get the large non-Gaussianity. In such a case, the curvature perturbation was effectively generated only from a single source at all orders.

On the other hand, here, we have assumed only $A_2 = 0$. From Eq. (166), we can find that this case is different from the single source case because the curvature perturbation can be generated from multi-source at the second (and also the third) order. Hence, the above expressions of non-linearity parameters are different from those in the pure single source case.

B. Linear potential model

Next let us briefly discuss the linear multi-brid model whose potential is given by [90, 94]

$$V = V_0 \exp(m_1 \phi_1 + m_2 \phi_2), \quad (195)$$

where

$$V_0 = \frac{1}{2} [g_1^2 (\phi_1 \cos \alpha + \phi_2 \sin \alpha)^2 + g_2^2 (-\phi_1 \sin \alpha + \phi_2 \cos \alpha)^2] \chi^2 + \frac{\lambda}{4} \left(\chi^2 - \frac{v^2}{\lambda} \right)^2. \quad (196)$$

For this potential, the slow-roll equation of motion is

$$\frac{d\phi_i}{dN} = m_i. \quad (197)$$

Hence the total e -folding number is evaluated as

$$N = \frac{1}{m_1} (\phi_1 - \phi_{1,f}), \quad (198)$$

where $\phi_{1,f}$ is the value of the scalar field at the end of inflation. As in a usual hybrid inflation model, the inflation ends when the following relation is satisfied:

$$v^2 = g_1^2 (\phi_{1,f} \cos \alpha + \phi_{2,f} \sin \alpha)^2 + g_2^2 (-\phi_{1,f} \sin \alpha + \phi_{2,f} \cos \alpha)^2. \quad (199)$$

We again parameterize $\phi_{1,f}$ and $\phi_{2,f}$ as in Eqs. (162) and (163). The field values at the end of inflation can be described in terms of the values of ϕ_1 and ϕ_2 at some time during inflation as

$$\frac{1}{m_1} \phi_1 - \frac{1}{m_2} \phi_2 = \frac{1}{m_1} \phi_{1,f} - \frac{1}{m_2} \phi_{2,f}. \quad (200)$$

Perturbing the above equation, we have the following relation,

$$\begin{aligned} \frac{1}{m_1} \delta \phi_1 - \frac{1}{m_2} \delta \phi_2 = & \left(\frac{1}{m_1} \frac{\partial \phi_{1,f}}{\partial \gamma} - \frac{1}{m_2} \frac{\partial \phi_{2,f}}{\partial \gamma} \right) \delta \gamma \\ & + \frac{1}{2} \left(\frac{1}{m_1} \frac{\partial^2 \phi_{1,f}}{\partial \gamma^2} - \frac{1}{m_2} \frac{\partial^2 \phi_{2,f}}{\partial \gamma^2} \right) \delta \gamma^2 + \frac{1}{6} \left(\frac{1}{m_1} \frac{\partial^3 \phi_{1,f}}{\partial \gamma^3} - \frac{1}{m_2} \frac{\partial^3 \phi_{2,f}}{\partial \gamma^3} \right) \delta \gamma^3. \end{aligned} \quad (201)$$

From Eq. (198), δN is given by

$$\delta N = \frac{1}{m_1} \delta \phi_1 - \frac{1}{m_1} \frac{\partial \phi_{1,f}}{\partial \gamma} \delta \gamma - \frac{1}{2} \frac{1}{m_1} \frac{\partial^2 \phi_{1,f}}{\partial \gamma^2} \delta \gamma^2 - \frac{1}{6} \frac{1}{m_1} \frac{\partial^3 \phi_{1,f}}{\partial \gamma^3} \delta \gamma^3. \quad (202)$$

Substituting Eq. (201) into Eq. (198), we have the expression of δN up to the third order,

$$\begin{aligned} \delta N = & \frac{1}{\tilde{F}(\gamma)} \left(-\tilde{A}_2(\gamma) \delta \phi_1 + \tilde{A}_1(\gamma) \delta \phi_2 \right) + \frac{\tilde{G}(\gamma)}{2\tilde{F}(\gamma)^3} (m_2 \delta \phi_1 - m_1 \delta \phi_2)^2 \\ & - \frac{\tilde{G}(\gamma) \tilde{F}'(\gamma)}{2\tilde{F}(\gamma)^5} (m_2 \delta \phi_1 - m_1 \delta \phi_2)^3, \end{aligned} \quad (203)$$

where

$$\tilde{A}_1(\gamma) = \frac{\partial \phi_{1,f}}{\partial \gamma}, \quad \tilde{A}_2(\gamma) = \frac{\partial \phi_{2,f}}{\partial \gamma}, \quad (204)$$

$$\tilde{F}(\gamma) = m_2 \tilde{A}_1(\gamma) - m_1 \tilde{A}_2(\gamma), \quad \tilde{G}(\gamma) = \tilde{A}'_1(\gamma) \tilde{A}_2(\gamma) - \tilde{A}'_2(\gamma) \tilde{A}_1(\gamma), \quad (205)$$

and we have used

$$\tilde{A}_1'' = -\tilde{A}_1, \quad \tilde{A}_2'' = -\tilde{A}_2. \quad (206)$$

From these equations, the non-linearity parameters can be calculated as

$$\frac{6}{5}f_{\text{NL}} = \frac{\tilde{G}}{\tilde{F}} \frac{(m_1\tilde{A}_1 + m_2\tilde{A}_2)^2}{(\tilde{A}_1^2 + \tilde{A}_2^2)^2}, \quad (207)$$

$$\tau_{\text{NL}} = \frac{\tilde{G}^2}{\tilde{F}^2} \frac{(m_1\tilde{A}_1 + m_2\tilde{A}_2)^2}{(\tilde{A}_1^2 + \tilde{A}_2^2)^3} (m_1^2 + m_2^2), \quad (208)$$

$$\frac{54}{25}g_{\text{NL}} = \frac{3\tilde{F}'(\gamma)\tilde{G}(\gamma)}{\tilde{F}^2(\gamma)} \frac{(m_1\tilde{A}_1 + m_2\tilde{A}_2)^3}{(\tilde{A}_1^2 + \tilde{A}_2^2)^3}. \quad (209)$$

By using the above expressions, we find that g_{NL} can be written with f_{NL} :

$$\frac{54}{25}g_{\text{NL}} = \left(\frac{6}{5}f_{\text{NL}}\right)^{\frac{3}{2}} \frac{3(m_1\phi_{2,f} - m_2\phi_{1,f})}{\sqrt{(\tilde{A}_1\phi_{2,f} - \tilde{A}_2\phi_{1,f})(m_2\tilde{A}_1 - m_1\tilde{A}_2)}}. \quad (210)$$

Thus, g_{NL} in the linear potential model is at least of the order of $f_{\text{NL}}^{3/2}$, and it can be relatively large compared to f_{NL} .

The spectral index and the tensor to scalar ratio are given by

$$n_s - 1 = -(m_1^2 + m_2^2), \quad r = \frac{8\tilde{F}^2(\gamma)}{\tilde{A}_1^2 + \tilde{A}_2^2}, \quad (211)$$

from which we find another simple relation among f_{NL} , n_s and r :

$$\frac{(6f_{\text{NL}}/5)^2}{\tau_{\text{NL}}} = 1 - \frac{r}{8(1 - n_s)}. \quad (212)$$

Although the expressions for the non-linearity parameters in this model are not so complicated, but still it is a bit difficult to see its size explicitly. Thus we look at some limiting cases in order.

I. Equal mass case ($m_1 = m_2 = M$)

Let us first consider the equal mass case. The expression of f_{NL} in this case is given by

$$\begin{aligned} \frac{6}{5}f_{\text{NL}} &= \frac{M}{v(g_1^2 \cos^2 \gamma + g_2^2 \sin^2 \gamma)^2} \\ &\times g_1^2 g_2^2 \frac{[-g_1 \cos \gamma (\cos \alpha - \sin \alpha) + g_2 \sin \gamma (\cos \alpha + \sin \alpha)]^2}{g_1 \cos \gamma (\cos \alpha + \sin \alpha) + g_2 \sin \gamma (\cos \alpha - \sin \alpha)}. \end{aligned} \quad (213)$$

Regarding τ_{NL} , from Eq. (212) we obtain the following relation

$$\tau_{\text{NL}} = \left(\frac{1 + \bar{R}}{\bar{R}} \right) \left(\frac{6}{5} f_{\text{NL}} \right)^2, \quad (214)$$

where the ratio \bar{R} is given by

$$\bar{R} = \left(\frac{\tilde{A}_1 + \tilde{A}_2}{\tilde{A}_1 - \tilde{A}_2} \right)^2. \quad (215)$$

We can also find the relation between f_{NL} and g_{NL} as

$$g_{\text{NL}} = 2 \frac{g_1^2 \cos^2 \gamma + g_2^2 \sin^2 \gamma}{g_1 g_2} \frac{g_1 \sin \gamma (\cos \alpha + \sin \alpha) - g_2 \cos \gamma (\cos \alpha - \sin \alpha)}{g_2 \sin \gamma (\cos \alpha + \sin \alpha) - g_1 \cos \gamma (\cos \alpha - \sin \alpha)} f_{\text{NL}}^2$$

$$= \begin{cases} O(g_1/g_2) \times f_{\text{NL}}^2, & g_1 \gg g_2 \\ O(g_2/g_1) \times f_{\text{NL}}^2, & g_2 \gg g_1 \end{cases} \quad (216)$$

In particular, $g_{\text{NL}} = 2f_{\text{NL}}^2$ for the case with $g_1 = g_2$.

II. Large mass ratio case ($m_1 \gg m_2$) with $\tilde{A}_2 \ll 1$

Now we briefly discuss the large mass ratio case. To study this case, we again set $\tilde{A}_2 = 0$ as we did for the counterpart in the quadratic potential case. Then the expressions for the non-linearity parameters become

$$\frac{6}{5} f_{\text{NL}} = \frac{m_1}{m_2} \frac{m_1 \phi_{2,f}}{\tilde{A}_1^2}, \quad (217)$$

$$\tau_{\text{NL}} = \left(\frac{1 + \bar{R}}{\bar{R}} \right) \left(\frac{6}{5} f_{\text{NL}} \right)^2, \quad \bar{R} = \frac{m_1^2}{m_2^2}, \quad (218)$$

$$g_{\text{NL}} = 2 \left(1 - \frac{m_2 \phi_{1,f}}{m_1 \phi_{2,f}} \right) f_{\text{NL}}^2. \quad (219)$$

Thus, the linear potential model generically predicts large g_{NL} relative to f_{NL} and in some limiting cases, we have $g_{\text{NL}} \sim f_{\text{NL}}^2$ as we have shown above.

3.4 Constrained multi-source model

In this section, we discuss a class of ‘‘constrained multi-source’’ model. In fact, models of this category are particularly related to so-called loop contributions. Thus we start with a general discussion including loop terms.

3.4.1 Expressions including loop contributions

In the discussions up to the previous section, we have neglected loop contributions in the expressions for the power spectrum and non-linearity parameters. However, if we include such loop terms, a new type of model can appear. The expression for P_ζ and the non-linearity parameters, including one loop contributions, are respectively given by

$$P_\zeta(k) = [N_a N^a + N_{ab} N^{ab} \mathcal{P}_\delta \ln(kL)] P_\delta(k), \quad (220)$$

$$\frac{6}{5} f_{\text{NL}} = \frac{N_a N_b N^{ab} + N_a{}^b N_b{}^c N_c{}^a \mathcal{P}_\delta \ln(k_{m1}L)}{(N_a N^a + N_{bc} N^{bc} \mathcal{P}_\delta \ln(k_i L))^2}, \quad (221)$$

$$\tau_{\text{NL}} = \frac{N_a N_b N^{ac} N_c{}^b + N_a{}^b N_b{}^c N_c{}^d N_d{}^a \mathcal{P}_\delta \ln(k_{m2}L)}{(N_a N^a + N_{bc} N^{bc} \mathcal{P}_\delta \ln(k_i L))^3}, \quad (222)$$

where L is the size of the box in which perturbations are defined and we have introduced the notations $k_{m1} = \min\{k_i\}$ and $k_{m2} = \min\{|k_i + k_j|, k_l\}$. In deriving the above equations, we have truncated the expansion of Eq. (1) at the second order in the field fluctuations. Strictly speaking, higher order terms contribute to the one-loop corrections. The full expressions for the one-loop correction are given in appendix B. In this section, we do not take into account such higher order effects since it turns out to be negligible in many cases. Since the current observations indicate that the primordial curvature perturbation is almost Gaussian, the power spectrum should not be dominated by the one-loop contributions, from which we have the following constraint:

$$1 > \frac{N_{ab} N^{ab}}{N_c N^c} \mathcal{P}_\delta \ln(kL) \simeq \frac{N_{ab} N^{ab}}{(N_c N^c)^2} \mathcal{P}_\zeta \ln(kL). \quad (223)$$

Now let us consider the relation between f_{NL} and τ_{NL} in the case where the one-loop contributions dominate in the non-linearity parameters. In such a case, f_{NL} and τ_{NL} are respectively given by

$$\frac{6}{5} f_{\text{NL}} = P_{ab} M^{ab} \mathcal{P}_\zeta \ln(k_{m1}L), \quad (224)$$

$$\tau_{\text{NL}} = M_{ab} M^{ab} \mathcal{P}_\zeta \ln(k_{m2}L), \quad (225)$$

where

$$P_{ab} \equiv \frac{N_{ab}}{N_d N^d}, \quad M_{ab} \equiv \frac{N_a{}^c N_{cb}}{(N_d N^d)^2}. \quad (226)$$

Using the Cauchy-Schwarz inequality, we find

$$\begin{aligned}
\left(\frac{6}{5}f_{\text{NL}}\right)^2 &= (P_{ab}M^{ab})^2 \mathcal{P}_\zeta^2 \ln^2(k_{m1}L) \\
&\leq (P_{ab}P^{ab}) (M_{cd}M^{cd}) \mathcal{P}_\zeta^2 \ln^2(k_{m1}L) \\
&= \tau_{\text{NL}} \frac{\ln^2(k_{m1}L)}{\ln(k_{m2}L)} (P_{ab}P^{ab}) \mathcal{P}_\zeta \\
&< \tau_{\text{NL}} \frac{\ln^2(k_{m1}L)}{\ln(k_{m2}L) \ln(kL)}, \tag{227}
\end{aligned}$$

where in the final inequality we have used Eq. (223). We have also assumed that k is any wavenumber that satisfies $\ln(kL) \simeq \ln(k_{m1}L) \simeq \ln(k_{m2}L) = O(1)$. Then we obtain an approximate inequality given by

$$\tau_{\text{NL}} \gtrsim \left(\frac{6}{5}f_{\text{NL}}\right)^2, \tag{228}$$

up to the logarithmic corrections. Hence, even in the case where the one-loop contribution dominates in the non-linearity parameters, “the local-type inequality” Eq. (14) should be satisfied under the condition where the contribution from the one-loop term should be subdominant in power spectrum.

3.4.2 Ungaussiton model

In some cases, the first terms in the numerators of Eqs. (221) and (222) are negligible compared to the second order terms. In such a case, the non-linear parameters are dominated by the one loop contributions. This kind of model has been discussed in [34–36, 95] and called “ungaussiton” in [36] and “quadratic model” in [95]. Let us consider the simplest case where the curvature perturbation is given by

$$\zeta = N_\phi \delta\phi + \frac{1}{2} N_{\sigma\sigma} \delta\sigma^2 + \dots, \tag{229}$$

where ϕ is the inflaton and σ is the so-called “ungaussiton.” In this model, the expression for the non-linearity parameters given by Eqs. (9) and (10) cannot be adopted in this case any more and f_{NL} , τ_{NL} and g_{NL} are given by

$$\frac{6}{5}f_{\text{NL}} = \frac{N_{\sigma\sigma}^3 \mathcal{P}_{\delta\sigma} \ln(k_{m1}L)}{N_\phi^4}, \tag{230}$$

$$\tau_{\text{NL}} = \frac{N_{\sigma\sigma}^4 \mathcal{P}_{\delta\sigma} \ln(k_{m2}L)}{N_\phi^6}, \tag{231}$$

$$\frac{54}{25}g_{\text{NL}} = \frac{3N_\sigma^2 N_{\sigma\sigma} N_{\sigma\sigma\sigma\sigma} \mathcal{P}_\sigma \log(k_{m1}L) + 3N_\sigma N_{\sigma\sigma}^2 N_{\sigma\sigma\sigma} \mathcal{P}_\sigma \log(k_{m1}L)}{N_\phi^6}. \tag{232}$$

Since N_σ and $N_{\sigma\sigma\sigma}$ are strongly suppressed in this model, the size of g_{NL} would be very small. Thus the trispectrum is dominated by τ_{NL} . From the above expressions, we find the relation between f_{NL} and τ_{NL} as

$$\tau_{\text{NL}} = CP_\zeta^{-1/3} f_{\text{NL}}^{4/3} \sim 10^3 f_{\text{NL}}^{4/3}, \quad (233)$$

where we adopt the normalization for the power spectrum $P_\zeta \sim 2 \times 10^{-9}$ and C is a constant defined as $C = (6/5)^{4/3} (\ln(k_{m1}L)/[\ln(k_{m2})]^{4/3})$. This equation clearly contradicts with Eq. (228) if f_{NL} is sufficiently large. However, it can be easily checked that, in such a case, the power spectrum is also dominated by the loop contribution, which does not satisfy our assumptions to derive Eq. (228). Also notice that the curvature perturbation induced from σ starts from the second order. Hence the fluctuations from σ are completely non-Gaussian, which cannot explain the observed fluctuations. Thus we need another source of fluctuations to account for the observed almost Gaussian fluctuations, which could be those from the inflaton. In this sense, this model requires multi-sources in nature. This motivates us to call this kind of models ‘‘constrained multi-source model.’’

In fact, when the initial value (the field value during inflation) of the scalar field σ_* is less than its quantum fluctuation during inflation $\delta\sigma_* \simeq H_{\text{inf}}/(2\pi)$, models of this category can be easily realized such as in the axion, the curvaton, the modulated reheating and so on.

3.5 Other models

In this paper, we have discussed various models generating large local-type non-Gaussianity focusing on models which can be accommodated in the framework of inflationary universe (fluctuations originating to quantum fluctuations during inflation) with adiabatic mode. However, there are other possibilities of generating large non-Gaussianity in some other frameworks and/or models where a simple parametrization of the non-linearity parameters may not be adopted. Here we briefly mention such other models of the local type.

When one considers the generation of dark matter and baryon asymmetry of the Universe, isocurvature perturbations can be generated in some situations. Since the shapes of the bispectrum and the trispectrum are different from the counterparts of the adiabatic ones, a simple parametrization of f_{NL} , τ_{NL} and g_{NL} cannot be easily compared with the ones defined for adiabatic fluctuations^{#21}. In fact, isocurvature fluctuations have already been severely constrained by cosmological observations such as CMB, however, the non-linear effect can be large in some cases, in particular, where fluctuations are dominated by the second order term. In this case, the situation is quite similar to the ungaussiton model discussed in the previous section. The issue of non-Gaussianity in models with

^{#21} However, we can have some approximate relation between f_{NL} and $f_{\text{NL}}^{(\text{iso})}$. While the former is defined in Eq. (6) and has been discussed in this paper, the latter is defined to parametrize non-Gaussianity in models with isocurvature mode [95]. We can estimate how large non-Gaussianity from isocurvature fluctuations can be compared to the counterpart in adiabatic mode by using the relation between these non-linearity parameters derived in [95].

isocurvature fluctuations has been investigated by several authors. We refer the reader to Refs. [95–100] for the detailed discussion on this issue.

Another local-type model is so-called the Ekpyrotic scenario [101–103], in which the scale-invariant curvature perturbation and large non-Gaussianity can be generated. The non-linearity parameters f_{NL} and g_{NL} in this models have been calculated and the relation between f_{NL} and g_{NL} is obtained as $g_{\text{NL}} \sim f_{\text{NL}}^2$ [103].

There are also several studies on the possibility of generating large non-Gaussianity during preheating phase [104–113]. In this case, the super-horizon scale fluctuations might be strongly coupled to the evolution of small scale fluctuations. In Ref. [112], the authors have introduced a new parameter F_{NL} , which describes the non-linearity of the curvature perturbations and claimed that during preheating era there seems to be a possibility of generating large non-Gaussianity whose form is quite different from the usual local-type non-Gaussianity.

Another possibility of local-type non-Gaussianity we would like to mention is a model in which the e -folding number is quite sensitive to the field value. In such a case, the truncation at the leading order or at the next leading order of Eq. (1) will no longer give a correct answer. We then need to go to the higher order calculations until the series converge or to resort to the full order calculations. In appendix C, we give a simple toy model belonging to this class and briefly discuss some interesting features of the bispectrum and trispectrum.

4 Discussion and Summary

In this paper, we made a classification of models generating large local-type non-Gaussianity by using some consistency relations between the non-linearity parameters f_{NL} , τ_{NL} and g_{NL} . The first key relation is the ratio of $\tau_{\text{NL}}/(6f_{\text{NL}}/5)^2$, by which we classify local-type models into three categories:

- single-source model ($\tau_{\text{NL}}/(6f_{\text{NL}}/5)^2 = 1$)
- multi-source model ($\tau_{\text{NL}}/(6f_{\text{NL}}/5)^2 > 1$)
- constrained multi-source model ($\tau_{\text{NL}} \propto f_{\text{NL}}^n$)

We have also shown that the “local-type inequality”

$$\tau_{\text{NL}} \gtrsim \left(\frac{6}{5}f_{\text{NL}}\right)^2 \quad (234)$$

holds true not only for the case where the tree level contribution dominates in the non-linearity parameters but also for the case where the loop contribution dominates there. This inequality has been shown under the condition that a loop contribution is subdominant in the power spectrum, which is required by current observations. To our knowledge,

since all models generating local-type large non-Gaussianity known today should satisfy the “local-type inequality,” if future observations confirm that this inequality does not hold, local-type models would be practically ruled out as a mechanism of generating large non-Gaussian primordial fluctuations.

On the other hand, if future observations find large f_{NL} of local type and probe the relation between τ_{NL} and f_{NL} with some accuracy, satisfying the local-type inequality, we can see what category of models would be favored. However, even if we can pick up the one of these categories, as we have discussed, there still remain many possibilities for each. Thus we need a further classification to pin down the model of large non-Gaussianity. For this purpose, we can make use of the relation between f_{NL} and g_{NL} . We have shown that models can be further divided into three types according to the relative size of g_{NL} compared to that of f_{NL} as follows:

- Suppressed g_{NL} type ($g_{\text{NL}} \sim [\text{suppression factor}] \times f_{\text{NL}}$)
- Linear g_{NL} type ($g_{\text{NL}} \sim f_{\text{NL}}$)
- Enhanced g_{NL} type ($g_{\text{NL}} \sim f_{\text{NL}}^n$ with $n > 1$ or $n = 2$ for many models)

Thus if we further probe the relation f_{NL} and g_{NL} in future observations, we may find that only a few models survive by using the above categorizations. Then we can figure out what type of models are favored as a mechanism of the generation of primordial fluctuations.

We have also worked out the above mentioned relations for various concrete models in this paper. Although models can be categorized rather rigorously by using the ratio $\tau_{\text{NL}}/(6f_{\text{NL}}5)^2$, the relation between f_{NL} and g_{NL} can significantly differ depending on some model parameters, in particular, in multi-source models. For example, let us take the multi-brid inflation model with quadratic potential, which was discussed in Section 3.3.3. This model predicts that $g_{\text{NL}} \sim \eta f_{\text{NL}}$ with being η a slow-roll parameter, which is of the suppressed g_{NL} type, for the equal mass case, while the relation becomes $g_{\text{NL}} \sim f_{\text{NL}}^2$, which is of the enhanced g_{NL} type, for the large mass ratio case. In other words, the relation between f_{NL} and g_{NL} should be carefully investigated to discriminate a model because a model can predict quite different relations depending on its model parameters. However, it also means that the relation would be useful to explore the parameters of a model.

In this paper, we have focused on non-Gaussianity in various models and not discussed much the tensor-to-scalar ratio or gravitational waves. In most models where large non-Gaussian primordial fluctuations are generated, the tensor-to-scalar ratio is considered to be very small in general. However, there are a few examples which can give a relatively large tensor-to-scalar ratio as well as generating large non-Gaussianity. One of such examples is a mixed model of inflaton fluctuations with some other source discussed in Section 3.3.1. In this model, the fluctuations from the inflaton can also be responsible for the curvature perturbation, and in such a case, the tensor-to-scalar ratio can be large, which could be detectable in near future observations. Another example is multi-brid inflation model discussed in Section 3.3.3. If both the tensor-to-scalar ratio and non-Gaussianity are found to be large in the future, above mentioned models may become the target of

detailed studies. This illustrates that a comprehensive investigation using non-Gaussianity and some other information such as gravitational waves can give much insight into the pursuit of the generation mechanism of primordial fluctuations.

If three non-linearity parameters f_{NL} , τ_{NL} and g_{NL} are well determined in future observations, we may be able to pin down the model of large non-Gaussianity and pick up a right model of generating primordial fluctuations. The classification by using the consistency relation among the above three parameters would be very useful to pursue the origin of the structure of the Universe and give a deep understanding of the early Universe.

Acknowledgments

T. T., M. Y. and S. Y. thank the Yukawa Institute for Theoretical Physics at Kyoto University, where this work was discussed during the YITP-W-09-09 on “The non-Gaussian universe,” “Gravity and Cosmology 2010” and the organizers and participants of these workshops for stimulating discussions. This work is partially supported by the Belgian Federal Office for Scientific, Technical, and Cultural Affairs through the Inter-University Attraction Pole Grant No. P6/11 (T. S.); by the Grant-in-Aid for Scientific research from the Ministry of Education, Science, Sports, and Culture, Japan, Nos. 19740145 (T. T.), 21740187 (M. Y.) and 22340056 (S. Y.). T. S. is supported by a Grant-in-Aid for JSPS Fellows. S. Y. acknowledges support from the Grant-in-Aid for the Global COE Program “Quest for Fundamental Principles in the Universe: from Particles to the Solar System and the Cosmos” from MEXT, Japan.

Appendix

A Full expression for ζ in multi-curvaton model

In Section 3.3.2, we have discussed the multi-curvaton model, but investigated only some limiting cases. Here we give the full expression for the curvature perturbation in the model up to the third order. In general, the curvature perturbation ζ can be written as

$$\begin{aligned} \zeta = & C_a \zeta_{a(1)} + C_b \zeta_{b(1)} + C_{aa} \zeta_{a(1)}^2 + C_{bb} \zeta_{b(1)}^2 + C_{ab} \zeta_{a(1)} \zeta_{b(1)} \\ & + C_{aaa} \zeta_{a(1)}^3 + C_{bbb} \zeta_{b(1)}^3 + C_{aab} \zeta_{a(1)}^2 \zeta_{b(1)} + C_{abb} \zeta_{a(1)} \zeta_{b(1)}^2. \end{aligned} \quad (235)$$

We list full expressions for the coefficients such as C_a and so on in the following.

For the first order,

$$C_a = -\frac{f_{a1}(f_{a1} + 3)(f_{b2} - 1)}{f_{a1} - 3f_{b1} + 3}, \quad (236)$$

$$C_b = \frac{f_{a1}(-f_{b1}f_{b2} + f_{b1} + f_{b2}) - 3(f_{b1} - 1)f_{b2}}{f_{a1} - 3f_{b1} + 3}. \quad (237)$$

For the second order,

$$\begin{aligned} C_{aa} = & \frac{1}{4(f_{a1} - 3f_{b1} + 3)^2} [f_{a1}(f_{b2} - 1) (2f_{a1}^4 - 2f_{a1}^3 (2f_{b1} + f_{b2}^2 + 3f_{b2} - 8) \\ & - 3f_{a1}^2 (2f_{b1}^2 + 4f_{b2}^2 + 12f_{b2} - 13) + 9f_{a1} (5f_{b1} - 2f_{b2}^2 - 6f_{b2} + 2) + 27(f_{b1} - 1))] , \end{aligned} \quad (238)$$

$$\begin{aligned} C_{bb} = & \frac{1}{4(f_{a1} - 3f_{b1} + 3)^2} [2f_{a1}^3 f_{b1}^2 (f_{b2} - 1) + f_{a1}^2 (-4f_{b1}^3 (f_{b2} - 1) - 2f_{b1}^2 (f_{b2}^3 + 2f_{b2}^2 - 11f_{b2} + 8) \\ & + f_{b1} (4f_{b2}^3 + 8f_{b2}^2 - 15f_{b2} + 3) + f_{b2} (-2f_{b2}^2 - 4f_{b2} + 3)) \\ & - 3f_{a1}(f_{b1} - 1) (2f_{b1}^3 (f_{b2} - 1) + 2f_{b1}^2 (f_{b2} - 1) + f_{b1} (4f_{b2}^3 + 8f_{b2}^2 - 15f_{b2} + 3) \\ & - 2f_{b2} (2f_{b2}^2 + 4f_{b2} - 3)) - 9(f_{b1} - 1)^2 f_{b2} (2f_{b2}^2 + 4f_{b2} - 3)] , \end{aligned} \quad (239)$$

$$\begin{aligned} C_{ab} = & \frac{1}{(f_{a1} - 3f_{b1} + 3)^2} [f_{a1}(f_{b2} - 1) ((9 - 2f_{a1}^2) f_{b1}^2 + (f_{a1} + 3)f_{b1} (f_{a1}^2 - f_{a1} (f_{b2}^2 + 3f_{b2} - 5) \\ & - 3(f_{b2}^2 + 3f_{b2} + 1)) - 3f_{a1} f_{b1}^3 + (f_{a1} + 3)^2 f_{b2} (f_{b2} + 3)] . \end{aligned} \quad (240)$$

For the third order,

$$\begin{aligned}
C_{aaa} = & \frac{-1}{12(f_{a1} - 3f_{b1} + 3)^3} [f_{a1}^2(f_{b2} - 1) (6f_{a1}^6 - 2f_{a1}^5 (12f_{b1} + 3f_{b2}^2 + 9f_{b2} - 37) \\
& + f_{a1}^4 (-12f_{b1}^2 + 2f_{b1} (6f_{b2}^2 + 18f_{b2} - 77) + 6f_{b2}^4 + 26f_{b2}^3 - 48f_{b2}^2 - 216f_{b2} + 343) \\
& + 3f_{a1}^3 (24f_{b1}^3 + 2f_{b1}^2 (3f_{b2}^2 + 9f_{b2} - 35) + f_{b1} (12f_{b2}^2 + 36f_{b2} - 23) \\
& + 3 (6f_{b2}^4 + 26f_{b2}^3 - 11f_{b2}^2 - 105f_{b2} + 77)) + 9f_{a1}^2 (6f_{b1}^4 + 2f_{b1}^3 + f_{b1}^2 (6f_{b2}^2 + 18f_{b2} - 55) \\
& + f_{b1} (-15f_{b2}^2 - 45f_{b2} + 128) + 3 (6f_{b2}^4 + 26f_{b2}^3 + 3f_{b2}^2 - 63f_{b2} + 15)) \\
& + 27f_{a1} (-9f_{b1}^3 + 9f_{b1}^2 - 3f_{b1} (6f_{b2}^2 + 18f_{b2} - 23) + 6f_{b2}^4 + 26f_{b2}^3 + 15f_{b2}^2 - 27f_{b2} - 17) \\
& - 243(f_{b1} - 1) (-2f_{b1} + f_{b2}^2 + 3f_{b2} - 2)], \tag{241}
\end{aligned}$$

$$\begin{aligned}
C_{bbb} = & \frac{-1}{24(f_{a1} - 3f_{b1} + 3)^3} [12f_{a1}^5 f_{b1}^3 (f_{b2} - 1) \\
& + 2f_{a1}^4 f_{b1}^2 (f_{b2} - 1) (-24f_{b1}^2 - 2f_{b1} (3f_{b2}^2 + 9f_{b2} - 37) + 6f_{b2}^2 + 18f_{b2} - 9) \\
& + 2f_{a1}^3 (-12f_{b1}^5 (f_{b2} - 1) + 2f_{b1}^4 (6f_{b2}^3 + 12f_{b2}^2 - 95f_{b2} + 77) \\
& + f_{b1}^3 (6f_{b2}^5 + 20f_{b2}^4 - 86f_{b2}^3 - 192f_{b2}^2 + 595f_{b2} - 343) \\
& - 3f_{b1}^2 (6f_{b2}^5 + 20f_{b2}^4 - 33f_{b2}^3 - 86f_{b2}^2 + 126f_{b2} - 33) \\
& + 6f_{b1} f_{b2} (3f_{b2}^4 + 10f_{b2}^3 - 4f_{b2}^2 - 18f_{b2} + 9) - f_{b2}^2 (6f_{b2}^3 + 20f_{b2}^2 + f_{b2} - 18)) \\
& + 6f_{a1}^2 (f_{b1} - 1) (24f_{b1}^5 (f_{b2} - 1) + 2f_{b1}^4 (3f_{b2}^3 + 6f_{b2}^2 - 32f_{b2} + 23) \\
& + 3f_{b1}^3 (4f_{b2}^3 + 8f_{b2}^2 - 37f_{b2} + 25) + 3f_{b1}^2 (6f_{b2}^5 + 20f_{b2}^4 - 29f_{b2}^3 - 78f_{b2}^2 + 108f_{b2} - 27) \\
& - 12f_{b1} f_{b2} (3f_{b2}^4 + 10f_{b2}^3 - 4f_{b2}^2 - 18f_{b2} + 9) + 3f_{b2}^2 (6f_{b2}^3 + 20f_{b2}^2 + f_{b2} - 18)) \\
& + 9f_{a1} (f_{b1} - 1)^2 (12f_{b1}^5 (f_{b2} - 1) + 28f_{b1}^4 (f_{b2} - 1) + 6f_{b1}^3 (f_{b2} - 1) (2f_{b2}^2 + 6f_{b2} - 3) \\
& + 6f_{b1}^2 (f_{b2} - 1) (2f_{b2}^2 + 6f_{b2} - 3) + 12f_{b1} (f_{b2} - 1) f_{b2} (3f_{b2}^3 + 13f_{b2}^2 + 9f_{b2} - 9) \\
& - 6f_{b2}^2 (6f_{b2}^3 + 20f_{b2}^2 + f_{b2} - 18)) + 54(f_{b1} - 1)^3 f_{b2}^2 (6f_{b2}^3 + 20f_{b2}^2 + f_{b2} - 18)], \tag{242}
\end{aligned}$$

$$\begin{aligned}
C_{aab} = & \frac{-1}{4(f_{a1} - 3f_{b1} + 3)^3} [f_{a1} (f_{b2} - 1) (54f_{a1}^2 f_{b1}^5 + 9f_{a1} (8f_{a1}^2 + 2f_{a1} - 15) f_{b1}^4 \\
& + (f_{a1} + 3)^3 f_{b2} (f_{b2} + 3) (2f_{a1}^2 - 2f_{a1} (3f_{b2}^2 + 4f_{b2} - 5) - 3) \\
& - 3f_{b1}^3 (4f_{a1}^4 - 2f_{a1}^3 (3f_{b2}^2 + 9f_{b2} - 35) - 3f_{a1}^2 (6f_{b2}^2 + 18f_{b2} - 43) - 45f_{a1} - 27) \\
& - (f_{a1} + 3) f_{b1}^2 (24f_{a1}^4 - 2f_{a1}^3 (6f_{b2}^2 + 18f_{b2} - 41) + 3f_{a1}^2 (2f_{b2}^2 + 6f_{b2} - 55) \\
& + 9f_{a1} (9f_{b2}^2 + 27f_{b2} - 25) + 27 (f_{b2}^2 + 3f_{b2} + 2)) + (f_{a1} + 3)^2 f_{b1} (6f_{a1}^4 \\
& - 2f_{a1}^3 (3f_{b2}^2 + 9f_{b2} - 19) + f_{a1}^2 (6f_{b2}^4 + 26f_{b2}^3 - 16f_{b2}^2 - 120f_{b2} + 49) \\
& + 3f_{a1} (6f_{b2}^4 + 26f_{b2}^3 + 23f_{b2}^2 - 3f_{b2} - 25) + 9 (2f_{b2}^2 + 6f_{b2} + 1))], \tag{243}
\end{aligned}$$

$$\begin{aligned}
C_{abb} = & \frac{-1}{4(f_{a1} - 3f_{b1} + 3)^3} [f_{a1}(f_{b2} - 1) (18 (4f_{a1}^2 + f_{a1} - 3) f_{b1}^5 \\
& + (f_{a1} + 3)^2 f_{b1} (f_{a1}^2 (4f_{b2}^2 + 12f_{b2} - 3) - f_{a1} (12f_{b2}^4 + 52f_{b2}^3 + 13f_{b2}^2 - 105f_{b2} + 15) \\
& - 3 (12f_{b2}^4 + 52f_{b2}^3 + 46f_{b2}^2 - 6f_{b2} - 3)) - 3f_{b1}^4 (4f_{a1}^3 - 2f_{a1}^2 (3f_{b2}^2 + 9f_{b2} - 35) \\
& - 3f_{a1} (6f_{b2}^2 + 18f_{b2} - 35) - 18) + f_{b1}^3 (-24f_{a1}^4 + 2f_{a1}^3 (6f_{b2}^2 + 18f_{b2} - 77) \\
& + 3f_{a1}^2 (8f_{b2}^2 + 24f_{b2} - 29) - 9f_{a1} (8f_{b2}^2 + 24f_{b2} - 45) - 27 (4f_{b2}^2 + 12f_{b2} - 5)) \\
& + (f_{a1} + 3) f_{b1}^2 (6f_{a1}^4 - 2f_{a1}^3 (3f_{b2}^2 + 9f_{b2} - 28) + f_{a1}^2 (6f_{b2}^4 + 26f_{b2}^3 - 38f_{b2}^2 - 186f_{b2} + 163) \\
& + 3f_{a1} (12f_{b2}^4 + 52f_{b2}^3 + 15f_{b2}^2 - 99f_{b2} - 1) + 9 (6f_{b2}^4 + 26f_{b2}^3 + 29f_{b2}^2 + 15f_{b2} - 8)) \\
& + 54f_{a1}f_{b1}^6 + (f_{a1} + 3)^3 f_{b2} (6f_{b2}^3 + 26f_{b2}^2 + 21f_{b2} - 9)] . \tag{244}
\end{aligned}$$

B Full expressions including one-loop corrections

In subsection 3.4, we have considered the one-loop terms in the expression for the power spectrum and the non-linear parameters, neglecting the third order terms in the δN formalism. Here, we show the full expressions for the one-loop correction terms, including higher order ones in the δN formalism [99].

The expression for the power spectrum including the full one-loop correction terms is given by

$$P_C(k) = [N_a N^a + N_{ab} N^{ab} \mathcal{P}_\delta \ln(kL) + N_a N^{ab} {}_b \mathcal{P}_\delta \ln(k_{\max} L)] P_\delta(k), \tag{245}$$

where k_{\max} is the cut-off scale of the power spectrum and the last term in principle can be removed by shifting the homogeneous value of the scalar field [30].

The non-linearity parameters including the one-loop corrections are given as follows. For f_{NL} , we obtain

$$\begin{aligned}
\frac{6}{5} f_{\text{NL}} = & [N_a N^a + N_{ab} N^{ab} \mathcal{P}_\delta \ln(k_i L) + N_a N^{ab} {}_b \mathcal{P}_\delta \ln(k_{\max} L)]^{-2} \\
& \times \left[N_a N_b N^{ab} + \left(N_{ab} N^{bc} N_c{}^a + 2N_a N_{bc} N^{abc} \right) \mathcal{P}_\delta \ln(k_{m1} L) \right. \\
& \left. + \left(N_a N^{ab} N_{bc}{}^c + \frac{1}{2} N_a N_b N^{abc} \right) \mathcal{P}_\delta \ln(k_{\max} L) \right], \tag{246}
\end{aligned}$$

where $k_{m1} = \min\{k_i\}$. Please notice that a term with k_{\max} again can be removed by shifting the homogeneous value of the scalar field. Here we have assumed that $\ln(k_1 L) \sim \ln(k_2 L) \sim \ln(k_3 L)$ and all of these are just represented as $\ln(k_i L)$, which enables us to factor out the dependence on such a factor in the power spectrum. Other two non-linearity parameters

are:

$$\begin{aligned}
\tau_{\text{NL}} = & \left[N_a N^a + N_{ab} N^{ab} \mathcal{P}_\delta \ln(k_i L) + N_a N^{ab} \mathcal{P}_\delta \ln(k_{\text{max}} L) \right]^{-3} \\
& \times \left[N_a N^{ab} N_{bc} N^c + 2 N_a N^{ab} N^{cd} N_{bcd} \mathcal{P}_\delta \ln(k_{m1} L) \right. \\
& \quad + (N_{ab} N^{bc} N_{cd} N^{da} + N_a N_{bc} N^b{}_d N^{acd} + N_a N_b N^{acd} N^b{}_{cd}) \mathcal{P}_\delta \ln(k_{m2} L) \\
& \quad \left. \left(+ N_a N^{ab} N_{bc} N^{cd}{}_d + N_a N^{ab} N_{bc}{}^{cd} N_d \right) \mathcal{P}_\delta \ln(k_{\text{max}} L) \right], \tag{247}
\end{aligned}$$

$$\begin{aligned}
\frac{54}{25} g_{\text{NL}} = & \left[N_a N^a + N_{ab} N^{ab} \mathcal{P}_\delta \ln(k_i L) + N_a N^{ab} \mathcal{P}_\delta \ln(k_{\text{max}} L) \right]^{-3} \\
& \times \left[N_a N_b N_c N^{abc} + 3 (N_a N_{bc} N^b{}_d N^{acd} + N_a N_b N_{cd} N^{abcd}) \mathcal{P}_\delta \ln(k_{m1} L) \right. \\
& \quad \left. + \left(\frac{1}{2} N_a N_b N_c N^{abcd}{}_d + \frac{3}{2} N_a N_b N^{abc} N_{cd}{}^d \right) \mathcal{P}_\delta \ln(k_{\text{max}} L) \right], \tag{248}
\end{aligned}$$

where $k_{m2} = \min\{|k_i + k_j|, k_l\}$.

C Full order calculation

In this appendix, we briefly discuss the higher order perturbation effects on the bispectrum and the trispectrum. So far, our analysis has been based on the perturbative expansion of the e -folding number in terms of the field fluctuations. In order to calculate the power spectrum, the bispectrum, and the trispectrum, it was sufficient to consider the lowest order contribution to those quantities (or the next lowest order if the lowest one vanishes like in the ungaussiton case). This perturbative expansion is extremely accurate and powerful in many models including all the models discussed in this paper since the higher order contributions are highly suppressed.

Yet, it is still logically possible to consider a model in which the e -folding number is quite sensitive to the field value. In such a case, the truncation at the leading order or at the next leading order will no longer give a correct answer. We then need to go to the higher order calculations until the series converge or to resort to the full order calculations.

To see what happens if the higher order terms are taken into account, we give a simple toy model that allows full order calculations at some level. Here, by at some level, it means that the final expressions of the bispectrum and the trispectrum involve multidimensional integrals that defeats analytic calculation. Nevertheless, we can derive some interesting consequences from these results, as we will see below.

Let us assume that the e -folding number depends on a field σ by

$$N(\vec{x}) = \exp\left(-\frac{\sigma(\vec{x})}{a}\right) \left/ \left\langle \exp\left(-\frac{\sigma(\vec{x})}{a}\right) \right\rangle \right., \tag{249}$$

where $\langle \dots \rangle$ denotes the spatial average. The magnitude of σ field perturbation is not necessarily smaller than a . This type of model may be realized in the context of modulated reheating scenario if the coupling constant for the inflaton decay is multiplied by a factor like $\exp(-\frac{\sigma}{2a})$. Then, using the δN formula, the curvature perturbation is given by

$$\zeta(\vec{x}) = \exp\left(-\frac{\delta\sigma(\vec{x})}{a}\right) \left/ \left\langle \exp\left(-\frac{\delta\sigma(\vec{x})}{a}\right) \right\rangle \right. - 1. \quad (250)$$

The full order calculation was also done in [114], where the authors calculate the power spectrum of the field which depends on the Gaussian field by the sine function rather than the exponential one.

By assuming that $\delta\sigma$ is Gaussian, we write the two-point function in Fourier space as

$$\langle \delta\sigma_{\vec{k}_1} \delta\sigma_{\vec{k}_2} \rangle = (2\pi)^3 P(k_1) \delta(\vec{k}_1 + \vec{k}_2). \quad (251)$$

We further assume the scale invariant power spectrum, i.e. $P(k) = H_*^2/(2k^3)$. Then, using the standard formula,

$$\begin{aligned} & \left\langle \exp\left(-\int d^3x b(\vec{x})\delta\sigma(\vec{x})\right) \right\rangle \\ &= \exp\left[\frac{1}{2}\int d^3x_1 d^3x_2 \int \frac{d^3q}{(2\pi)^3} P(q) e^{i\vec{q}\cdot(\vec{x}_1-\vec{x}_2)} b(\vec{x}_1)b(\vec{x}_2)\right], \end{aligned} \quad (252)$$

we find that the connected part of the three-point function of ζ is given by

$$\begin{aligned} \langle \zeta_{\vec{k}_1} \zeta_{\vec{k}_2} \zeta_{\vec{k}_3} \rangle &= \int d^3x_1 d^3x_2 d^3x_3 e^{i\vec{k}_1\cdot\vec{x}_1+i\vec{k}_2\cdot\vec{x}_2+i\vec{k}_3\cdot\vec{x}_3} \\ &\times \exp\left[\frac{1}{a^2}\int \frac{d^3q}{(2\pi)^3} P(q)(e^{i\vec{q}\cdot\vec{x}_{12}} + e^{i\vec{q}\cdot\vec{x}_{23}} + e^{i\vec{q}\cdot\vec{x}_{31}})\right], \end{aligned} \quad (253)$$

where $\vec{x}_{ij} \equiv \vec{x}_i - \vec{x}_j$. This is non-vanishing only when $\vec{k}_1 + \vec{k}_2 + \vec{k}_3 = 0$. Then after a suitable change of integration variables, we can show that the bispectrum of ζ is given by

$$\begin{aligned} B_\zeta(\vec{k}_1, \vec{k}_2, \vec{k}_3) &= \int d^3x_1 d^3x_2 e^{i\vec{k}_1\cdot\vec{x}_1+i\vec{k}_2\cdot\vec{x}_2} \\ &\times \exp\left[\frac{1}{a^2}\int \frac{d^3q}{(2\pi)^3} P(q)(e^{i\vec{q}\cdot\vec{x}_1} + e^{i\vec{q}\cdot\vec{x}_2} + e^{i\vec{q}\cdot\vec{x}_{12}})\right]. \end{aligned} \quad (254)$$

The momentum integration can be done analytically [114],

$$\exp\left[\frac{1}{a^2}\int \frac{d^3q}{(2\pi)^3} P(q) e^{i\vec{q}\cdot\vec{x}}\right] = \left(\frac{L}{x}\right)^{2\beta}, \quad (255)$$

where L is the size of the box and $\beta \equiv H_*^2/(8\pi^2 a^2)$. Then the bispectrum becomes

$$B_\zeta(\vec{k}_1, \vec{k}_2, \vec{k}_3) = \int d^3x_1 d^3x_2 e^{i\vec{k}_1\cdot\vec{x}_1+i\vec{k}_2\cdot\vec{x}_2} \left(\frac{L}{x_1}\right)^{2\beta} \left(\frac{L}{x_2}\right)^{2\beta} \left(\frac{L}{x_{12}}\right)^{2\beta}. \quad (256)$$

It is not easy to do the integration over the real space coordinates. However, we can extract the scale dependence of the bispectrum. Indeed, under the scaling transformation $\vec{k}_i \rightarrow \lambda \vec{k}_i$ with λ being constant, the bispectrum scales as

$$B_\zeta(\lambda \vec{k}_1, \lambda \vec{k}_2, \lambda \vec{k}_3) = \lambda^{-6+6\beta} B_\zeta(\vec{k}_1, \vec{k}_2, \vec{k}_3). \quad (257)$$

Or, equivalently, the bispectrum runs with the scale as

$$\frac{d \log B_\zeta}{d \log k} = -6 + 6\beta. \quad (258)$$

The derivative should be understood that the shape of the triangle is kept unchanged. Therefore, the larger β is, the larger the bispectrum is on small scales. On the other hand, it is difficult to extract the shape dependence from Eq. (256) and we stop pursuing it further.

We can do the same for the four-point function. The trispectrum is given by

$$\begin{aligned} T_\zeta(\vec{k}_1, \vec{k}_2, \vec{k}_3, \vec{k}_4) &= \int d^3 x_1 d^3 x_2 d^3 x_3 e^{i\vec{k}_1 \cdot \vec{x}_1 + i\vec{k}_2 \cdot \vec{x}_2 + i\vec{k}_3 \cdot \vec{x}_3} \\ &\times \left(\frac{L}{x_1}\right)^{2\beta} \left(\frac{L}{x_2}\right)^{2\beta} \left(\frac{L}{x_3}\right)^{2\beta} \left(\frac{L}{x_{12}}\right)^{2\beta} \left(\frac{L}{x_{23}}\right)^{2\beta} \left(\frac{L}{x_{31}}\right)^{2\beta}. \end{aligned} \quad (259)$$

Therefore, the trispectrum scales as

$$T_\zeta(\lambda \vec{k}_1, \lambda \vec{k}_2, \lambda \vec{k}_3, \lambda \vec{k}_4) = \lambda^{-9+12\beta} T_\zeta(\vec{k}_1, \vec{k}_2, \vec{k}_3, \vec{k}_4), \quad (260)$$

and therefore, the trispectrum runs as

$$\frac{d \log T_\zeta}{d \log k} = -9 + 12\beta. \quad (261)$$

Due to the same reason as the case of the ungaussiton, we assume that the leading contribution to the power spectrum comes from inflaton fluctuations. Therefore,

$$P_\zeta(k) = \frac{1}{4\epsilon M_{\text{Pl}}^2 k^3}, \quad (262)$$

where ϵ is again the slow-roll parameter. From (258) and (261), we find that a ratio

$$\left(\frac{B_\zeta}{P_\zeta^2}\right)^2 \bigg/ \left(\frac{T_\zeta}{P_\zeta^3}\right) = \frac{B_\zeta^2}{P_\zeta T_\zeta}, \quad (263)$$

does not run with the scale. But it will in general depend on the shape of the triangle and the quadrilateral.

References

- [1] E. Komatsu *et al.*, arXiv:1001.4538 [astro-ph.CO].
- [2] J. Q. Xia, M. Viel, C. Baccigalupi, G. De Zotti, S. Matarrese and L. Verde, *Astrophys. J.* **717**, L17 (2010) [arXiv:1003.3451 [astro-ph.CO]].
- [3] F. De Bernardis, P. Serra, A. Cooray and A. Melchiorri, arXiv:1004.5467 [astro-ph.CO].
- [4] J. Q. Xia, A. Bonaldi, C. Baccigalupi, G. De Zotti, S. Matarrese, L. Verde and M. Viel, *JCAP* **1008**, 013 (2010) [arXiv:1007.1969 [astro-ph.CO]].
- [5] L. Senatore, K. M. Smith and M. Zaldarriaga, *JCAP* **1001**, 028 (2010) [arXiv:0905.3746 [astro-ph.CO]].
- [6] [Planck Collaboration], arXiv:astro-ph/0604069.
- [7] E. Silverstein and D. Tong, *Phys. Rev. D* **70**, 103505 (2004) [arXiv:hep-th/0310221].
- [8] M. Alishahiha, E. Silverstein and D. Tong, *Phys. Rev. D* **70**, 123505 (2004) [arXiv:hep-th/0404084].
- [9] N. Arkani-Hamed, P. Creminelli, S. Mukohyama and M. Zaldarriaga, *JCAP* **0404**, 001 (2004) [arXiv:hep-th/0312100].
- [10] D. Seery and J. E. Lidsey, *JCAP* **0506**, 003 (2005) [arXiv:astro-ph/0503692].
- [11] X. Chen, M. x. Huang, S. Kachru and G. Shiu, *JCAP* **0701**, 002 (2007) [arXiv:hep-th/0605045].
- [12] C. Cheung, P. Creminelli, A. L. Fitzpatrick, J. Kaplan and L. Senatore, *JHEP* **0803**, 014 (2008) [arXiv:0709.0293 [hep-th]].
- [13] M. Li, T. Wang and Y. Wang, *JCAP* **0803**, 028 (2008) [arXiv:0801.0040 [astro-ph]].
- [14] M. LoVerde, A. Miller, S. Shandera and L. Verde, *JCAP* **0804**, 014 (2008) [arXiv:0711.4126 [astro-ph]].
- [15] E. Sefusatti, M. Liguori, A. P. S. Yadav, M. G. Jackson and E. Pajer, arXiv:0906.0232 [astro-ph.CO].
- [16] C. T. Byrnes, S. Nurmi, G. Tasinato and D. Wands, *JCAP* **1002**, 034 (2010) [arXiv:0911.2780 [astro-ph.CO]].
- [17] C. T. Byrnes, M. Gerstenlauer, S. Nurmi, G. Tasinato and D. Wands, arXiv:1007.4277 [astro-ph.CO].

- [18] C. T. Byrnes, K. Enqvist and T. Takahashi, arXiv:1007.5148 [astro-ph.CO].
- [19] Q. G. Huang, arXiv:1008.2641 [astro-ph.CO].
- [20] C. T. Byrnes, M. Sasaki and D. Wands, Phys. Rev. D **74**, 123519 (2006) [arXiv:astro-ph/0611075].
- [21] K. Enqvist and T. Takahashi, JCAP **0809**, 012 (2008) [arXiv:0807.3069 [astro-ph]].
- [22] K. Enqvist and T. Takahashi, JCAP **0912**, 001 (2009) [arXiv:0909.5362 [astro-ph.CO]].
- [23] J. Smidt, A. Amblard, A. Cooray, A. Heavens, D. Munshi and P. Serra, arXiv:1001.5026 [astro-ph.CO].
- [24] V. Desjacques and U. Seljak, Phys. Rev. D **81**, 023006 (2010) [arXiv:0907.2257 [astro-ph.CO]].
- [25] J. Smidt, A. Amblard, C. T. Byrnes, A. Cooray and D. Munshi, arXiv:1004.1409 [astro-ph.CO].
- [26] A. A. Starobinsky, JETP Lett. **42** (1985) 152 [Pisma Zh. Eksp. Teor. Fiz. **42** (1985) 124];
- [27] M. Sasaki and E. D. Stewart, Prog. Theor. Phys. **95**, 71 (1996). [arXiv:astro-ph/9507001];
- [28] M. Sasaki and T. Tanaka, Prog. Theor. Phys. **99**, 763 (1998). [arXiv:gr-qc/9801017].
- [29] D. H. Lyth, K. A. Malik and M. Sasaki, JCAP **0505**, 004 (2005) [arXiv:astro-ph/0411220].
- [30] C. T. Byrnes, K. Koyama, M. Sasaki and D. Wands, JCAP **0711**, 027 (2007) [arXiv:0705.4096 [hep-th]].
- [31] S. Yokoyama, T. Suyama and T. Tanaka, JCAP **0902**, 012 (2009) [arXiv:0810.3053 [astro-ph]].
- [32] D. H. Lyth and Y. Rodriguez, Phys. Rev. Lett. **95**, 121302 (2005) [arXiv:astro-ph/0504045].
- [33] L. Alabidi and D. H. Lyth, JCAP **0605**, 016 (2006) [arXiv:astro-ph/0510441].
- [34] A. D. Linde and V. F. Mukhanov, Phys. Rev. D **56**, 535 (1997) [arXiv:astro-ph/9610219].
- [35] L. Boubekeur and D. H. Lyth, Phys. Rev. D **73**, 021301 (2006) [arXiv:astro-ph/0504046].

- [36] T. Suyama and F. Takahashi, JCAP **0809**, 007 (2008) [arXiv:0804.0425 [astro-ph]].
- [37] T. Suyama and M. Yamaguchi, Phys. Rev. D **77**, 023505 (2008) [arXiv:0709.2545 [astro-ph]];
- [38] K. Enqvist and M. S. Sloth, Nucl. Phys. B **626**, 395 (2002) [arXiv:hep-ph/0109214].
- [39] D. H. Lyth and D. Wands, Phys. Lett. B **524**, 5 (2002) [arXiv:hep-ph/0110002].
- [40] T. Moroi and T. Takahashi, Phys. Lett. B **522**, 215 (2001) [Erratum-ibid. B **539**, 303 (2002)] [arXiv:hep-ph/0110096].
- [41] T. Moroi and T. Takahashi, Phys. Rev. D **66**, 063501 (2002) [arXiv:hep-ph/0206026].
- [42] D. H. Lyth, C. Ungarelli and D. Wands, Phys. Rev. D **67**, 023503 (2003) [arXiv:astro-ph/0208055].
- [43] D. H. Lyth and D. Wands, Phys. Rev. D **68**, 103516 (2003) [arXiv:astro-ph/0306500].
- [44] N. Bartolo, S. Matarrese and A. Riotto, Phys. Rev. D **69**, 043503 (2004) [arXiv:hep-ph/0309033].
- [45] K. A. Malik and D. H. Lyth, JCAP **0609**, 008 (2006) [arXiv:astro-ph/0604387].
- [46] M. Sasaki, J. Valiviita and D. Wands, Phys. Rev. D **74**, 103003 (2006) [arXiv:astro-ph/0607627].
- [47] Q. G. H. Huang, Phys. Lett. B **669**, 260 (2008) [arXiv:0801.0467 [hep-th]].
- [48] T. Multamaki, J. Sainio and I. Vilja, Phys. Rev. D **79**, 103516 (2009) [arXiv:0803.2637 [astro-ph]].
- [49] M. Beltran, Phys. Rev. D **78**, 023530 (2008) [arXiv:0804.1097 [astro-ph]].
- [50] T. Moroi and T. Takahashi, Phys. Lett. B **671**, 339 (2009) [arXiv:0810.0189 [hep-ph]].
- [51] T. Takahashi, M. Yamaguchi and S. Yokoyama, Phys. Rev. D **80**, 063524 (2009) [arXiv:0907.3052 [astro-ph.CO]].
- [52] K. Enqvist and S. Nurmi, JCAP **0510**, 013 (2005) [arXiv:astro-ph/0508573].
- [53] Q. G. Huang, JCAP **0811**, 005 (2008) [arXiv:0808.1793 [hep-th]].
- [54] K. Enqvist, S. Nurmi, G. Rigopoulos, O. Taanila and T. Takahashi, JCAP **0911**, 003 (2009) [arXiv:0906.3126 [astro-ph.CO]].
- [55] K. Enqvist, S. Nurmi, O. Taanila and T. Takahashi, JCAP **1004**, 009 (2010) [arXiv:0912.4657 [astro-ph.CO]].

- [56] Q. G. Huang and Y. Wang, JCAP **0809**, 025 (2008) [arXiv:0808.1168 [hep-th]].
- [57] M. Kawasaki, K. Nakayama and F. Takahashi, JCAP **0901**, 026 (2009) [arXiv:0810.1585 [hep-ph]].
- [58] P. Chingangbam and Q. G. Huang, JCAP **0904**, 031 (2009) [arXiv:0902.2619 [astro-ph.CO]];
- [59] K. Y. Choi and O. Seto, arXiv:1008.0079 [astro-ph.CO].
- [60] G. Dvali, A. Gruzinov and M. Zaldarriaga, Phys. Rev. D **69**, 023505 (2004) [arXiv:astro-ph/0303591].
- [61] L. Kofman, arXiv:astro-ph/0303614.
- [62] T. Takahashi, M. Yamaguchi, J. Yokoyama and S. Yokoyama, Phys. Lett. B **678**, 15 (2009) [arXiv:0905.0240 [astro-ph.CO]].
- [63] K. Kamada, K. Kohri and S. Yokoyama, arXiv:1008.1450 [astro-ph.CO].
- [64] M. Zaldarriaga, Phys. Rev. D **69**, 043508 (2004) [arXiv:astro-ph/0306006];
- [65] K. Ichikawa, T. Suyama, T. Takahashi and M. Yamaguchi, Phys. Rev. D **78**, 063545 (2008) [arXiv:0807.3988 [astro-ph]];
- [66] F. Bernardeau and J. P. Uzan, Phys. Rev. D **67**, 121301 (2003) [arXiv:astro-ph/0209330].
- [67] F. Bernardeau, L. Kofman and J. P. Uzan, Phys. Rev. D **70**, 083004 (2004) [arXiv:astro-ph/0403315].
- [68] D. H. Lyth, JCAP **0511**, 006 (2005) [arXiv:astro-ph/0510443].
- [69] M. P. Salem, Phys. Rev. D **72**, 123516 (2005) [arXiv:astro-ph/0511146].
- [70] L. Alabidi and D. Lyth, JCAP **0608**, 006 (2006) [arXiv:astro-ph/0604569].
- [71] M. Kawasaki, T. Takahashi and S. Yokoyama, JCAP **0912**, 012 (2009) [arXiv:0910.3053 [hep-th]].
- [72] T. Matsuda, Class. Quant. Grav. **26**, 145011 (2009) [arXiv:0902.4283 [hep-ph]].
- [73] D. H. Lyth and E. D. Stewart, Phys. Rev. D **53**, 1784 (1996) [arXiv:hep-ph/9510204].
- [74] D. J. H. Chung, E. W. Kolb, A. Riotto and I. I. Tkachev, Phys. Rev. D **62**, 043508 (2000) [arXiv:hep-ph/9910437].
- [75] O. Elgaroy, S. Hannestad and T. Haugboelle, JCAP **0309**, 008 (2003) [arXiv:astro-ph/0306229].

- [76] A. E. Romano and M. Sasaki, Phys. Rev. D **78**, 103522 (2008) [arXiv:0809.5142 [gr-qc]].
- [77] D. Langlois and L. Sorbo, JCAP **0908**, 014 (2009) [arXiv:0906.1813 [astro-ph.CO]].
- [78] K. Ichikawa, T. Suyama, T. Takahashi and M. Yamaguchi, Phys. Rev. D **78**, 023513 (2008) [arXiv:0802.4138 [astro-ph]].
- [79] D. Langlois and F. Vernizzi, Phys. Rev. D **70**, 063522 (2004) [arXiv:astro-ph/0403258];
- [80] T. Moroi, T. Takahashi and Y. Toyoda, Phys. Rev. D **72**, 023502 (2005) [arXiv:hep-ph/0501007];
- [81] T. Moroi and T. Takahashi, Phys. Rev. D **72**, 023505 (2005) [arXiv:astro-ph/0505339];
- [82] K. Y. Choi and J. O. Gong, JCAP **0706**, 007 (2007) [arXiv:0704.2939 [astro-ph]].
- [83] H. Assadullahi, J. Valiviita and D. Wands, Phys. Rev. D **76**, 103003 (2007) [arXiv:0708.0223 [hep-ph]].
- [84] C. T. Byrnes, K. Y. Choi and L. M. H. Hall, JCAP **0810**, 008 (2008) [arXiv:0807.1101 [astro-ph]].
- [85] C. T. Byrnes, K. Y. Choi and L. M. H. Hall, JCAP **0902**, 017 (2009) [arXiv:0812.0807 [astro-ph]].
- [86] C. T. Byrnes and K. Y. Choi, arXiv:1002.3110 [astro-ph.CO].
- [87] S. Yokoyama, T. Suyama and T. Tanaka, JCAP **0707**, 013 (2007) [arXiv:0705.3178 [astro-ph]].
- [88] T. Tanaka, T. Suyama and S. Yokoyama, Class. Quant. Grav. **27**, 124003 (2010) [arXiv:1003.5057 [astro-ph.CO]].
- [89] E. D. Stewart, Phys. Rev. D **65**, 103508 (2002) [arXiv:astro-ph/0110322].
- [90] M. Sasaki, Prog. Theor. Phys. **120**, 159 (2008) [arXiv:0805.0974 [astro-ph]].
- [91] Q. G. Huang, JCAP **0906**, 035 (2009) [arXiv:0904.2649 [hep-th]].
- [92] L. Alabidi, JCAP **0610**, 015 (2006) [arXiv:astro-ph/0604611].
- [93] A. Naruko and M. Sasaki, Prog. Theor. Phys. **121**, 193 (2009) [arXiv:0807.0180 [astro-ph]].
- [94] Q. G. Huang, JCAP **0905**, 005 (2009) [arXiv:0903.1542 [hep-th]].

- [95] C. Hikage, K. Koyama, T. Matsubara, T. Takahashi and M. Yamaguchi, *Mon. Not. Roy. Astron. Soc.* **398**, 2188 (2009) [arXiv:0812.3500 [astro-ph]].
- [96] D. Langlois, F. Vernizzi and D. Wands, *JCAP* **0812**, 004 (2008) [arXiv:0809.4646 [astro-ph]].
- [97] M. Kawasaki, K. Nakayama, T. Sekiguchi, T. Suyama and F. Takahashi, *JCAP* **0811**, 019 (2008) [arXiv:0808.0009 [astro-ph]].
- [98] M. Kawasaki, K. Nakayama, T. Sekiguchi, T. Suyama and F. Takahashi, *JCAP* **0901**, 042 (2009) [arXiv:0810.0208 [astro-ph]].
- [99] E. Kawakami, M. Kawasaki, K. Nakayama and F. Takahashi, *JCAP* **0909**, 002 (2009) [arXiv:0905.1552 [astro-ph.CO]].
- [100] D. Langlois and A. Lepidi, arXiv:1007.5498 [astro-ph.CO].
- [101] K. Koyama, S. Mizuno, F. Vernizzi and D. Wands, *JCAP* **0711**, 024 (2007) [arXiv:0708.4321 [hep-th]].
- [102] E. I. Buchbinder, J. Khoury and B. A. Ovrut, *Phys. Rev. Lett.* **100**, 171302 (2008) [arXiv:0710.5172 [hep-th]].
- [103] J. L. Lehners, arXiv:1001.3125 [hep-th].
- [104] E. W. Kolb, A. Riotto and A. Vallinotto, *Phys. Rev. D* **71**, 043513 (2005) [arXiv:astro-ph/0410546].
- [105] K. Enqvist, A. Jokinen, A. Mazumdar, T. Multamaki and A. Vaihkonen, *Phys. Rev. Lett.* **94**, 161301 (2005) [arXiv:astro-ph/0411394].
- [106] K. Enqvist, A. Jokinen, A. Mazumdar, T. Multamaki and A. Vaihkonen, *JCAP* **0503**, 010 (2005) [arXiv:hep-ph/0501076].
- [107] N. Barnaby and J. M. Cline, *Phys. Rev. D* **75**, 086004 (2007) [arXiv:astro-ph/0611750].
- [108] A. Chambers and A. Rajantie, *Phys. Rev. Lett.* **100**, 041302 (2008) [Erratum-ibid. **101**, 149903 (2008)] [arXiv:0710.4133 [astro-ph]].
- [109] A. Chambers and A. Rajantie, *JCAP* **0808**, 002 (2008) [arXiv:0805.4795 [astro-ph]].
- [110] C. T. Byrnes, *JCAP* **0901**, 011 (2009) [arXiv:0810.3913 [astro-ph]].
- [111] K. Kohri, D. H. Lyth and C. A. Valenzuela-Toledo, *JCAP* **1002**, 023 (2010) [arXiv:0904.0793 [hep-ph]].

- [112] J. R. Bond, A. V. Frolov, Z. Huang and L. Kofman, Phys. Rev. Lett. **103**, 071301 (2009) [arXiv:0903.3407 [astro-ph.CO]].
- [113] A. V. Frolov, Class. Quant. Grav. **27**, 124006 (2010) [arXiv:1004.3559 [gr-qc]].
- [114] K. Yamamoto, M. Nagasawa, M. Sasaki, H. Suzuki and J. Yokoyama, Phys. Rev. D **46**, 4206 (1992).